Energy Research and Development Division
FINAL PROJECT REPORT

MT SURVEY FOR RESOURCE ASSESSMENT AND ENVIRONMENTAL MITIGATION AT THE GLASS MOUNTAIN KGRA

Prepared for: California Energy Commission – Geothermal Resources Development Account
Prepared by: Cumming Geoscience
GSY-USA, Inc.

MARCH 2007
CEC-500-2013-063

Prepared by:

Primary Author(s):
William Cumming

Cumming Geoscience
4728 Shade Tree Lane
Santa Rosa CA 95405-7841

Randall Mackie

GSY-USA, Inc.
2261 Market St.
San Francisco, CA 94114-1600

Contract Number: GEO-02-007

Prepared for:

California Energy Commission
Geothermal Resources Development Account

Gail Wiggett
Project Manager

Linda Spiegel
Office Manager
Energy Generation Research Office

Laurie ten Hope
Deputy Director
RESEARCH AND DEVELOPMENT DIVISION

Robert P. Oglesby
Executive Director

ACKNOWLEDGEMENTS

The authors are especially grateful to the following individuals who contributed greatly to the success of this project:

Mr. Mitch Stark, Resource Manager of Calpine Corporation, who provided access to the existing data sets, obtained permission for their public release and supported the project both technically and administratively;

Ms. Charlene Wardlow who, as Calpine Corporation's Geothermal Government Affairs and Community Relations Manager, managed and negotiated the particularly complex permitting process for the field work conducted as part of this project;

Dr. Gail Wiggett of the California Energy Commission, who patiently provided valuable encouragement and coaching on the GRDA process;

Dr. Joseph Moore and his team at the Energy and Geoscience Institute at the University of Utah, especially Mr. Steven Clausen and Ms. Emily Jackson, who supported the petrography and geology components of this study;

Mr. Gregg Nordquist who, as Consulting Geophysicist at Unocal Corporation (now Chevron), supported the translation of the Glass Mountain legacy data used in this project from a digital format proprietary to Unocal. In the 1980's and 1990's, Mr. Nordquist, with Mr. Daniel Carrier and Mr. Randy Thompson of Unocal Corporation, completed the proprietary analyses and reports that became the foundation for the Glass Mountain geophysics and petrography interpretation of this study.

PREFACE

The California Legislature created the Geothermal Resources Development Account (GRDA) and the Geothermal Program in 1980. Funding comes from revenues paid to the United States government by geothermal developers for leases on federal land in California. Under the Geothermal Program, the California Energy Commission has assisted numerous eligible private entities and local jurisdictions in geothermal research, development, demonstration, commercialization, planning, mitigations, and environmental enhancement projects related to geothermal energy. The purpose of the program is to enhance and promote geothermal development in California. For more information on the Geothermal Program, please visit the California Energy Commission's Web site at. http://www.energy.ca.gov/geothermal/index.html

The California Energy Commission Energy Research and Development Division supports public interest energy research and development that will help improve the quality of life in California by bringing environmentally safe, affordable, and reliable energy services and products to the marketplace.

The Energy Research and Development Division conducts public interest research, development, and demonstration (RD&D) projects to benefit California.

The Energy Research and Development Division strives to conduct the most promising public interest energy research by partnering with RD&D entities, including individuals, businesses, utilities, and public or private research institutions.

Energy Research and Development Division funding efforts are focused on the following RD&D program areas:

- Buildings End-Use Energy Efficiency
- Energy Innovations Small Grants
- Energy-Related Environmental Research
- Energy Systems Integration
- Environmentally Preferred Advanced Generation
- Industrial/Agricultural/Water End-Use Energy Efficiency
- Renewable Energy TechnologiesTransportation

MT Survey for Resource Assessment and Environmental Mitigation in the Glass Mountain KGRA is the final report for the Geothermal Reserouces Development Account contract number GEO-02-007 conducted by GSY-USA, Inc. The information from this project contributes to Energy Research and Development Division's Renewable Program.

For more information about the Energy Research and Development Division, please visit the California Energy Commission's Web site at www.energy.ca.gov/research/ or contact the Energy Commission at 916-327-1549.

ABSTRACT

The objectives of this project were to use non-invasive methods to indirectly image the permeable geothermal reservoir geometry and mitigate the drilling costs and environmental impact of future geothermal development at Glass Mountain Known Geothermal Resource Area. This was done by more efficiently focusing exploration wells on the most promising target zones. Significant advances were achieved in three dimensional magnetotelluric imaging, allowing three dimensional imaging to be given greater weight than two dimensional imaging in interpreting the data. Magnetotellurics is a geophysical investigation technique that images the earth's subsurface by measuring natural variations of electric and magnetic fields at the surface. Magnetotelluric resistivity patterns were correlated with detailed data on subsurface temperatures, downhole resistivity logging, patterns of rock alteration zones and water entry zones from wells along geologic cross-sections. This confirmed that reservoir interpretation based on correlating magnetotelluric resistivity with temperature sensitive clay alteration was feasible. The magnetotelluric resistivity maps and cross-sections extended these correlations to undrilled areas, revealing the likely geometry of the geothermal system.

Conceptual models based on the resistivity images indicated that major northeast trending structures and the Medicine Lake Volcano rim structure form permeable zones and reservoir boundaries in the Glass Mountain Known Geothermal Resource Area. Several areas that appear to host a relatively shallow permeable reservoir were identified. The magnetotelluric interpretation also indicated that a significant part of the Medicine Lake Volcano was unlikely to host a developable geothermal resource. Depending on the resource development strategy and supporting studies, follow-up magnetotelluric surveys could be justified. The conceptual resource model derived from this study's integrated interpretation illustrates well-targeting strategies that can be reviewed with respect to engineering and environmental issues. By more efficiently directing well targeting, magnetotelluric resistivity imaging can reduce dry hole costs, as well as focus planning efforts and mitigate the environmental impacts of resource development.

Keywords: electromagnetic survey, geothermal exploration, geophysics resistivity, magnetotellurics, petrography, Medicine Lake, Glass Mountain Known Geothermal Resource Area

Please use the following citation for this report:

Cumming, William. (Cumming Geoscience). Mackie, Randall. (GSY-USA, Inc.) 2007. ***MT Survey for Resource Assessment and Environmental Mitigation at the Glass Mountain KGRA.*** California Energy Commission, GRDA Geothermal Resources Development Account. CEC-500-2013-063.

TABLE OF CONTENTS

LIST OF FIGURES

LIST OF TABLES

EXECUTIVE SUMMARY

Introduction

The Glass Mountain Known Geothermal Resource Area is in northern California, about 50 kilometers (30 miles) northeast of Mt. Shasta. Exploration wells drilled since the 1980s demonstrate that 243 to 278°C (470 to 532°F) geothermal reservoirs exist in two areas, the Fourmile Hill and Telephone Flat Areas, for which Calpine Corporation has obtained power purchase agreements. Exploration has also identified other prospects, including the Southwest and Pumice Mine areas. The most important data sets used to target the geothermal wells at Glass Mountain are temperature gradient holes, geological structure analysis and subsurface geophysical information, specifically resistivity surveys, and most particularly time domain electromagnetics (TDEM) and magnetotellurics (MT).

Acquiring subsurface geophysical information is widely used in exploration for characterizing the geologic attributes that control the flow of geothermal fluids. Geophysical techniques can be used for inferring critical properties of the geothermal reservoir, such as fracture orientation, fracture density, temperature and fluid saturation. MT surveys in geothermal exploration are powerful tools for detecting and imaging resistivity anomalies associated with critical reservoir structural features, such as faults that might provide conduits for the flow of geothermal fluids, other potentially productive geothermal structures and lower permeability features that may constrain the reservoir geometry. The data obtained through these geophysical surveys also allow for estimating geothermal reservoir temperatures at various depths.

Magnetotellurics is a geophysical investigation technique that pictures, or images, the earth's subsurface by measuring natural variations of electric and magnetic fields at the surface. It is capable of investigation as deep as 10,000 meters below the surface, and is relatively low cost compared to other portable resistivity methods that are unable to image so deeply. The method is widely used in geothermal, petroleum, and groundwater investigations. Dozens of MT geothermal exploration surveys have been completed worldwide since the 1980s. As an academic discipline, research applications include deep-crust exploration, earthquake investigations, and research experimentation towards refining the techniques for deriving better subsurface information. Combining and correlating the geophysical data with available data from other sources, such as surface geologic mapping, well logs, microscopic examination ("petrographic analysis") of rock composition in samples, direct temperature measurements from wells and water chemistry, among others, creates a more complete analysis. This was the approach used in this project.

Time domain electromagnetic (TDEM) methods measure the electrical conductivity of soil and rock by inducing pulsating currents in the ground with a transmitter coil and monitoring induced current decay over time with a separate receiver coil. TDEM measurements are primarily used for determining depth and thickness of natural geologic and hydrologic conditions; although MT surveys have become a standard method for geothermal well targeting. The existing MT data at Glass Mountain have not been integrated into an updated resource interpretation since the early 1990s, partly because of the obsolete format of the Glass

Mountain data sets recorded in the 1980s. For targeting the most recent well 88A-28, drilled in the Fourmile Hill area in 2002, TDEM was given more emphasis, although it has a much smaller depth of investigation than MT. The 88A-28 well indicates the existence of a nearby reservoir, but the well is not economic for production.

Although legal and commercial issues have delayed the drilling program at Glass Mountain, interest in geothermal resource development in the United States is increasing, raising expectations that drilling will resume. At the same time, environmental standards covering the area are changing and the value of minimizing the impact of any geothermal development has increased.

Project Purpose

The following specific objectives were planned to achieve the overall goals:

- Analyze and interpret all available geophysical and geological data and incorporate this data into a unified conceptual model. Complete processing of the MT data, including correcting for distortions caused by electric charges on near-surface inhomogeneities ("static shift") using TDEM and one-, two- and three-dimensional) manipulation ("inversion") of the MT into resistivity images in the subsurface.
- Validate a geologic interpretation model for the resistivity patterns in and around the geothermal reservoir using microscopic examination and interpretation of rock samples ("petrography") and other well data.
- Interpret resource geometry and average permeability patterns from correlations of the resistivity patterns with existing well data and extend these to exploration and development targets.
- Identify the most likely conceptual model for the Glass Mountain Known Geothermal Resource Area.
- Review drill targets based on the MT and TDEM interpretation and the actual results of wells.

In order to demonstrate the applicability of MT and TDEM data to well targeting and resource assessment at Glass Mountain, the project provided for the release of sufficient well data to confirm the interpretation approach and show that the methodology would most likely improve the success rate of geothermal well targeting.

Project Results

This study focused on the effective use of MT and TDEM resistivity data for imaging the geothermal resource geometry and inferring patterns of permeability. As part of match share for this project, Calpine released a large amount of previously-obtained "legacy" data sets. All of the 105 legacy MT and 200 legacy TDEM stations identified for release in the original statement of work were included in this analysis, and the quality and utility of each MT station were tabulated. Because Calpine actually released much more data than anticipated when the original proposal was written, a further 148 TDEM stations and the results from 838 gravity stations were included in the analysis. However, after an initial review, several data sets were

not considered because they were obsolete, unusable or irrelevant to Glass Mountain well targeting. All of the geophysical data that were used were assembled in a single database for analysis.

The legacy MT data was reformatted to a modern digital standard and analyzed to plan a field survey including 50 full MT stations, 40 lower- cost high-frequency MT stations, and 40 TDEM stations collocated with MT stations. The survey design was adjusted as the analysis of legacy data and Calpine's well targeting priorities dictated. A total of 91 new sites were recorded as full MT stations with collocated TDEM. However, the most serious data acquisition restriction was the inability to acquire stations on the Glass Mountain rhyolite flow because of dangerous access and the difficulty of acquiring high quality MT electric field data using electrodes on blocky lava with large void spaces.

Data tables and plots for the 105 legacy MT stations identified for release in the original proposal and 91 MT stations acquired in the 2005 survey were compiled in Appendix 2 and in the attachments to this report. The MT digital data can be largely regenerated from the plots and tables in these reports, but to facilitate further research relevant to geothermal development in California, the MT data were also released in digital formats that are familiar standards for industrial and academic MT practitioners.

In preparing the resistivity maps and cross-sections used in the interpretation, the 1D and 3D inversions were given more emphasis than the 2D inversions. The 2D inversions required identifying a pseudo-2D orientation, a sometimes problematic task that produces misleading results if done incorrectly. Over twenty 3D inversion runs were completed. The most significant advance was that smaller model elements and more densely sampled MT frequencies were required to image geothermal targets. Careful editing of the data set proved to be more important than expected. Numerous adjustments to the algorithm also resulted in incremental improvements to the images. This is likely to become a standard public domain test data set for 3D inversion because well data are available to "ground truth" the results.

The "smectite-illite transition" refers to a change in chemistry and crystal structure of certain clay minerals that occur widely in geothermal settings. "Smectite" refers to any of a group of clay minerals that contain water loosely bound in their crystalline structure. "Illite" is a type of clay mineral that differs chemically from the smectites and does not contain water. Under conditions of rising temperature in the subsurface, the smectites gradually give up their water content and are altered, chemically and physically, to illite. This results in a low resistivity, low permeability hydrothermal smectite cap over a higher temperature, more permeable geothermal reservoir. The transition can be used as a geothermometer for determining the likely temperatures at depth and indicating the movement of hot geothermal fluids. Many geothermal reservoirs are known or thought to have a shallow "cap" near the top of the reservoir, overlying the hotter, potentially productive zones. The standard smectite-illite conceptual model used to explain resistivity patterns at most geothermal reservoirs, albeit seldom emphasized in publications on California geothermal MT data sets, was confirmed at Glass Mountain by correlating 1D and 3D MT imaging results with a resistivity induction log and alteration zoning from well 17A-6 and a smectite clay log and temperature logs from well

88A-28. The most reliable indication of the average (bulk) permeability pattern in a geothermal reservoir was the pattern of natural-state isotherms (contour lines showing temperature patterns) supplemented by information on water entries into wells. These patterns were provided in two cross-sections and correlated with the alteration zones and the 1D and 3D MT results. Correlating resistivity patterns with existing well properties including temperature and permeability information was used to extend the interpretation of permeability to undrilled areas. In this report, the annotated resistivity cross-sections with overlaid isotherms and likely flow arrows illustrated the resource conceptual model and how it is constrained by the MT data.

Resource areas at Glass Mountain identified in earlier drilling and surveys have been confirmed, although the new MT analysis suggested that the existing wells targeted the periphery of the areas likely to have high permeability.

In the Telephone Flat area, the pattern of clay alteration inferred from MT resistivity and temperature in the wells suggested that a >290°C (550°F) upflow existed northwest of well 68-8, probably beneath the Glass Mountain rhyolite flow. Wells 68-8 and 31-17 appeared to be located on a margin of this upflow, consistent with their relatively low permeability. In many reservoirs that have extensive zones with relatively low permeability, more prolific production has been achieved by targeting deep exploration wells away from the margins of the reservoir across the structural trend that hosts the higher temperature upflow. The lack of MT data over the Glass Mountain rhyolite flow was a significant source of uncertainty in this interpretation that is difficult to mitigate, but its risk can be considered in a reservoir engineering analysis of the viability of targeting deeper, higher temperature zones.

The high temperature fluids produced from well 87-13 seemed likely to originate from a local upflow, although it is possible that this area is connected to the upflow postulated to exist to the north below the Glass Mountain rhyolite lava flow. The MT imaged a permeable interval associated with the entry in well 87-13.

In the case of the Fourmile Hill, more intense alteration capped the reservoir to the south and southwest, suggesting that the source of the >240°C (460°F) upflow supporting the high temperature zone encountered in well 88A-28 may be located in this direction.

The target areas derived from the MT were consistent with entries shown in wells along the cross-section images. Areas where the resistivity pattern indicated that smectite alteration was poorly developed or that the base of the smectite zone became very deep are higher risk for geothermal well targeting.

Considering the MT data alone would exaggerate the uncertainty of these conclusions. For example, the gap in MT station coverage on the Glass Mountain rhyolite lava makes interpreting a hydrothermal upflow beneath it suspect if based only on the MT. However, the borehole temperature and alteration data implied that an upflow existed nearby and the adjacent MT was consistent with it being located beneath the lava flow. The integration of the MT with geology, alteration and temperature data significantly leveraged the value of the MT.

Locations and priorities for targeting wells in the Glass Mountain KGRA must consider issues other than MT imaging, such as environmental impacts, regulatory constraints and reservoir engineering assessment of resource risk. The conclusions of the MT imaging identified areas where such aspects can be given a higher review priority. For example, the relative risk of targeting certain identified areas of interest could be evaluated by relatively low-cost reservoir engineering analyses supported by geology and geochemistry reviews that consider the results of the MT imaging.

As improvements in multi-processor computing reduce the cost and reliability of three-dimensional MT inversion continues to improve, revising MT images at geothermal fields will become a more attractive option, particularly when new MT becomes available or significant investment decisions are being made. At Glass Mountain, this project's recovery and editing of the legacy MT data and making it available in a readily accessible format has already overcome the main hurdle to revising the MT resistivity imaging. There may be cases where the recovery of legacy MT data sets would be not be the most cost-effective approach to imaging resistivity at a geothermal field. For example, if the data are not available in an industry standard format, the cost of fully and reliably reformatting the data may be high relative to the quality of the older data. A low-cost alternative would be to initially use simpler one-dimensional analysis of legacy data for evaluating whether acquiring new data for three-dimensional imaging would be more effective. MT and TDEM survey costs can be reduced by changes in survey design, but approaches to this are site specific.

Benefits to California

Improved well targeting leads to fewer wells being drilled, fewer well pads and reduced surface disturbance, as well as reduced costs in future exploration and development in the Glass Mountain area. Permitting costs and times are likely to be reduced in the area. Additionally, a fuller appreciation of the likely geometry of the resource will foster improved long-term land use planning.

The advances in technique and knowledge and the experience gained in this project and the demonstration of non-invasive surface geophysical surveys in a sensitive environment are likely to benefit exploration in other California geothermal areas. The availability of a public domain data set in industry standard format with well data to provide explicit constraints will provide a basis for researchers to improve the three-dimensional MT imaging of geothermal reservoirs.

The direct comparisons of borehole geological data and MT resistivity data performed (as a key component of this project) provided important confirmation of the clay-oriented interpretation of geothermal resistivity data at Glass Mountain, and is transferable on a conceptual basis for improving interpretations of resistivity data at other geothermal fields in California.

Lastly, the Fourmile Hill and Telephone Flat projects in this geothermal resource area are expected to benefit Siskiyou County by creating jobs, creating several million dollars in annual property tax revenue, and providing new renewable energy that can help utilities meet California's Renewable Portfolio Standard.

CHAPTER 1:
Introduction

1.1 Geological Setting

This project area is in the Glass Mountain Known Geothermal Resource Area (KGRA) on the eastern flank of the Cascade Range in Northern California, about 50 km (35 miles) northeast of Mt. Shasta. Figure 1 shows the Medicine Lake Volcano. With a surface area of over 2000 km2 (772 square miles) and a volume of 600 km3 (144 cubic miles, it is the largest shield volcano in the Cascades , despite its low relief of about 1200 m (3900 ft). because of its area of square miles). Most of the volcanic surface expression ("edifice") has been built over a period of about 500 thousand years (ka). Initial eruptions were Pliocene basalt and basaltic-andesite, followed by andesite and rhyolite, (Donnelly-Nolan 1988, 1990). Much of the rhyolite is very young; the last eruption is dated only 900 years ago at Glass Mountain. The largest rhyolite flow from Glass Mountain gives its name to the KGRA.

Figure 1: Glass Mountain Study area with Shaded Relief Topography, Geothermal Features and Exploration Area Outlines

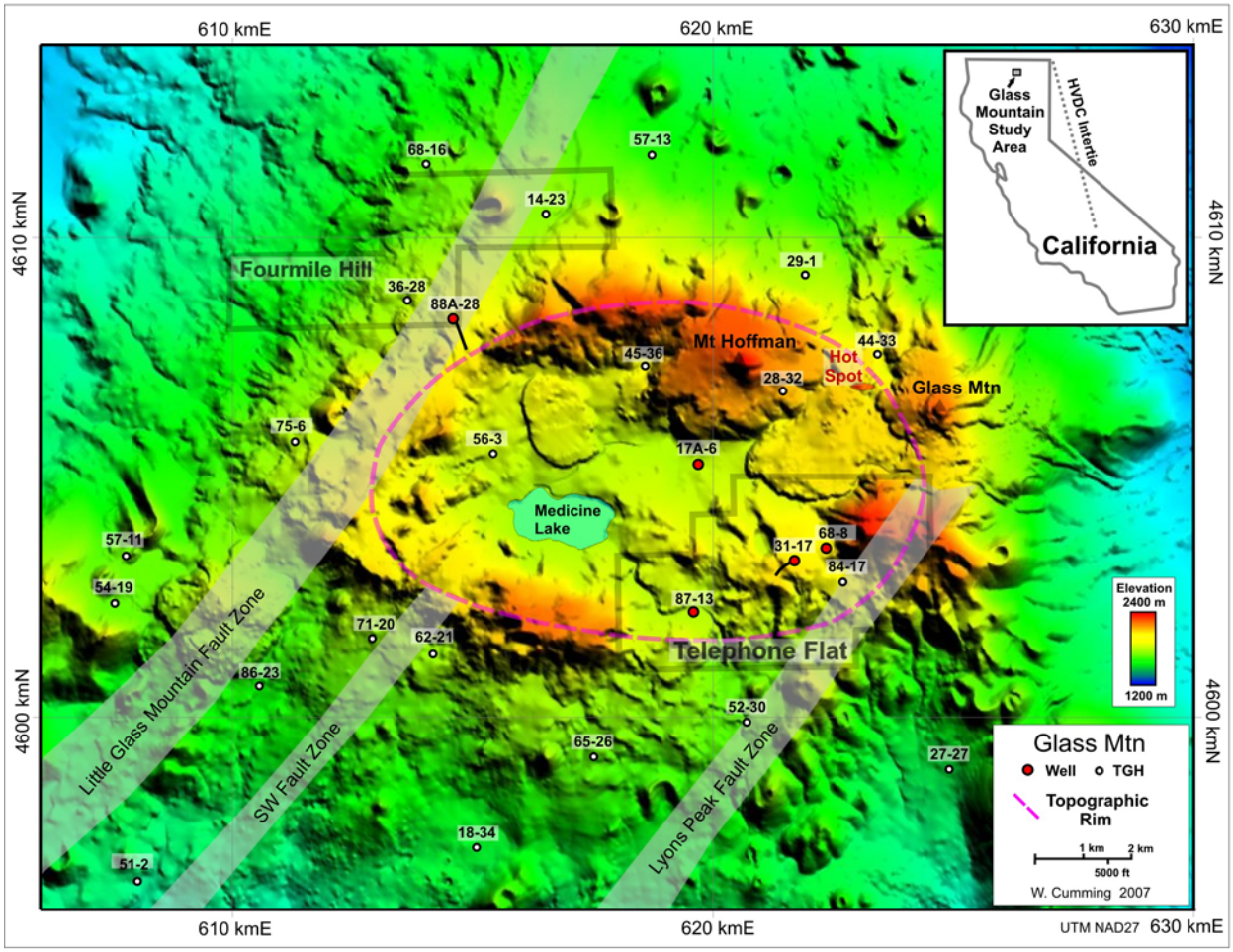

A ring of eruptive centers, highlighted by the magenta dashed line in Figure 1, encloses the central basin that hosts Medicine Lake, leading Anderson (1941) and Donnelly-Nolan (1988) to conclude that the ring is a caldera collapse feature. However, the absence of significant thicknesses of ash flow tuff in deep well cores may indicate, instead, that the elliptical ridge-line is a coalescence of eruptive centers along a ring fracture system (Clausen et al. 2006). Elevation monitoring suggests that the ring fracture is probably related to vertical deformation, currently going on at 8 mm/y subsidence at the summit and symmetrically decreasing on the flanks of the volcano (Dzurisin et al. 2002; Poland et al. 2003; Lisowski et al. 2004). Therefore, local structures are influenced by a combination of volcanism and regional extension associated with the transition from the Cascades to the west and the Basin and Range to the east (Hulen and Lutz 1999). Medicine Lake Volcano is elongated along the active, northerly trending, extensional Klamath Falls-Falls River Graben where it is intersected by the northeasterly trending Mt- Shasta-Medicine Lake fault zone (Donnelly-Nolan 1990). Within three recently active northeasterly fault zone strands shown in Figure 1, fractures are deflected where they intersect the ring fracture (Clausen et al. 2006). Such intersections have been the target of earlier geothermal exploration in this area (Calpine-Siskiyou Geothermal Partners L.P. 2004).

The likely heat source for the geothermal system at Medicine Lake Volcano is ongoing basaltic magma intrusion that has re-melted crust and generated many small granite bodies beneath the volcano over the past 100,000 years (100 ka) (Lowenstern et al. 2003). Granite xenolith fragments that are ubiquitous in the volcanic rocks have been radiometrically age-dated from 20 to 100 ka. Most of the granite fragments are unaltered, suggesting that they originate from much deeper depths than the current geothermal system, below the brittle-ductile transition. Granite intrusive rocks encountered by two wells within the geothermal system appear to be older, about 300 ka, based on hydrothermal alteration dated at 171 ka. This indicates that the hydrothermal system is long-lived, probably has had several episodes of renewed hydrothermal activity, and shows evidence of being much hotter in the past than at present (Lutz et al. 2000). Geophysical imaging has not detected magma (Evans and Zucca 1988), although smaller igneous bodies with a volume less than 2 km3 (0.5 cubic miles) such as dikes would be below the detection threshold of those studies (Donnelly-Nolan 1988). The pattern of volcanism implies that the more recent eruptions originate from dikes intruded along structures (Fink and Pollard 1983). These sources continue to heat the shallow crust within the constructional rim of the Medicine Lake Volcano, creating the currently active geothermal systems.

1.2 Initial Geothermal Exploration

In 1971, the United States Geological Survey (USGS) defined the Glass Mountain KGRA based on the pattern of volcanism younger than 11 ka and the presence of one weak fumarole known as the Hot Spot, on the north margin of the rhyolite flow from Glass Mountain (Figure 1). Although spring and fumarole geochemistry and alteration mapping play a crucial role in the exploration for most geothermal prospects, information available from the regional

geochemistry and the Hot Spot fumarole had limited utility for geothermal exploration at the Glass Mountain KGRA. This situation is similar to other geothermal prospects in the Cascades (Hulen and Lutz 1999, Mariner at al. 1998). To promote geothermal exploration, the USGS and other research groups acquired a variety of geophysical data including a gravity survey reported by Finn and Williams (1982), a time domain electromagnetic (TDEM) survey (Anderson et al. 1983a, b and c), vertical electrical soundings (VES) reported by Zohdy and Bisdorf (1982), telluric profiling (Broker et al. 1982), seismic tomography (Evans and Zucca 1988), regional heat flow (Mase et al. 1982) and earthquake monitoring (McNutt 1989). Donnelly-Nolan (1985) presented a general assessment of geothermal potential for the Medicine Lake Volcano.

Industry, principally Unocal Corp., CalEnergy, Inc., and Occidental Geothermal Inc., supplemented the data published by the USGS on the Glass Mountain KGRA with proprietary surveys, acquiring over 200 magnetotelluric (MT) stations of widely varying quality, over 400 generally high quality time domain electromagnetic (TDEM) stations, over 60 vertical electrical soundings (VES), and over 600 gravity stations. Some of the reconnaissance and experimental surveys, for example the early single-site MT and the helicopter electromagnetics, are now obsolete. However, most of these data are still relevant to current geothermal exploration issues.

Figure 2: Geothermal Prospect Definition Based on Previous Exploration

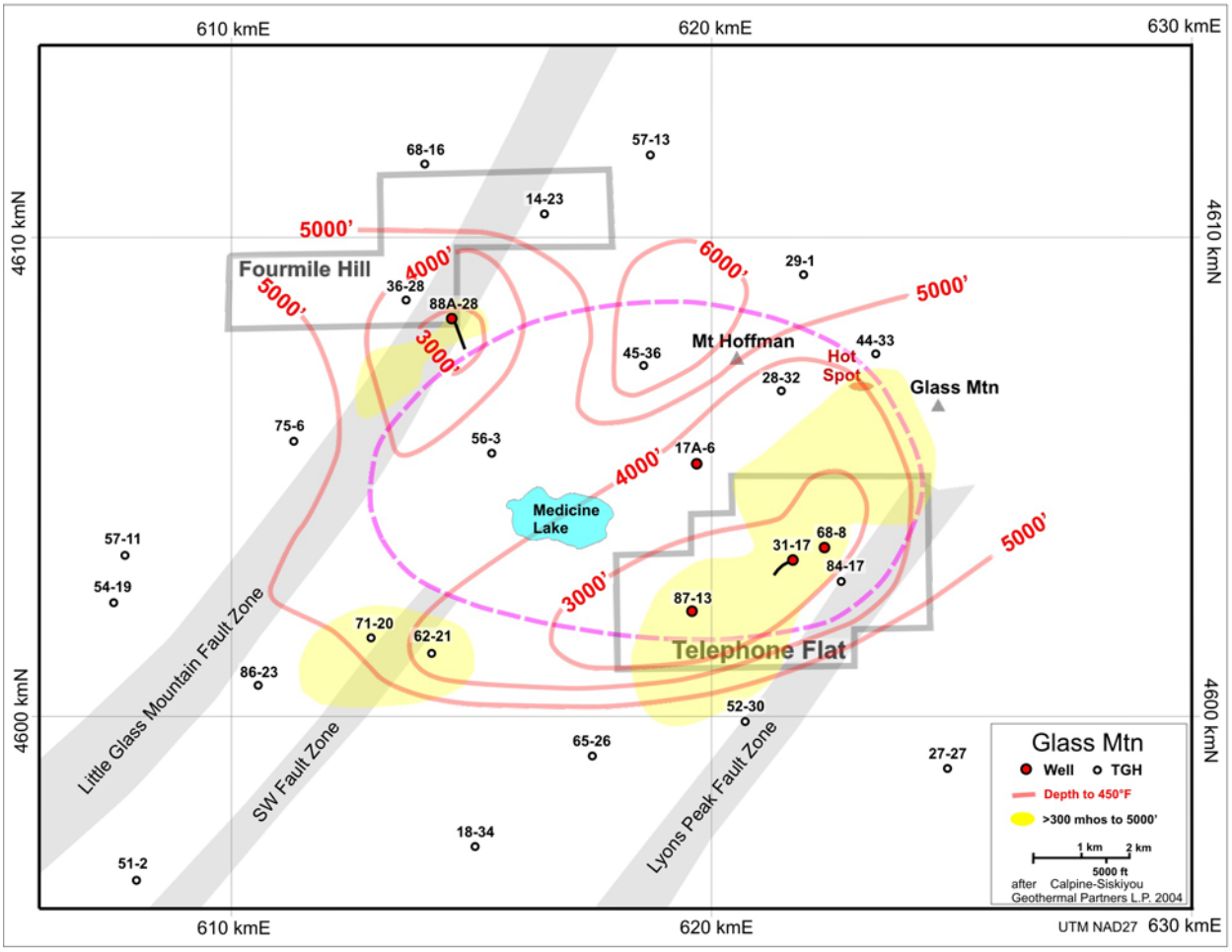

As shown in Figure 2, temperatures extrapolated from 24 temperature gradient holes (TGHs) and patterns of low resistivity, mainly derived from TDEM but also from MT stations, were emphasized in targeting exploration wells (Calpine-Siskiyou Geothermal Partners L.P. 2004). The contoured depth to the 232°C (450°F) isotherm in Figure 2, based on measured TGH and well temperatures and extrapolated gradients, outlines two prospective areas called Fourmile Hill and Telephone Flat. A third prospect, called the Southwest Area, was based on resistivity data such as the 1-dimensional (1D) MT conductance to 1500 m (5000 ft) depth shaded in yellow in Figure 2 and on its less prominent but still high thermal gradient. Each of the three areas roughly coincides with the intersection of the northwesterly structure trends and the volcanic rim.

Since 1984, five deep exploration wells have been drilled in the Glass Mountain KGRA, shown with red highlight in Figures 1 and 2. Of these, the three drilled at Telephone Flat in the 1980's were the most successful. These wells encountered a resource with interpreted temperatures from 243 to 268°C (470 to 515°F) and less than 2500 parts per million (ppm) average dissolved solids. However, the relatively low permeability of the wells limited their deliverability to between 3 and 5 MW per well. The geochemistry of the produced fluids and temperature patterns indicated that the permeable zones in the wells were peripheral to the main upflow of the system. The naturally under-pressured geothermal reservoir has a well-developed clay cap that isolates it from the overlying perched groundwater aquifers that form a cold "rain curtain" over most Cascades volcanoes (Hulen and Lutz 1999).

Well 17A-6, drilled just northwest of the Telephone Flat block, encountered mechanical problems before it could be tested, but it and TGH 17-6 at the same location and TGH 28-32 to its northeast all encountered temperatures over 260°C (500°F), albeit at greater depth than where similar temperatures were reached at Telephone Flat.

Reviewing the nature of permeability in the Glass Mountain wells, Clausen et al. (2006) concluded that open fractures in dense rocks accounted for most of the field-wide permeability, whereas the open space associated with the primary permeability in the breccias at volcanic flow boundaries tended to be filled. Clausen et al. attributed the relatively low permeability in the Glass Mountain KGRA to the intense propylitic hydrothermal alteration. Much of this alteration originated in older, higher temperature geothermal systems that may have reduced porosity and permeability. On the other hand, test data for wells 31-17 and 68-8 indicated that permeability near the well bore wall was probably reduced by the drilling procedures, especially the practice of injecting the drilling sump contents into the well (Calpine-Siskiyou Geothermal Partners L.P. 2004).

1.3 Recent Exploration Drilling at 88A-28

The most recent exploration well at Glass Mountain was 88A-28, drilled in 2002 in the Fourmile Hill Area. Because this well was the subject of a California Energy Commission GRDA grant, the detailed rationale for it is explained in the project report (Calpine-Siskiyou Geothermal Partners L.P. 2004). An earlier TGH at this location showed that a shallow apex in the temperatures coincided with high MT conductance to 1500 m (5000 ft) depth (Figure 2). The

high MT conductance was interpreted as local high intensity clay alteration above the reservoir. This was consistent with apparent resistivity maps from 38 new and 22 older (“legacy”) TDEM stations located in the area. New TDEM data was acquired instead of supplementing the existing MT data with new data because the cost of TDEM stations was lower than MT, and the obsolete format of the old MT data made it difficult to integrate with new data. The 88A-28 well deviation to the southeast was chosen largely on structural grounds, targeting the ring fracture system.

Well 88A-28 proved to be a sub-commercial producer with a maximum temperature of 230°C (443°F) at 914 m (3000 ft) depth over a temperature reversal. Only limited permeability was found, and that was in an underlying cooler 210°C (411°F) zone. The temperature pattern, well test geochemistry and conceptual models imply that the 230°C (443°F) zone in 88A-28 is heated by a nearby upflow zone.

1.4 Improving Well Targeting at Glass Mountain

Because of the lack of surface thermal manifestations, exploration efforts at Glass Mountain have relied primarily on resistivity methods, temperature gradient holes and surface geology to target deep exploration wells. Due to the thick low temperature aquifers overlying the deep clay reservoir cap (often called the “rain curtain" effect of the Cascades), drilling TGH wells deep enough to unambiguously characterize a resource would require 900 to 1200 m (3,000 to 4,000 ft) wells at a per-well cost $500,000 to $1,500,000 more than shallow 100 to 300 m (300 to 1000 ft) wells. Because larger rigs are required for such deep wells, they would also be subject to more regulatory requirements than a typical TGH.

Although the US Department of Energy (DOE) and the California Energy Commission fund research on geophysical methods that might improve on the performance of MT and TDEM resistivity methods, currently available alternatives are not applicable to Glass Mountain. For example, a more powerful TDEM system than the system used for this study could have a reliable depth of investigation below the thick low resistivity clay cap at Glass Mountain, but its cost would be comparable to MT and it would require a very heavy generator-transmitter that would make access and permitting problematic. In fact, most of the alternatives would be more difficult to permit than MT. The most commonly proposed non-resistivity methods, reflection and refraction seismic surveying, have had little or no exploration success confirmed by direct correlation to wells in geothermal fields on volcanoes. Refraction seismic is likely to produce reliable images but, relative to MT, it is less sensitive to the hydrothermal alteration that is diagnostic of reservoir permeability, it has poorer resolution at reservoir depths, and it is more expensive for comparable coverage. Reflection seismic would be particularly expensive at Glass Mountain. Seismic reflection quality is usually poor over geothermal reservoirs and usable data is seldom acquired in volcanic areas covered by a mixture of high density lavas and low density tuffs. There are no case histories where a reflection seismic survey in a geological environment like Glass Mountain imaged a permeable zone confirmed by drilling. On the other hand, there are dozens of successful geothermal case histories for MT resistivity imaging (Anderson et al.

2000; Cumming et al. 2000; Uchida, 2005), making it the most promising geophysical method to reduce exploration risk at Glass Mountain.

Since the original MT data was acquired and processed in the 1980's at the Glass Mountain KGRA, the ongoing development of MT instrumentation and analysis have improved the quality of MT data acquisition and the ability to extract more meaningful information from both new and reasonably good quality older data, especially with respect to imaging three-dimensional patterns of resistivity. Moreover, geothermal interpretation methods have rapidly evolved, and numerous international publications have promoted what is usually called the smectite-illite model for interpreting geothermal reservoir geometry and targeting wells based on resistivity images. The MT and TDEM methods have virtually no environmental impact and are normally allowed to proceed as a casual use activity not requiring a permit by regulatory agencies like the Bureau of Land Management (BLM).

This project was designed to improve the targeting of wells that would follow-up 88A-28 by using existing Glass Mountain well data to confirm the applicability of the smectite-illite approach to interpreting state-of-the-art 3-dimensional (3D) resistivity images from about 105 existing and 90 new MT stations, about 200 existing TDEM stations, and 40 new TDEM stations. After demonstrating how resistivity patterns can be used to infer the geometry of a geothermal reservoir based on the smectite-illite model, the following sections herein outline the MT and TDEM methods for obtaining resistivity images. A detailed discussion of the legacy data sets released by Calpine explains which data were used, which were emphasized and which were not used beyond an initial evaluation. A summary of the acquisition of the new data and its integration with the legacy data introduces a presentation of the validation of the resistivity data relative to well data. Following that, the resistivity images are presented as maps and cross-sections that illustrate a geothermal conceptual model that supports well targeting recommendations.

CHAPTER 2:
Resistivity Methods in Geothermal Exploration

The MT method of imaging resistivity, usually combined with TDEM to correct MT static distortion, has become a standard component of international geothermal exploration programs (Cumming et al. 2000). MT applications to geothermal exploration were pioneered in the USA. However, in the 1970's and 1980's, published case histories of efforts to apply MT to geothermal prospects in the western USA were disappointing, an outcome attributed by Wight et al. (1985) to poor data quality, inadequate interpretation models and misapplication of the method, particularly an inappropriate focus on deep imaging of magma. However, Wight et al. (1985) continued to assume that a fractured, high temperature geothermal reservoir would be imaged as a low resistivity zone, an assumption that was inconsistent with the proprietary experience of geothermal developers and accumulating published evidence, mostly from international geothermal resource areas. Most reservoirs appeared to be resistive relative to overlying and adjacent rocks. Despite international improvements in MT data quality and interpretation reliability, the MT method remained underutilized in California geothermal prospects when this project commenced.

Many international case histories have established a resistivity interpretation approach in geothermal exploration that emphasizes the pattern of hydrothermal clay alteration (e.g. Ussher et al. 2000, Anderson et al. 2000, Cumming et al. 2000, Flóvenz et al. 2005 and Uchida 2005). Correlations of temperature-sensitive clay alteration with temperature, petrology, permeability and other rock property data from boreholes illustrate the utility of clay-oriented MT resistivity interpretation in geothermal reservoir characterization and well targeting. Although the use of MT resistivity imaging to target geothermal wells and characterize resources is well established internationally, few publications confirm the application of modern MT imaging to the development of conventional geothermal resources in California.

The following outline of the geological properties of geothermal systems illustrates why MT and TDEM techniques have become the predominant methods used in geothermal exploration worldwide. The descriptions of the MT and TDEM methods and field procedures demonstrate the methods' minimal environmental impact, a particularly important issue in permitting the field work conducted as part of this study. By comparing Glass Mountain MT resistivity images to existing well bore resistivity log and petrography data, this study confirms the applicability of a geothermal resistivity interpretation approach based primarily on clay alteration.

2.1 Geothermal Reservoir Properties

The thermodynamic and geological bases for the interpretation of resistivity data to explore geothermal reservoirs are illustrated by the reservoir conceptual models sketched in Figure 3. In areas of uniform and generally impermeable rocks, like many sedimentary basins, heat from the earth's interior is conducted to the surface evenly. Contours of equal temperature, called isotherms, are almost parallel to the surface in such areas and temperature slowly gets hotter with greater depth. Variations in the heat conductivity of rocks can cause small variations but

by far the biggest changes in the temperature pattern are caused when either cold water moves down due to gravity or hot water moves up due to thermal buoyancy. At some scale usually much larger than a geothermal field, hot rising water cools, becomes dense, sinks, reheats and rises, and cools again, forming a convection cell.

Most rocks in the subsurface are water saturated. If they become fractured and permeable due to deformation and are also heated by volcanic activity or deep circulation, the water in the permeable fractures rises by thermal buoyancy. This water movement carries heat much faster than would be possible if only heat conduction was occurring. This is generically called convective heat flow in the geothermal industry, even if no return flow path is specifically identified. When depicting such a pattern, the isotherms appear to outline the hot water flow and conform to the margins of the permeable volume. Because the isotherm pattern defines the temperature distribution and implies a permeability distribution, cross-sections with plotted isotherms are an essential part of a geothermal conceptual model. The two cases sketched in Figure 3 use isotherms to illustrate geothermal reservoirs that differ in temperature range, type of permeability, and likely method of production. Nevertheless, the pattern of resistivity with respect to their permeable reservoirs would likely be very similar.

Figure 3: Conceptual models of generic geothermal systems, >250°C (482°F) and <200°C (392°F)

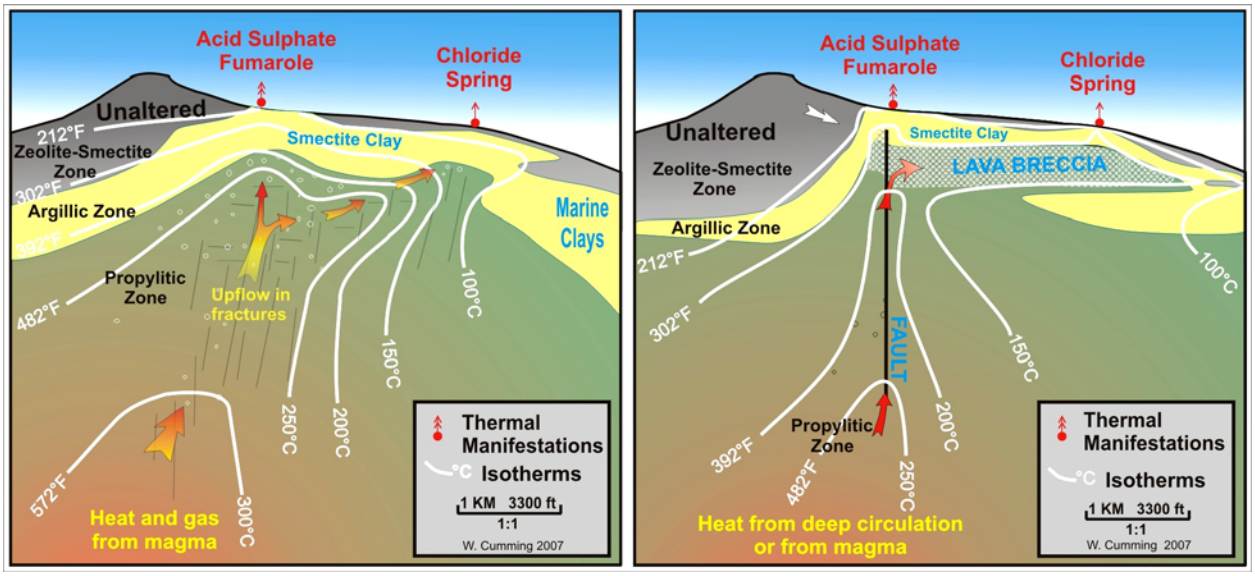

The reservoir at left in Figure 3 is a >250°C (482°F) upflow with the hot fluid rising by thermal buoyancy in fractures. Whether producing water or steam, most of the total mass (weight) of produced fluid is extracted from matrix porosity consisting of the original rock open space porosity, secondary porosity created by hydrothermal dissolution of minerals, and microfracturing. However, commercial geothermal wells require very high flow rates and so do not produce directly from the matrix porosity but from very permeable fractures that interconnect a large volume of the matrix porosity. Geothermal wells are typically drilled 300 m to 3500 m (1000 to 10,000 ft) deep with an uncased open section exposed to the formation over

100 to 1000 m (300 to 3000 ft). In this type of reservoir, wells usually produce from only one or two fracture zones, although they may intersect hundreds or even thousands of fractures. Most fractures are not permeable because stress has closed them, hydrothermal mineral deposition filled the open space, or fault motion filled them with impermeable gouge. Wells in geothermal fields containing water with reservoir temperature over 200°C (392°F) are produced by flashing the water to steam in the well bore to lift the fluid to the surface.

The reservoir at right in Figure 3 is a shallow, <150°C (300°F) tabular outflow in a lava breccia that originates from a >200°C (392°F) upflow hosted in a limited zone of fracturing associated with a fault. The temperatures in this figure are typical of these systems but could span a broad range. Commonly, the volume of deeper fluid that is connected to the fracture system is small relative to that available in the outflow breccia and so, although it is much lower temperature, the tabular outflow can sustain higher generation capacity. Many, perhaps most, shallow tabular outflows have sufficient distributed permeability to support economic production rates throughout most of the formation that hosts the outflow, not just at a few faults, greatly reducing targeting risk. Reservoirs under 200°C (392°F) are typically produced by pumping rather than by partial flashing.

2.1.1Alteration Zones and Permeability

The alteration zone terminology commonly used at Glass Mountain and similar geothermal fields is included in Figure 3 (Clausen et al. 2006). Hydrothermal alteration occurs over a broad range of temperature from about 60°C to over 350°C (140 to over 662°F). Alteration of porous rocks in the reservoir is usually dominated by the illite-chlorite clay mineralogy characteristic of the propylitic alteration zone found in porphyry mineral deposits. Above the reservoir, gas and water leak upward to form the low permeability argillic (smectite-illite clay) alteration halo shown in yellow in Figure 3. The zeolite-smectite alteration zone shown in gray is characteristic of the meteoric zone affected more by rain water than by the geothermal system. This meteoric zone is often relatively unaltered and permeable.

An impermeable cap is a conceptually important element of a geothermal resource model and, in all but a few special cases, the low permeability in the cap is caused by smectite clay alteration. The smectite clay alteration created over and adjacent to most geothermal reservoirs reduces permeability, even where the rock is fractured. The impermeable cap inhibits thermally buoyant flow and the dissipation of heat. This trapping of hot water is important to the characteristics of a developable reservoir: shallow enough to drill, high enough temperature to efficiently generate power, and large enough volume to sustain an economically significant rate and period of production.

Because both temperature and permeability affect the conversion of smectite to illite (Essene and Peacor, 1995), this mineralogical transition usually follows the isotherm(s) that mark the transition to the permeable geothermal reservoir. Because of its partial dependence on permeability, the transition occurs over a wide range of temperature from about 70 to 200°C (158 to 392°F). Therefore, although the average reservoir temperature difference between the

two models depicted in Figure 3 is about 100°C (212°F), isotherms near the top of the permeable reservoir conform to the base of the smectite clay cap.

2.2 Resistivity Variation near Geothermal Reservoirs

Ussher et al. (2000) present a basic model for thematically predicting geothermal resistivity based on various rock and alteration properties found in cuttings and cores. Resistivity variations in geothermal field areas are related to changes in salinity, water saturation, temperature, porosity, and cation-exchange capacity in hydrated clays, particularly smectite clay and mixed-layer smectite-illite clay. Numerous case histories show that the variation in cation exchange capacity, mainly related to smectite clay content, is by far the most important factor in determining resistivity variation in geothermal fields. The emphasis of clay alteration in geothermal resistivity interpretation is sometimes called the "smectite-illite" approach based on the two predominant clay types involved in the transition from the impermeable, lower-temperature cap containing smectite clay to the higher temperature permeable reservoir where illite clay usually replaces smectite.

Inferring a permeable reservoir target from resistivity is done in two ways; 1) through the pattern of isotherms implied by the resistivity pattern, and 2) through the intensity of the alteration suggested by resistivity values. The natural state temperature pattern is the primary constraint on bulk permeability. Because low resistivity is correlated with low permeability, temperature sensitive smectite alteration, imaging the base of the low resistivity clay gives a direct constraint on the transition from low to high permeability at the top of the reservoir and an indirect constraint on temperature. In many cases, inferring the temperature and permeability pattern using resistivity data provides sufficient information to target wells on zones with a higher probability of encountering permeable fractures (Anderson et al. 2000).

Even in cases where the reservoir is dominated by a single fracture, the intersection of the fracture with the clay cap can usually be inferred with a lateral resolution less than the depth to the fracture. Highly permeable fractures within a reservoir tend to leak more gas, causing more intense overlying alteration. Sometimes the smectite-illite transition is pushed higher at the apex of the fracture by the higher temperature upflow, as illustrated by the base of the cap below the fumarole in the models in Figure 3.

2.2.1 Outflows and Low Resistivity below the Smectite-Illite Transition

Depending on depth and geology, low resistivity zones below the top of a geothermal reservoir can have a variety of plausible interpretations. Most commonly, like in Figure 3 on the right, a low resistivity zone below a reservoir is smectite clay alteration in a low permeability, low temperature zone below an outflow. In fact, the pattern of a low resistivity cap, a tabular resistive zone, and an underlying low resistivity zone is a pattern diagnostic of an outflow over an impermeable zone. The lack of such a pattern, however, does not preclude the existence of an outflow. For example, deeper rocks below geothermal outflows often have little hydrated smectite because they are often cooled from a previous hotter period when conversion of

smectite to illite took place and illite does not convert back to smectite when temperature declines.

2.2.2 Resistivity Patterns within Geothermal Reservoirs

Well logs indicate that, compared to the variations from 1 to 1000 ohm-m above the smectite-illite transition, bulk resistivity does not vary much within geothermal reservoirs, typically 10 to 100 ohm-m, but commonly just a very gradual increase with depth. A common diagnostic for noise influencing a surface measurement of resistivity is an exceptionally high or low value at reservoir depths. A relatively smooth variation in bulk resistivity is expected since the rock is compacted and the water content of all clays is low in the propylitic alteration zone. At temperatures over 200°C (392°F), the variation of resistivity with respect to temperature is small (Ussher et al. 2000). A variation in salinity within a reservoir large enough to cause a detectable resistivity change could only occur where permeability is low, which is not characteristic of geothermal reservoirs.

Acid zones of geothermal fields are a special case in resistivity interpretation. Although several geothermal fields have isolated zones that are acidic, because of limited economic interest in producing such zones, their rock physics has not been thoroughly investigated and published. Based on reported mineralogy and resistivity images, it appears that clay has a significant effect on resistivity in acid zones but that a wider range of clays besides smectite may be involved. Salinity and porosity are also important in an acid zone resistivity pattern, especially in the transition to a neighboring neutral geothermal reservoir. Although this may be an issue in some geothermal prospects, it is unlikely to be a factor at Glass Mountain because it lacks an active volcanic vent containing sulfur-depositing fumaroles, a characteristic of most acid-cored systems.

In a manner analogous to the smectite-illite transition at the top of geothermal reservoirs, the transition from chlorite and illite derived from smectite to more crystalline illite clay may include intermediate clay types at temperatures between 200 and 300°C (392 and 572°F). Based on the core studies of Flóvenz et al. (2005), it is plausible to expect that changes in resistivity related to intermediate clays in this transition could make high permeability, high temperature upflow zones appear to be resistive relative to other parts of the permeable reservoir. A similar pattern might be expected if higher temperature resulted in greater induration and loss of matrix porosity. At Glass Mountain, both chlorite and illite clay are found in most parts of the reservoir at temperatures over 200°C (392°F) (Carrier, 1989b). Although this is a plausible suggestion, unlike the smectite-illite approach to interpreting resistivity at the top of reservoirs, this has not been well established by case histories and so it is not emphasized in this Glass Mountain interpretation.

2.2.3 Reservoir Fracturing and Resistivity

At a typical depth to the top of a high temperature geothermal reservoir of 300 to 1000 m (984 to 3281 ft), the depth to the top of a productive fracture is probably at least 10,000 and commonly over 100,000 times greater than its narrowest dimension. Although the height of a near-vertical open fracture in a reservoir might be comparable to its depth, its thickness is likely to be less

than 0.03 m (0.1 ft). Filled with reservoir water, the conductance of such a fracture is a small fraction of the conductance of the overlying clay cap. Therefore, it is unlikely that the open space saturated with reservoir water associated with a single potentially productive fracture could be resolved by any existing surface method of imaging resistivity.

A variety of borehole imaging logs use arrays of very small resistivity "buttons" to map the resistivity of borehole walls in great detail and, in the case of geothermal applications, map the resistivity of fractures within a geothermal reservoir. Such a tool has not been run in the wells at Glass Mountain but it is expected to be similar to other volcanic areas. These very detailed resistivity logs show that, on a scale of less than 0.01 m (0.05 ft), fractures filled with reservoir fluid are low resistivity features. A group of such fractures might collectively increase bulk porosity to such an extent that they would be detectible within a volume of rock with bulk matrix porosity less than 1 percent. However, based on core measurements (Elliot 1982 and Carrier 1989a), the Glass Mountain reservoir is likely to have a bulk matrix porosity that fits the typical range for conventional geothermal reservoirs of 2 to 20 percent (Ussher et al. 2000). Even if a well intersected hundreds or even thousands of fractures, the open space in these fractures, when averaged over a reservoir volume that could be detected by a surface resistivity method, does not add significantly to the total rock porosity typical of volcanic reservoirs. Therefore, on a reservoir scale of tens to hundreds of meters (hundreds of feet) that might conceivably be resolved by a surface resistivity method, fracture porosity is unlikely to significantly affect the average resistivity of volcanic reservoir rocks.

A recently published three-dimensional (3D) MT study of Coso Geothermal Field by Hoversten et al. (2006) interprets a low resistivity zone within a geothermal reservoir as direct evidence of fracture permeability. This survey is directed, in part, at imaging targets suitable for developing an unconventional enhanced geothermal system (EGS). It is possible that the rock matrix porosity is low enough that a fracture system would have this relative effect on resistivity. However, because rock properties related to this feature have not yet been elucidated by well data, its practical significance for the interpretation of a conventional geothermal target like Glass Mountain is uncertain.

2.2.4 Resistivity Deeper than Geothermal Reservoir Production Zones

Low resistivity zones have been detected below the production zones of other geothermal fields at depths greater than 4000 m (13124 ft). A variety of explanations for these have been proposed but the most common interpretation in volcanic areas is that it is molten rock, magma. A limited number of rock measurements indicate that magma bodies with high water and gas content are likely to be low resistivity, 1 to 10 ohm-m. Other explanations for deep low resistivity are also generally accepted as being plausible (Simpson and Bahr, 2005). Several investigators have hypothesized that high salinity water trapped in the transition to ductile rocks at 350 to 450°C (662 to 842°F) might cause low resistivity, although others argue that the very low permeability of this zone would isolate the low resistivity fluid in a resistive matrix. Graphitic shale is commonly proposed as an explanation for deep low resistivity features, although this is usually associated with very old rocks, not geologically young volcanoes like Glass Mountain. If a large low resistivity zone were detected at Glass Mountain below 4000 m (13124 ft) depth, the most

likely explanation would be noise or an imaging artifact and the most likely geological explanation would be magma.

Given the distribution and very high conductance of shallow smectite alteration at Glass Mountain, only very large zones with high conductance are likely to be reliably detected below 4000 m (13124 ft) depth. Lateral resolution of such bodies would be at a scale too large to be relevant to conventional Glass Mountain geothermal resource targets. However, the released MT data set could be integrated into a regional MT survey designed to address resistivity variation below 4000 m (13124 ft) depth. This is outside the scope of the current project.

2.2.5 Conceptual Uncertainty in Geothermal Resistivity Interpretation

Uncertainty in geothermal resistivity interpretation is commonly accommodated using risk analysis tools such as probabilistic decision trees and tables for well targeting and resource assessment (Newendorp and Schuyler, 2000). The reliability of such an approach depends not only on the reliability of the resistivity imaging itself but also on how effectively it is integrated with the types of supporting information that have proven to be most relevant in case histories.

There are many geological features that could have low resistivity zones but that are not geothermal fields. The ambiguity in geothermal resistivity interpretation has usually been manageable unless the resistivity data is interpreted without adequate consideration of the geological and hydrological context. The most frequent mistake is targeting wells on the extremely low resistivity values where hydrothermal water leaks from a reservoir into clays in a neighboring sedimentary basin, like the basin in Figure 3. Taken in context, this is obviously a high risk target.

It is rare that a clay cap over a geothermal reservoir that has cooled is mistaken for the cap of an active geothermal reservoir. Importantly, the geochemistry and geologic context are often decisive in differentiating these cases. Moreover, if the clay cap is quickly buried after the reservoir cools, it tends to compact and become higher resistivity than would be expected for active hydrothermal smectite alteration. If local volcanoes stop erupting but do not subside, the hydrothermal smectite alteration is usually rapidly eroded and the high temperature propylitic alteration is exposed at the surface. In several cases where a dormant eroded volcano became active again, a new geothermal system began but stayed relatively small because a smectite clay cap could not form in rocks already altered to a higher temperature propylitic rank. In these cases, resistivity imaging is diagnostic of both the lack of a clay cap and the relatively small resource size.

Although most geothermal reservoirs are encased by a more or less continuous clay cap, the thickness of the cap and the intensity of the clay alteration in the cap usually vary. The ease with which the primary rock can be altered is related to its porosity, with dense andesitic lava resisting alteration more than porous andesitic ash. Some types of rock contain more of the types of minerals that are susceptible to alteration, given a particular temperature or water chemistry. Smectite alteration in a cap is attenuated if rocks have already been altered to illite clay in an earlier period when they were hotter than present day. This type of geologic context is particularly important in establishing a resistivity value expected to correlate with smectite

alteration because, for volcanic lavas it might be 10 ohm-m and for sediments it might be less than 1 ohm-m.

2.3 Geothermal Resource Assessment Based on Resistivity Data

Three common approaches to geophysical exploration interpretation, anomaly hunting, anomaly stacking and conceptual model targeting, play prominent roles in geothermal exploration. Anomaly hunting is a low-cost preliminary step to choose an area where a higher cost investigation would focus to develop a conceptual model. Anomaly stacking should always be done while building a conceptual model but it is a poor management presentation tool. Conceptual model interpretation, when integrated with a case-oriented risk analysis, would justify the much larger investment in drilling deep wells. Anomaly hunting and conceptual model targeting lead to different definitions for a resource boundary.

2.3.1 Anomaly Hunting

Anomaly hunting is a standard interpretation approach that works by direct analogy. For example, low resistivity is associated with geothermal reservoirs, albeit only indirectly associated with the reservoir itself. If a shallow regional resistivity survey could inexpensively detect average resistivity at about 200 m (600 ft) depth, the clay cap of most existing geothermal fields would be detected. Of course, many lake basins and other features not associated with geothermal fields might also be detected. Nevertheless, the simplicity of this anomaly hunting approach makes it useful for identifying likely prospects in reconnaissance surveys, provided that the data can be acquired at low cost.

In some cases, typically where there is little topographic variation, a particular resistivity contour might correlate with the perimeter of the production wells in a geothermal field. By analogy, this resistivity “anomaly” pattern is sometimes used to outline other potential geothermal resources. It is also used, albeit less frequently in the last decade, to target wells and define resource boundaries for geothermal fields. However, without conceptual models to establish the relevance of the underlying analogy on which anomaly hunting depends, its prediction of resource boundaries or even resource existence often fails. Therefore, a resource boundary based on anomaly hunting might be more appropriately considered to be an outline of the area where further analyses will be directed to prepare a resource conceptual model.

2.3.2 Anomaly Stacking

Anomaly stacking is an extension of the anomaly hunting approach that involves overlaying or stacking several contours or “anomalies” in a way that increases confidence about a decision without closely examining the conceptual basis for that confidence. Anomaly stacking depends on psychology for its impact and it is often more effective in influencing commercial and academic decision makers than an objective risk assessment. For example, if two closely related anomalies are prepared but the first is based on a data set that is much more reliable than the second, then even if they match, the second is probably redundant in terms of objectively reducing decision risk. However, such correlations often increase confidence, even among experts. Although overlaying and correlating data is an essential step in building conceptual

models, such work should be used to in a way that avoids basing decisions on the anomalies themselves rather than on the conceptual models that they support.

Stacked anomalies often have a common origin that has less relevance to the conceptual objective than is assumed. For example, a dry lake bed near a volcano will almost always have locally low values of shallow resistivity, gravity and magnetic field. It may mark an area of structural extension likely to enhance deep permeability or it might just be a lake bed created when a lava flow blocked drainages. However, because this pattern of anomalies is also typical of a geothermal clay cap, stacking the anomalies will almost always reduce the perception of risk unless the conceptual ambiguity of the geologic setting is recognized. This is not to say that the results of different data sets should not be overlaid and compared but that such overlays and comparisons should be integrated into one or more conceptual models that are consistent with the combined data.

2.3.3 Geothermal Resource Conceptual Models

When making decisions like targeting a geothermal well or committing to power plant construction, a conceptual model approach to resource evaluation is justified. A geothermal conceptual model suitable for well targeting should normally include predicted clay transitions from the cap to the permeable reservoir and predicted isotherms. Based on well cuttings analyses (Gunderson et al. 2000) and temperature log interpretation, a geoscientist can determine if the well is consistent with the predicted conceptual model and decide whether to continue the drilling strategy unchanged. Besides providing a basis for efficiently testing and adjusting exploration hypotheses, resource conceptual models can directly support economic risk assessments and reservoir engineering analyses of resource capacity.

A conceptual model approach leads to a different definition of reservoir boundaries than is used for anomalies. Instead of a boundary associated with a resistivity contour value, it will be defined based on conceptual elements that might include; an upflow, a high permeability shallow structure trend, a tabular <200°C outflow, and so on. The elements of a geothermal conceptual model can usually be more effectively illustrated in cross-section. Isotherms are the most important element, along with an indication of what data support the isotherm geometry, such as MT resistivity, surface geochemistry, and well data. Other supporting graphics for a conceptual model typically include a map of the elevation of the base of the low resistivity zone because this usually conforms to the top of the reservoir (Anderson et al. 2000). However, the upflow and the most attractive target areas are often obscured in such maps by prominent reservoir outflow zones. A map of conductance to the base of the shallower part of the clay cap will often outline the apex of the reservoir and identify any intensely altered area that may be correlated with shallow reservoir permeability. Another map showing the deeper conductance pattern on the field margins can outline the reservoir edge. To synthesize the results of all of these sections and maps, the boundaries of the conceptual elements interpreted in each are transferred to a resource conceptual model map that reconciles them as boundaries for at least one upflow and several reservoir zones. Producing such a map is an important objective of this study.

2.3.3.1 Supporting Data for Interpretations of Geothermal Resistivity Patterns

Although information can be ranked with respect to its likely practical impact on drilling success and resource assessment, the interpretation of each data set depends to some extent on the context provided by the other data sets. For prospects like Glass Mountain, case histories suggest an emphasis on; bore hole temperature, bore hole permeability, geochemistry relevant to temperature and fluid flow, resistivity in cross-section and map view, alteration type and intensity, hydrology, lithology, structure, and so on. Because it can characterize clay alteration throughout the entire system at relatively low cost, resistivity is ranked high on this list. However, other information like hydrology, alteration and lithology information are important to establish context for the resistivity interpretation.

Because resistivity well logs are rarely taken in the unstable upper parts of geothermal wells, the smectite-illite model for interpreting resistivity at a geothermal field is usually confirmed by comparing resistivity to petrographic analyses of well cores and cuttings. To produce a well log showing qualitative variations in the amount of smectite in cuttings, the methylene-blue (MeB) method is commonly used at new wells in geothermal fields (Gunderson et al. 2000). Using standard geological microscope analysis, supplemented by X-ray diffraction (XRD) which is more reliable than MeB in detecting mixed-layer smectite-illite, a petrological model for a geothermal field can be assembled to confirm the applicability of the smectite-illite approach. The temperature logs and petrographic data from five deep exploration wells and 24 TGHs at Glass Mountain provide an extensive data set to correlate with the MT. The resistivity log in well 17A-6 provides a rare opportunity to more directly correlate MT resistivity with measured resistivity from above a geothermal clay cap into a reservoir.

2.4 MT and TDEM Method, Procedures and Environmental Impacts

The details of the field procedures for the MT and TDEM surveys proved to be of far greater importance in getting permits to do the surveys than was initially expected based on earlier experience at Glass Mountain and on recent experience permitting similar geothermal surveys elsewhere in California. In order to process the permits, several iterations of descriptions of the field procedures were required for the US Forest Service (USFS) and the Bureau of Land Management (BLM). A summary of this information is provided below to illustrate how the permitting process affected the MT and TDEM survey designs. In addition, these survey procedure descriptions can be adapted to the permitting requirements of future MT and TDEM surveys for geothermal exploration on federal lands in California.

2.4.1 MT Field Procedures and Environmental Impacts

The MT method illustrated in Figure 4 uses two sets of grounded electrical field measurement lines, Ex and Ey, and three coil magnetometers, Hx, Hy and Hz, to measure the natural electric and magnetic fields at the earth's surface caused by electromagnetic waves radiated from the sun and from distant electrical storms (Vozoff, 1991). The magnetic field varies slowly with respect to ground resistivity while the electric field is more directly related to the resistivity at each station. Impedance, a complex parameter analogous to resistance that is used when electric fields vary in time, can be estimated from the electric and magnetic fields. Apparent resistivity

can be calculated from the impedance. It is proportional to the square root of the ratio of the electric to the orthogonal magnetic field, while the phase can be thought of as the delay, measured as an angle, between the peaks of the electric and orthogonal magnetic field waves. An MT sounding is made by computing the impedance for a range of frequencies, typically 0.01 to 300 Hz for geothermal applications. The electric field of a high frequency electromagnetic wave dissipates at shallow depths whereas the field at low frequencies responds to a much thicker and deeper section of the earth. Therefore, by recording MT at a wide range of frequencies, resistivity can be imaged for a wide range of depths. Because MT uses natural signals, there is no option to increase the signal strength if cultural noise from power lines or roads disturbs the measurements but the MT signal sources, the sun and worldwide lightning, have generally proven to be robust and reliable.

MT is subject to several types of distortion that must be allowed for or corrected. One type is called static shift, a potential source of distortion shared by all resistivity methods that use electrodes. In Figure 4, the apparent resistivity data measured for Ex and Ey are separated at high frequency. They would be equal in a uniform earth. However, in the field layout diagram in Figure 4, the yellow low resistivity body near the Ey electrode is causing a local distortion in the electric field that the Ex dipole does not detect, so the two apparent resistivity curves calculated from these electric fields, called modes, are separated by a constant offset through a wide range of frequencies. Because TDEM does not use electrodes, MT is commonly supplemented by TDEM data to correct static distortion (Pellerin and Hohmann 1990). The MT apparent resistivity curves in Figure 4 show an additional distortion. At low frequency, the apparent resistivity curves for the Ex and Ey electrodes diverge due to lateral changes in resistivities that are the subject of 2D and 3D inversions.

Figure 4: MT Station Layout, Data Recording and 1D Resistivity Models

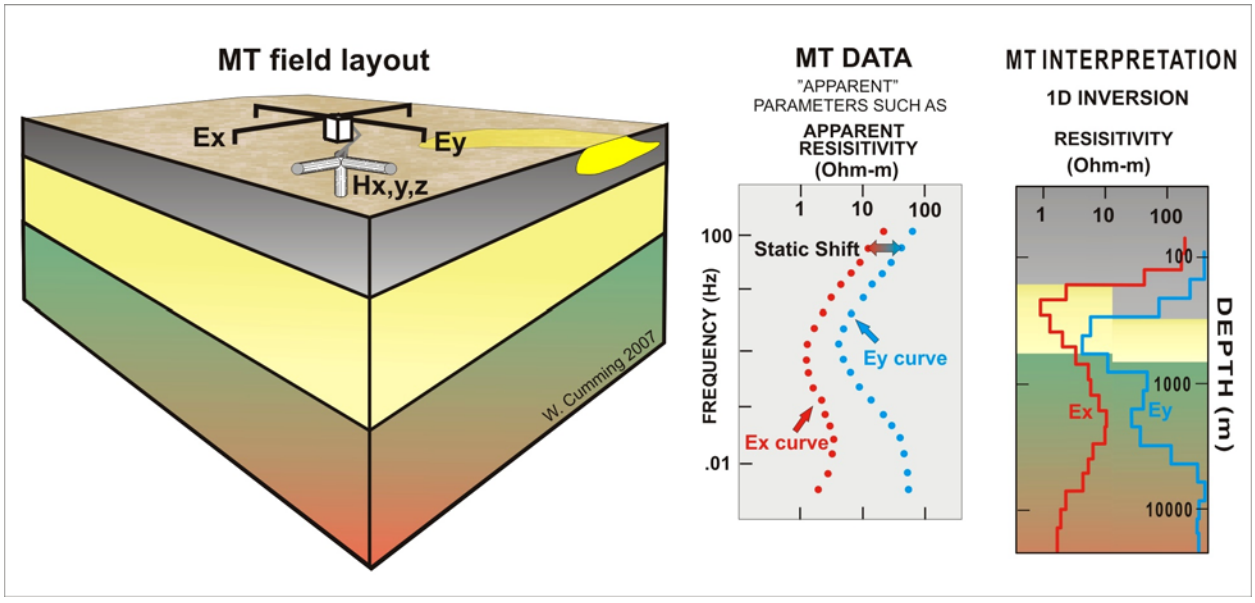

The MT interpretation in Figure 4 schematically illustrates 1D inversions of the data from the E_x and E_y electrodes. They differ because of the static and dimensional distortion in the two apparent resistivity curves already described. An effective and simple approach is to invert an average or invariant resistivity curve and that is the approach taken in this study for 1D analysis. For 2D analysis, a cross-section must be chosen that has little perpendicular variation, a situation that is difficult to arrange and so 2D cross-sections must make many iterative compromises with effects that can be difficult to assess. Therefore, when 3D inversions are available, MT analysis tends to focus on average 1D inversion for quality assurance and 3D inversion for final interpretation.

2.4.1.1 MT Station Layout

A set of MT equipment used to record a station for the planned survey consists of four insulated wires attached to five electrodes inserted into the ground, three coil magnetometers in PVC tubes about 1.2 m (48 inches) long and 0.1 m (4 inches) wide, a recording system about the size of a small piece of carry-on luggage, and a sealed battery.

Four insulated wires, each about 50 m (150 ft) long, are laid out by hand in a plus-sign pattern and are electrically connected to the ground through five electrodes of two possible types. Porous electrodes are usually buried in small holes about 0.15 to 0.3 m (6 to 12 inches) deep and 0.15 m (6 inches) wide using a post-hole digger. If steel stake or steel plate electrodes are used, they are usually hammered or dug in to refusal or to a maximum of about 0.4 m (18 inches). In cases where it is difficult to achieve a good electrical contact with the rock or soil, a few quarts of fresh or slightly salty water and/or wet bentonite clay may be placed in the bottom of a hole dug for a porous electrode or poured beside a steel stake. The steel electrodes are faster to install but the electrically more stable porous electrodes are required when recording for times much longer than an hour.

The MT receiver and electrode lines are shown at left with the operator and field crew while a magnetometer is shown being buried in a 0.15 m (6 inch) wide, 0.15 to 0.3 m (6 to 12 inch) deep trench at right. These photos are from a desert survey where it is easier to see the system than at Glass Mountain where vegetation obscures most sites. After the magnetometers and electrodes are recovered and the soil and vegetation replaced, the disturbance is usually so small that it is difficult to find without accurate coordinates and GPS positioning.

Figure 5: MT Equipment Field Layout Illustrating its Environmental Impact.

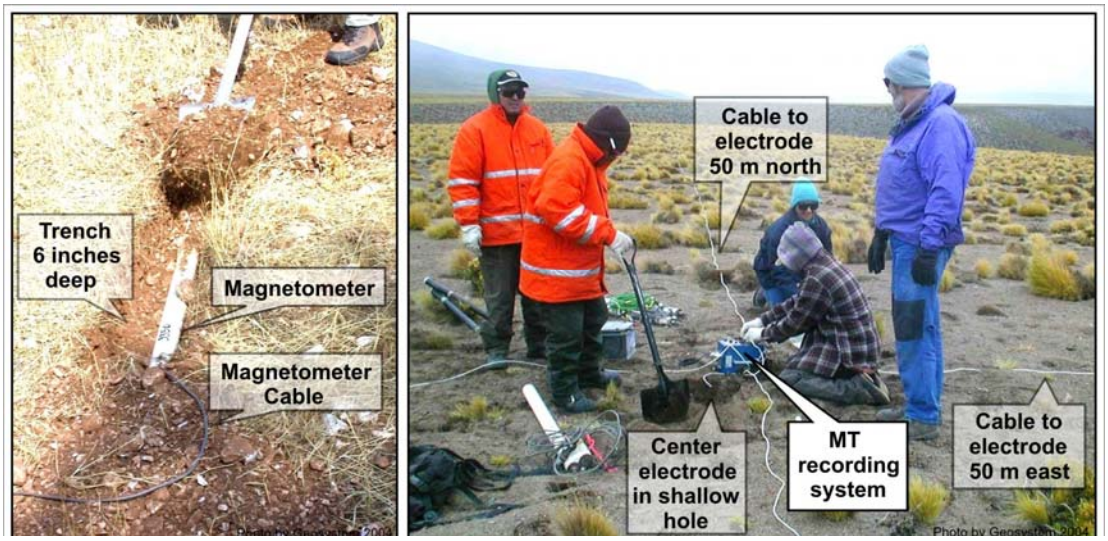

Photo Credit: Geosystem

To avoid wind vibration and resulting noise, the two horizontal magnetometers are usually buried in two 1.2 m (48 inch) long, 0.15 m (6 inch) deep trenches and the vertical magnetometer is partially buried in a 0.6 m (24 inch) deep hole dug with a post-hole digger. A plastic pail is placed over the protruding vertical coil to shield it from the wind.

The recording system is then connected to the electrode wires and the magnetometer signal cables and data acquired. The system may be left out overnight unattended to collect 14 hours of data. Shallower data can be recorded in less than an hour. Depending on variations in the subsurface resistivity, the spacing between MT stations may vary from several kilometers (miles) to a hundred meters (few hundred feet).

2.4.1.2 Survey Operation

Survey operations are conducted by two or three independent crews, each consisting of two to five workers. They usually use only one vehicle per crew unless safe operation requires more. If the station site is not accessible by vehicle, the equipment can be easily carried to the site by three to five people using backpacks. The number of stations recorded by each crew varies depending on access and the depth of investigation required. It takes 20 to 60 minutes to lay out a station, 1 to 14 hours to acquire the data, and 30 minutes to pick up the station and move on. Each crew carries 1 to 3 recording systems and can record 2 to 6 MT soundings per day, depending on access and recording duration. For recordings of 14 hours duration, the equipment is usually left running overnight at the station, to be picked up the next morning.

2.4.1.3Telluric Station Option

In areas where restrictions are placed on the minimal soil disturbance caused by the emplacement of MT coils and electrodes or where burying coils is impractical, as seemed to be a possibility on the glass flows at Glass Mountain, an alternative method called T-MT can be used. In this method, telluric-only stations (the T part of the T-MT acronym) are recorded at the

same time as two or more standard MT stations are recorded within 15 km (10 miles) of the telluric stations.

Telluric stations in this context are MT stations without magnetic field measurements. They are acquired by carrying an MT recorder to the station location and connecting it using four wires 50 m (150 feet) long to five small porous electrodes. In areas where digging is impractical or impossible, the porous electrodes are placed on the surface of the ground in contact with the underlying soil or rock. A quart of water may be poured on the ground to improve the electrode contact. If the electrode is placed on a hard surface like the volcanic lavas of Glass Mountain, wet clean clay would be patted onto the surface in a layer less than 0.1 m (4 inches) wide and 0.025 m (1 inch) thick and the electrode would be placed on that. The two to four person crew would leave the recorder to acquire data by itself for 1 to 12 hours and would then return to pick up the equipment. Any clay that was used would be removed after the measurement was completed for re-use at other stations. Acquiring a telluric station typically leaves no disturbance more significant than would occur if a "Leave No Trace" hiker walked through the area. If the resistivity variations are smooth and have few shallow vertical conductive zones, as is typical of geothermal prospects, there would be no loss of resolution from collecting telluric stations instead of MT stations.

Although using telluric stations with electrodes installed on the ground surface has a higher risk of collecting incomplete or noisy data, in cases where even minimal disturbance of the soil is of concern, it can be an effective option. Because variable sources of noise like wind have greater effect on surface electrodes, the surface installations are most effective when used as part of a larger conventional survey, so that the data can be acquired on the least windy days.

2.4.1.4 MT Environmental Impact

In the Medicine Lake area, more than two hundred MT soundings were acquired by geothermal operators and academic groups in the 1980's. These surveys left no permanent impact on the environment. Transient impacts may include vehicle traffic, foot traffic, and the easily restored minor soil disturbance caused by installing the electrodes and magnetometers. Sealed batteries are used so the survey has no generator noise. Safety concerns are minimal. The detection wires are measuring natural currents and so have no live current in them except in the very rare event of a direct lightning strike.

2.4.2 TDEM Field Procedures and Environmental Impact

For both transmission and detection of signals, the time domain electromagnetic (TDEM or TEM) method relies on electromagnetic induction between an ungrounded wire loop and the earth. Because it requires no electrical contact with the earth, it is not subject to the *static* distortion that can affect any method that measures the resistivity of the earth using electrodes. The most common TDEM approach is to send a steady current into a large wire loop laid out on the ground to generate a vertical magnetic field and then suddenly switch off the current, inducing decaying "smoke rings" of current in the earth as the magnetic field decays. The decaying vertical magnetic field generates a voltage in a detection coil in the center of the loop that is recorded. The voltage decay in the detector depends on the resistivity pattern of the

underlying rocks. An apparent resistivity versus recording time is directly calculated from the voltage versus time and this is later inverted to a true resistivity versus depth. Because the practical depth of investigation of TDEM is lower than of MT, the TDEM interpretation in Figure 6 shows only the top of the yellow conductor resolved.

Figure 6: TDEM Central Loop Field Layout, Data Recording and Resistivity Model

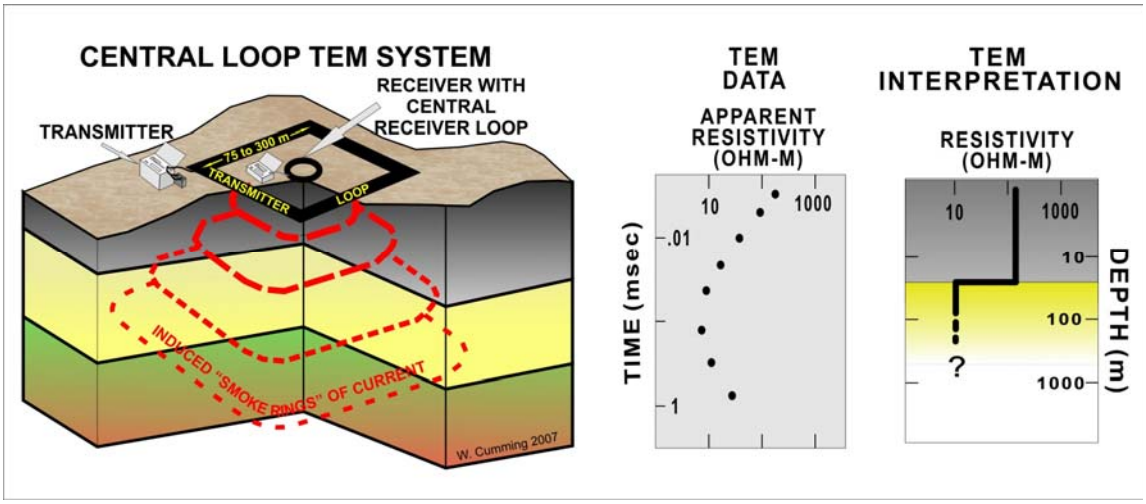

The geothermal applications of TDEM are mapping the shallow geometry of the clay cap without dimensional distortion and correcting MT statics. For both of these applications, a central loop TDEM geometry has significant advantages over non-symmetrical TDEM geometries such as moving the detector outside the transmitter large loop.

2.4.2.1 Field Procedures

TDEM survey operations are conducted by a crew of two to five workers, usually using only one vehicle. If the station site is not accessible by vehicle, TDEM equipment can be easily carried using backpacks. Depending on the size of loop used, it takes 15 minutes to several hours to lay out a station, 5 to 20 minutes to acquire the data, and 10 to 30 minutes to pick up the station and move on. Therefore, from 1 to 9 TDEM soundings per day can be acquired by a single crew, depending on loop size, with a 1000 m (1000 ft) diameter loop taking a full day or more and a 50 m (150 ft) diameter loop taking less than an hour. A large loop requires a large generator that usually cannot be moved far from road access.

Depending on expected variations in the subsurface resistivity and the objectives of the survey, the TDEM loops may be laid out as individual stations separated by up to several km, along continuous profile lines where the edge of one station coincides with an edge of an adjacent station, or at locations collated with an MT station. The TDEM soundings released by Calpine in support of this project include both several hundred distributed stations using 300 m (1000 ft) loops and over 100 stations in profiles in which 300 m (1000 ft) diameter loops are spaced at 300 m (1000 ft) intervals so that one loop shares a common side with an adjacent loop. The budget submitted to the CEC for the TDEM survey conducted as part of this project includes

supplementing the existing TDEM data with 40 more stations at 40 of the new MT stations for which static control from nearby existing TDEM stations might not be available.

Figure 7: Sirotem TDEM Receiver/Transmitter and Crew

Photo Credit: Geosystem

The transmitter/receiver setup is shown at left and the operator with the field crew logging a measurement is shown at right. When using a TDEM system in a forested area, as in the photographs, the transmitter wire is laid as close to the ground as possible, making it difficult to see amongst the vegetation. The minimal impact of this method, similar to a few leave-no-trace hikers walking through an area, is important to permitting such surveys.

In the case of a Sirotem TDEM system like that used in the 2005 GSY-USA survey at Glass Mountain, the TDEM survey equipment consists of a wire loop antenna, a transmitter/receiver unit and a sealed battery. The loop antenna is a single strand of insulated wire laid out in a square about 100 m (300 ft) on a side. The briefcase-sized transmitter/receiver box is connected at one corner of the loop and energizes the wire with a current from a sealed battery. The same loop is typically used to both transmit and then detect the signal response. The loop is normally laid out and retrieved by walking along its sides and paying out or re-coiling the wire by hand.

The Geonics EM37 system used by earlier TDEM surveys at Glass Mountain has a larger but still portable receiver/transmitter, a small gasoline generator to power the transmitter, and an auxiliary receiver coil that is hand carried to the center of the loop. With this system, a much larger loop with diameter over 300 m (1000 ft) is typically used in geothermal exploration. The system can still be made portable for a dedicated TDEM crew, but it is more difficult to include in a typical MT crew's equipment than is the much lighter-weight Sirotem system.

2.4.2.2 TDEM environmental Impact

The most prominent transient impacts of a TDEM survey are on-road vehicle traffic and hiking around the station location. For the larger loops that require a generator, there are a few minutes of local noise less intrusive than a snowmobile engine. Safety concerns are minimal. Because the TDEM transmitter loop is insulated, ungrounded, and the loop voltage and amperage is low in the types of portable TDEM systems used for this application, there is no electrocution hazard. Fire hazard is minimal, mainly related to a motor generator if one is used. In any case the risk is much lower than typical vehicle and small engine use in forested areas because it is run for short periods while stationary in a controlled location. The most significant public concern for TDEM surveys is usually the remote possibility of damage to vehicles getting tangled in the transmitter wire. For this reason loops are not laid across roads.

Earlier TDEM surveys collected at Glass Mountain using Geonics EM-37 systems in the 1980's and a Geonics Protem system in 2002, all with generators and 300 m (1000 ft) loops, had no significant impact on the environment. Sirotem systems have no generator and so can reduce the already minimal noise impact of the surveys. The impact of a TDEM survey done in support of an MT survey can be virtually eliminated if a Sirotem system is used and the TDEM data is acquired by the MT crew at the same time the MT station is set up.

2.5 MT Resolution of Geothermal Conceptual Targets

Some investigators are skeptical regarding the ability of the MT method to independently resolve both the resistivity of a geothermal clay cap and the depth to its base. The skepticism is rooted in observations like that of Simpson and Bahr (2005) who point out that MT can resolve the conductance (thickness divided by resistivity) of a buried low resistivity layer but not the resistivity and thickness independently. However, Simpson and Bahr (2005) go on to clarify that this is applicable to relatively thin zones with abrupt boundaries that lie beneath rocks that have similar or greater conductance to the surface. A geothermal clay cap typically has 10 to 100 times the conductance of the overlying unaltered rocks, it is usually of comparable thickness, and its base tends to be a smooth transition rather than an abrupt boundary. Widespread experience at geothermal fields (Anderson et al. 2000, Cumming et al. 2000) demonstrates that, in such conditions, the resistivity of a geothermal clay cap and the depth to its base can usually be independently determined well enough to characterize the geometry of the top of a geothermal reservoir. Moreover, this study and that of Uchida (2005) suggest that 3D inversion can probably characterize large scale smooth variations of resistivity within a geothermal reservoir itself.

Some parts of a permeable geothermal reservoir may be too thin and/or too deep to be resolved by MT as a relatively resistive zone below a low resistivity clay cap. In the right hand <200°C (392°F) model in Figure 3, the 150°C (300°F) outflow is covered by a clay cap less than 250 m (800 ft) thick, whereas the underlying reservoir is 600 m (2000 ft) thick. Where the smectite clay zone extends beneath the reservoir outflow, the outflow would be easily imaged by MT as a resistive zone between two conductors. However, if the outflow was much thinner, perhaps 30 m (100 ft), and was sandwiched between a 500 m (1600 ft) thick clay cap and an underlying low

resistivity smectite zone, then it would probably not be resolved using MT. Such thin, deep reservoir zones are probably not developable but they are important to understanding the geometry and chemistry of hot springs and fumaroles.

CHAPTER 3:
Data Recovery and Acquisition

3.1 Legacy Data

To support this project, Calpine released data from 105 MT stations, more than 200 TDEM stations and petrography data from all the Glass Mountain wells and TGHs.

When preparing for the release of data, numerous geophysical data sets were discovered in Calpine's data storage systems that were not included in the project proposal. These included older MT and TDEM data, other types of resistivity data and gravity data. Calpine agreed to the release of these data in support of this project, although it was unclear without more detailed analyses what its relevance would be. During the course of this project all of these data were compiled and reviewed. However, the additional MT data proved to be noisy, incomplete or located outside the area of interest and, therefore, were not included in the final analysis. On the other hand, much of the additional TDEM and gravity data were integrated into the interpretation. In any case, all of the data are included with the released materials.

All of the Calpine data reports released in support of this project were scanned to digital PDF files to facilitate the analysis and to provide a means for publicly distributing the data in a standard format. These files are listed as Attachments I through XXII. The complete released data set includes more than 4000 report pages.

3.1.1 Legacy MT Data Sets

Besides the 105 legacy MT stations that were included in the original proposal for this project, Calpine also released several other MT data sets summarized in Table 1. The Geonomics (1975) MT data are of such low quality that, besides the review completed to reach this conclusion, they were not otherwise used in this study. Very little background information is available on the MT surveys reported in Waff (1984) and Waff (1985) and, because of the low resolution of the station locations, the high levels of noise and the limited depth of investigation, this data could not be effectively integrated in the resistivity imaging conducted in this study, although it might have some application to regional exploration near the Glass Mountain KGRA.

MT acquired to resolve the overall structure of the base of the smectite clay zone capping geothermal resources like the Glass Mountain resource are typically specified to be recorded with a remote reference, that is, with at least two stations recorded at the same time so that each can use recordings from the other station to evaluate and exclude noise. The Geonomics data did not include a remote reference. It is not clear whether the Waff (1984 and 1985) data included a remote reference but the data looks like it did not, or at least did not use it effectively. The other MT data listed in Table 1 were all recorded with a remote reference.

Table 1: TMT Data Sets and Station Label Formats

Contractor	Year	Client	Contractor Station Label Format	Unocal Station Label Format	This Report Station Label Format	Stations In Data Release	Stations Used For Maps In This Report
Geonomics	1975	Union	nn			38	0
Woodward-Clyde	1981	Union	WCnn	WCnn	Wnn	22	22
CGG	1982	Unocal	Ann	Cnn	Cnn	17	17
Waff	1985	CalEnergy	Name			26	0
Waff	1986	CalEnergy	SHASTnn			53	0
Phoenix	1986	Unocal	Pnn	Pnn	Pnn	17	17
Phoenix	1988	Unocal	Pnn	nn	nn	49	49
GSYUSA	2005	CEC/Calpine	n-nnn, b-nnn		n-nnn, b-nnn	91	91

Although the basic analyses of the released MT data could be completed by digitizing the MT parameter plots in the attachments to this report, the data could be more easily and thoroughly analyzed if it were available in the standard electronic digital interchange (EDI) format for MT specified by the Society of Exploration Geophysics (Wight, 1991). Of the MT stations identified for release by Calpine in the original proposal, 88 had digital data available in a Unocal Corporation proprietary format that included the information required to generate standard EDI files. Part of this project included paying an independent contractor, Ken Peskett, who had helped Unocal develop processing applications for its proprietary MT format, to translate the proprietary format to EDI format. Of the 105 legacy MT stations included in the analysis, 17 recorded by Companie Générale de Géophysique (CGG) were in an idiosyncratic format that could not be translated directly to EDI MT impedances. These CGG stations were integrated into the analysis by digitizing the paper plots into standard text files containing MT parameters. The standard EDI and tabular text data were imported into the WinGlink® Geosystem geophysical software system and validated using comparisons to plots in the original contractors' reports in the attachments to this report. Although no MT field time series recordings are included in the data release, to promote further use of this data set in 3D MT imaging software development, both the original data plots in the Attachments and the MT EDI files and test tables were included in the released data sets.

Comments on all of the MT stations are tabulated in Appendix A, including any limitations of each station and its final status in the 3D inversion. This table provides general quality

comments on all MT stations that a non-expert could use to check the reliability of a resistivity image near a specific station. However, Appendix A also contains specific details about data characteristics and processing options that will usually be fully appreciated only by those familiar with MT interpretation techniques.

To be effective in resolving the base of a clay cap of a geothermal reservoir, the minimum range of MT frequencies required is typically specified to be 0.01 to 100 Hz, although this varies depending on the geological environment. For example, 1 to 1000 Hz data might be higher priority in generally high resistivity areas such as granite terrain, or 0.01 to 10 Hz might be given greater emphasis in very low resistivity areas like the sediments of the Salton Trough. At Glass Mountain, the important data range to resolve the base of the clay cap is typically 0.1 to 100 Hz and all of the released Calpine MT data nominally meets this requirement. However, data quality varies and the reliability with which specific stations constrain the base of the low resistivity clay cap is noted in the detailed station summaries tabulated in Appendix A.

Figure 8: MT Station Locations for the Surveys Listed in Table 1 and Analyzed in this Study

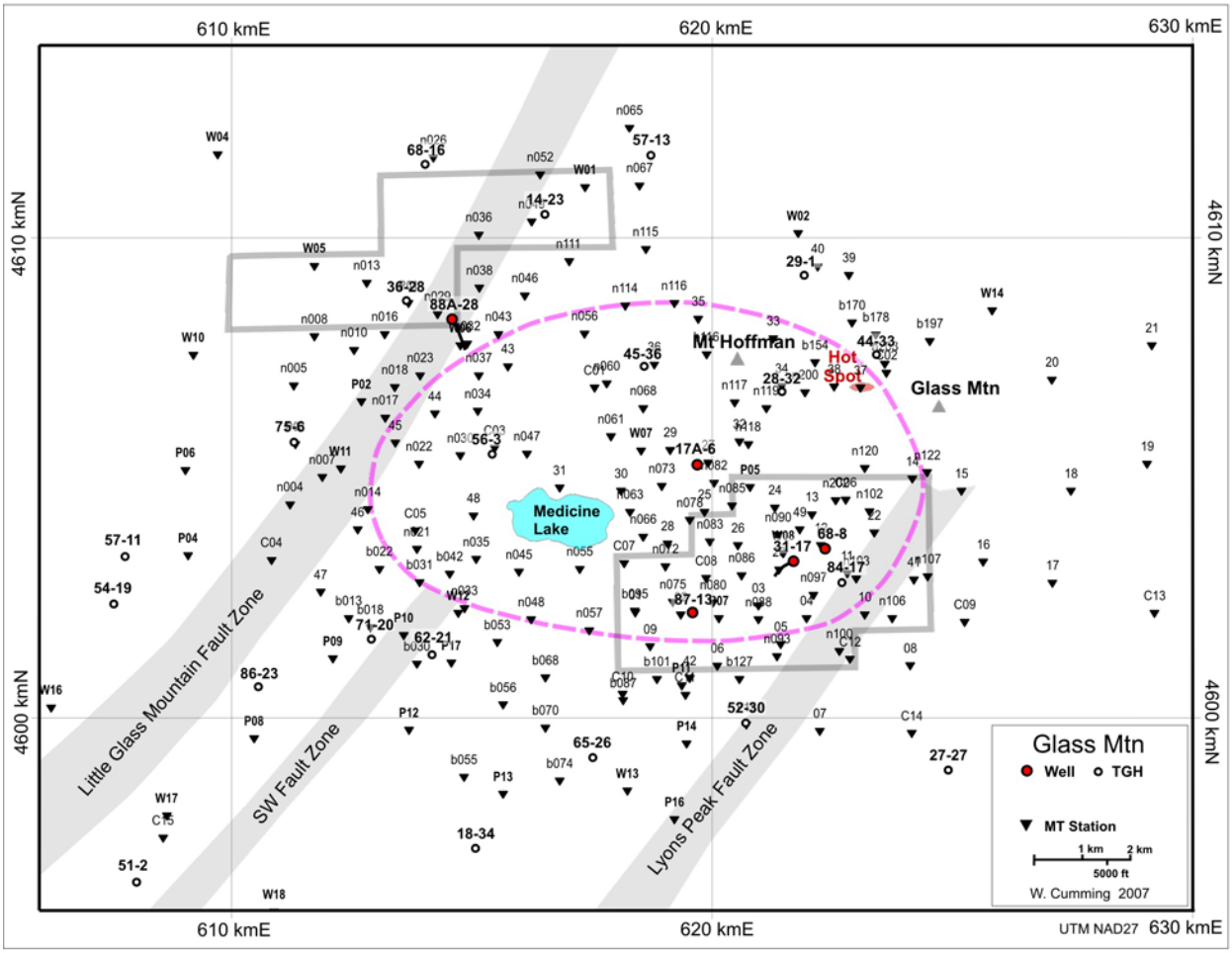

The MT station map in Figure 8 illustrates the layout of the legacy stations, labeled according to the key in Table 1.Also included in the map are the MT stations collected in 2005 as part of this project to fill in the legacy coverage. Gaps in coverage are mainly related to access issues. For example, the gap east of Glass Mountain is caused by poor access on the rhyolite lava flow visible in Figure 1. Seven Woodward-Clyde stations are located west and southwest of this map and two CGG stations are located to the southeast but, because they extend the properties of stations on the edge of the map that are less prospective, these stations are not shown on individual maps. However, they are included in the processing data base and in the detailed processing descriptions in Appendix A.

3.1.1.1 Geonomics MT Data

The report by Geonomics (1975) included in the attachments to this report details an experimental MT survey acquired for Union Oil Company. The data were not acquired using remote reference recording or processing and, as a result, the data quality is very low. Comparisons of Geonomics data to MT stations recorded in the 1980's and in 2005 using remote reference methods show that the Geonomics MT data is more likely to be misleading than helpful in understanding the resistivity structure at Glass Mountain.

3.1.1.2 Woodward-Clyde MT Data

Information on the 22 MT stations acquired for Union Oil Company in 1981 (Woodward-Clyde Consultants 1981) are provided in voluminous detail in the attachments. These were the most advanced MT data being collected in the early 1980's, with cryogenic magnetometers used to produce good quality results at most stations. The Woodward-Clyde system frequency range of 0.002 to 50 Hz did not go as high as is typical of more modern surveys, making correlation with TDEM sometimes more difficult. Noisier data were obtained for particular frequency bands at some stations where the natural signal was weak (W03, W04, W07, W08), wind in high trees created low frequency magnetic noise (W13, W18), or shorter than planned recording times impacted low frequency data quality (W09, W15). Descriptions of the contribution of each Woodward-Clyde station to the results of this study are tabulated in Appendix A.

3.1.1.3 Phoenix Geoscience MT Data

Phoenix Geoscience collected two MT surveys in the Glass Mountain area for Unocal Corporation (Phoenix Geoscience 1986 and 1989). Although these data were of reasonable quality, some stations in both surveys were heavily edited for the 3D inversion. Lightning was the most serious noise problem, significantly reducing the data quality at several stations. Poor quality data near 60 Hz was attributed to noise from AC transmission lines running through the Tule Lake area about 30 km (19 miles) to the east. Logging activity affected a few stations. Low frequency E-field noise was noticed but was not attributed to any source, although it may be due to interference from the HVDC power line located near the California-Nevada border 120 km (75 miles) to the east. Details of which stations are affected by noise and what this implies for their contribution to the MT imaging are tabulated in Appendix A.

3.1.1.4 CGG MT Data

The 17 stations acquired for Union Oil Company of California by CGG in 1982 (CGG, 1982) were recorded in an idiosyncratic digital format that could not be translated to standard EDI format files. Therefore, the scanned parameter plots were digitized by hand into a tab-delimited text file (readable in Word) containing the standard xy and yx modes of apparent resistivity, phase and rotation. Four columns of phase data are included in these tables; two for xy and yx are consistent with the non-standard CGG definition of MT phase and another two are consistent with the conventional definition of MT phase. A separate file with the data in a tab-delimited text format table was prepared describing each CGG station recorded at Glass Mountain.

Because most of the CGG stations are on the periphery of the survey area, they were mainly used to constrain the outer edges of models and maps. The initial analysis of the CGG data indicated that several of the stations like C01, C02, C05, C06 and C10 were located in important parts of the model and so new stations were added near them in the 2005 survey. The new data made the nearby CGG stations redundant and they were excluded from the 3D inversion. Because the CGG data was partly duplicated and partly peripheral, it was given less weight than the other digital data but all of the CGG stations were integrated into the interpretation as detailed in Appendix A.

3.1.1.5 Waff MT Data

Little background information is available on the 79 stations of the MT surveys reported in Waff (1984) and Waff (1985). These data sets were recorded for CalEnergy, Inc. by a geophysical group associated with Professor Harve Waff of the University of Oregon, Eugene. Because the data were recorded using custom equipment and software that was apparently evolving as the survey progressed, assessing the reliability is difficult. The most serious problem is that no station location map was found for these data and the station reports themselves give locations accurate only to the Section, Township and Range, providing about 1500 m (5000') resolution. Therefore, even if the data were high quality, the stations could not be reliably integrated into the 3D MT imaging data set. However, most of the stations in both of the Waff surveys are very noisy, with very little reliable data at frequencies lower than 1 Hz, and so they do not reliably resolve the base of the clay cap. The high frequency data from the Waff MT stations outside the area of coverage of the other MT and TDEM surveys might provide a thematic guide to shallow resistivity that could be used to plan regional resistivity surveys.

3.1.2 Legacy TDEM Data Sets

Calpine proved to have much more TDEM data in its files than the 200 stations estimated in the original proposal for this Energy Commission project. Over 400 TDEM soundings acquired in the Glass Mountain area between 1981 and 2002 are included in the data sets released by Calpine. With the 91 stations collected in 2005, TDEM is by far the most intensively used geophysical technique at Glass Mountain. The operators favored TDEM because experiments with vertical electrical sounding (VES), out-of-loop TDEM and other resistivity methods were disappointing. MT was initially unreliable and then seemed less cost-effective because of its higher cost per station. Among the geothermal exploration companies involved in Glass

Mountain KGRA exploration, only Unocal had in-house MT imaging and interpretation technology in the 1980's that could effectively map the base of the low resistivity clay cap over the reservoir. Therefore, mapping the top of the clay cap using TDEM became the default geophysical strategy of the geothermal developers at the Glass Mountain KGRA.

A total of 348 stations were included in the data base used to generate Figure 9. Table 2 summarizes the TDEM station labels used in the contractor reports, the station label format of the Unocal compilation maps used to generate coordinates for most of the stations, and the station label format used in this report. Besides the USGS, three contractors, ElectroMagnetic Surveys, Inc. (EMS), Earth Technology Corporation (ET) and Quantech Consulting, Inc. collected the legacy TDEM data.

Table 2: TDEM Data Sets and Station Label Formats

Contractor	Year	Client	Contractor Station Label Format	Unocal Station Label Format	This Report Station Label Format	Stations In Data Release	Stations used for maps in this report
EMS	1982	Occidental	n-z1	OPn	OPn	3	3
EMS	1982	Occidental	Rxnn			51	0
EMS	1983	Union	nnn	nnn	nnn	102	56
USGS	1983	USGS	nn	Unn	Unn	20	20
EMS	1985a	Unocal	GMnn	Snn	Snn	25	25
EMS	1985b	Occidental	MLnn			76	0
EMS	1985c	Santa Fe	Rnn, DRnn	Rnn, ORnn	Rnn, ORnn	36	36
ET	1985	Unocal	n-nn	n-nn	n-nn	109	109
ET	1986	Unocal	nn	Mnn	Mnn	61	61
Quantech	2002	Calpine	Txnn		Txnn	38	38
GSYUSA	2005	CEC/ Calpine	n-nnn, b-nnn		n-nnn, b-nnn	91	91

All of the legacy TDEM data used in this report were recorded using similar equipment. The TDEM data from the 1980's were recorded using Geonics EM37 systems, 300 m diameter transmitter loops and the largest Geonics central detection coils available. The 2002 survey by Quantech Consulting, Inc. used very similar equipment, with the Geonics Protem receiver replacing the EM37. This equipment was and probably still is a reasonable compromise between portability and depth of investigation using a TDEM system for geothermal exploration at the Glass Mountain KGRA.

The EMS, ET and USGS TDEM data are tabulated in the reports included in the attachments as layered inversions of depth and resistivity and as "combined frequency" time series of both detector voltage and calculated apparent resistivity. To evaluate the layered resistivity inversions provided in the reports, time series for about 13 EMS, 23 ET, and 5 USGS TDEM stations were digitized by sight reading from paper plots because attempts to scan the reports and use Optical Character Recognition (OCR) software to recover the data resulted in too many visually small but numerically significant errors like misplaced decimal points. Because standards for recording TDEM data have changed since the 1980's, the data were re-inverted assuming that the best constrained earlier models were correct. This showed that the 1D resistivity models were consistent and comparisons between TDEM stations and MT data showed that, within the constraints of the TDEM method, the existing inversions seemed valid. This was consistent with inversion tests of digital data available for the 38 stations recorded by Quantech Consulting, Inc. using Geonics systems in 2002. Therefore, all of the 1D TDEM layered models from the original contractor reports included in the attachments to this report were digitized, entered into the data base and used as the primary TDEM data for this study.

Figure 9:Station Locations for Legacy TDEM Surveys Recorded from 1982 - 2002 Listed in Table 2

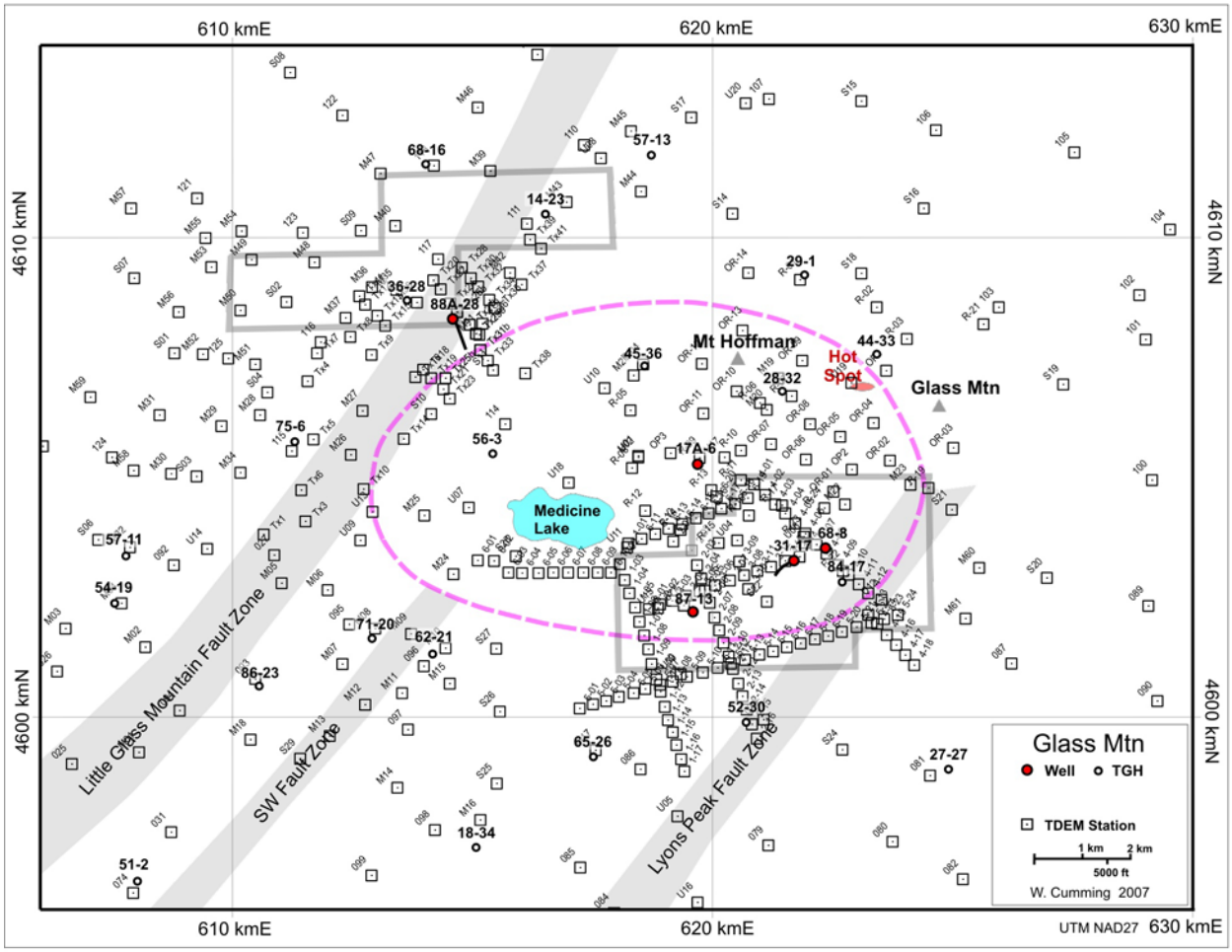

3.1.2.1 Electromagnetic Surveys TDEM Data

Five TDEM data sets collected by ElectroMagnetic Surveys, Inc. were released by Calpine. All of these data were collected using Geonics EM37 systems running at 3 and 30 Hz using 300 m (1000 ft) diameter transmitter loops and receiver coils with 100 m^2 and 1700^2 m effective areas.

A 51 station out-of-loop TDEM experiment conducted in 1982 for Occidental Geothermal, Inc. was reported as being relatively unsuccessful and the data was never successfully inverted to make a reliable image of resistivity. The contractor's report recommended that further surveys use an in-loop approach instead (ElectroMagnetic Surveys, Inc. 1982). Three conventional in-loop soundings were completed and were included in this study as layered model data based on a re-analyses done for Santa Fe Geothermal, Inc. in 1985 that is attached to the original report. All of the plots and results for both the out-of-loop and in-loop TDEM data are included in the attachments.

A 1983 survey for Union Oil Company (ElectroMagnetic Surveys, 1983b) included 146 recorded stations but 44 stations were excluded from the copy of the report received by Calpine because they were in areas not covered by the Calpine asset purchase from Union Oil Company. Of the 102 stations in the report, 56 were located in the study area and so the TDEM models were entered into the data base. The 46 stations not included in this analysis may of interest for regional geothermal exploration.

In 1985, a 25 station survey following up the 1983 survey for Union Oil Company was collected at scattered locations around the Medicine Lake Volcano outside the Telephone Flat area (ElectroMagnetic Surveys, Inc. 1985a). Models for all these data are included in the analysis.

A 76 station TDEM survey conducted for Occidental Geothermal, Inc. in 1985 (ElectroMagnetic Surveys, Inc. 1985b) was not included in the analysis because the station location map was not found. Because a map for a 1982 out-of-loop TDEM survey for Occidental Geothermal had a similar number of stations and a compendium map of TDEM stations prepared by Unocal included a category for Occidental TDEM data, the initial assessment concluded that locations were available for this survey. However, subsequent reviews of the released data and Calpine's file system did not uncover locations for these stations. Therefore, the data were included in the attachments but were not integrated into the analysis.

A 36 station TDEM survey was collected for Santa Fe Geothermal, Inc., mainly northeast of Telephone Flat near the Glass Mountain rhyolite flow (ElectroMagnetic Surveys, Inc. 1985c). A total of 37 locations were occupied but one station was unusable. All 36 of the usable stations are included in the analysis data base.

3.1.2.2 Earth Technologies TDEM Data

The data for two large TDEM surveys were collected by Earth Technology Corporation for Unocal Corporation and are included in the attachments and the analysis data base. A TDEM survey including 108 stations was recorded along six continuous profiles in the Telephone Flat area (Earth Technology Corporation 1985). Measurements were made at 3 and 30 Hz using a Geonics EM-37 TDEM system with 300 m (1000 ft) diameter loops and receiver coils with 100 m^2

and 1000^2 m effective areas. This was followed up by a survey of 61 stations scattered throughout the Medicine Lake Highland, with the majority located around the Telephone Flat area. Resistivity models for all of these stations were included in the analysis data base.

3.1.2.3 USGS TDEM Data

A USGS TDEM data set acquired on the Medicine Lake Volcano was initially reported in a series of USGS Open File Reports (Anderson et al. 1983a, b and c) but the results used for this study were those from the follow-up USGS study reported by Anderson (1988). The standard 1D model inversions are consistent with the results produced in the contract studies by Earth Technology Corporation and ElectroMagnetic Surveys, Inc.

3.1.2.4Quantech Consulting TDEM data

To support targeting of the 88A-28 well at Fourmile Hill, in 2002,Calpine contracted a 38 station TDEM survey to cover likely target areas near the Fourmile Hill block (Quantech Consulting Inc., 2002). This is available as digital data in the native format of the Geonics Protem acquisition system (RAW files), as digital TEX files in the format used by the TEMIX program used to compute the 1D models, and as plots and tables similar to those available for the other legacy data sets. The plots and tabulated data are included in the attachments.

The quality of the 2002 soundings is comparable to those recorded in the 1980's. All of these TDEM surveys used almost identical 300 m (1000 ft) transmitter loops. The Protem receiver used in 2002 is, in theory, more capable of suppressing noise by averaging data than the EM37 receivers used in the 1980's. On the other hand, the EM57 transmitter with 1.85 kw generator used in 2002 is less powerful than the EM37 generator-transmitter, and the current of 8.5 A was less than half what was typically used in the surveys in the 1980's. The Geonics 3D-3 surface coil used in 2002 was also less sensitive than the larger of the two sets of detector coils used in the 1980's. The earlier surveys apparently offset their less sophisticated digital recording capability by using a larger transmitter signal and a more sensitive detector. Therefore, the surveys using Geonics systems from the 1980's and from 2002 produced similar results; consequently, their 1D models were merged in the analysis data base.

3.1.3 Legacy VES Resistivity Soundings

Two vertical electrical sounding (VES) surveys acquired at Glass Mountain were evaluated for this interpretation. A nine station proprietary survey acquired for Occidental Geothermal, Inc. was released by Calpine (Electromagnetic Surveys Inc. 1983a). A fifty station survey acquired by the USGS in 1982 was integrated into this study based on the results reported in Zohdy and Bisdorf (1982). These data were evaluated both as resistivity soundings in their own right and as sources of ancillary information to correct MT statics.

Unfortunately, the analysis conducted for this study confirmed the conclusion of Zohdy and Bisdorf (1982) that compromises introduced to make the VES acquisition more efficient resulted in calculated resistivities that were unrealistically high. Of the VES stations, only one, D18, was consistent with the results of nearby MT and TDEM stations. The rest of the VES stations produced models with unrealistically high resistivity, often by more than an order of magnitude. Zohdy and Bisdorf (1982) noticed this problem and attributed it to running the VES

soundings along crooked roads. Although simple geometric corrections were done to allow the data to be modeled as if it was recorded along straight line, a more appropriate treatment would have required that the spatial pattern of the electric field be measured and inverted as a vector field. Because the initial results of the VES surveys were unusable except for very generally characterizing patterns of shallow resistivity, this technique was not pursued further at Glass Mountain in the 1980's and the existing data were not integrated into the interpretation beyond the initial evaluation.

3.1.4 Legacy Gravity Data

Besides the published survey of 74 USGS gravity stations reported in Finn and Spydell (1982), gravity data released by Calpine in a Wheeler (1985) compilation includes about 85 stations from a proprietary survey collected in 1984 for Occidental (BRW Geotechnical, Inc. 1984) and a proprietary 306 station gravity survey acquired in 1983 for Occidental (Summit Engineering Inc. 1983). The gravity compilation map by Wheeler (1985) may include data from a separate 373 station Unocal survey completed in 1985 for which the data listing is missing. A review of the Occidental station maps showed that all of the significant gravity features would be resolved by the data in the listings. However, the compiled gravity map by Wheeler (1985) uses a reasonable Bouguer reduction density of 2450 kg/m^3 and so is used directly in the interpretation of this study.

The initial Finn and Williams (1982) analysis of the gravity data is still valid in terms of the overall model geometry, and drilling did confirm the existence of the predicted shallow granite intrusion. However, comparisons of the gravity to resistivity and well data at different depth intervals suggest that, besides intrusions, indurated volcanic rocks in the high temperature propylitic alteration zone could be modeled as part of a high density body. Density variations within shallow volcanics may also contribute to the overall gravity pattern.

3.1.5 Legacy Well Data

As required in the project agreement, Calpine released sufficient well data to validate the resistivity interpretation, most importantly data from X-ray diffraction crystallography (XRD) and petrography analyses of core and cuttings from 24 temperature gradient wells and 5 exploration wells. An induction resistivity log data in well 17A-6 proved to be important. As agreed in their letter of support for the project, Calpine also provided sufficient abstracted temperature and deliverability data from the wells to validate the resistivity interpretation.

3.1.5.1 Well Petrography

The original proposal for this project included a subcontract for a geological consultant to compile the rock property data from the 24 TGHs and 5 wells and prepare a petrologic model to confirm the resistivity interpretation. One option to complete this task that was mentioned in the proposal was to employ a part-time consultant already working on Glass Mountain exploration issues for Calpine Corporation. However, at the time this part of the project was initiated, Calpine Corporation was not employing consulting geologists. Following the review and consent of the California Energy Commission, Dr. Joseph Moore of the Energy and Geoscience Institute (EGI) at the University of Utah was contracted by GSY-USA, Inc. to supply

these services, leveraging other work being conducted by EGI as part of a US Department of Energy funded project to improve the understanding of the relationship between fracture systems and permeability in the development of enhanced geothermal systems (Moore, 2006).

In preparation for this project and with the agreement of Calpine, in January 2005, the petrography data sets at Glass Mountain that had been collected and scanned for this project were sent to Dr. Moore at EGI. The collection of supporting documentation (Gunderson, 1991) includes original x-ray diffraction (XRD) and thin section petrography analyses of cores and cuttings from the University of Utah Research Institute (UURI), fluid inclusion analyses by James Reynolds, and core plug wet density and susceptibility data from well GMF 56-3 completed by Elliot Geophysical Co. The available information included more than 1000 thin section, 300 petrography, 500 XRD (bulk and clay), and 400 whole rock analyses. Moore also relied on the interpretation reports of Carrier (1987, 1989a and 1989b) who had focused on the most relevant Glass Mountain analyses from more than 370 bulk rock and 120 clay analyses.

The EGI group provided a spreadsheet compiling the information from the released analyses. They also conceptually combined the petrology data released as part of this project with core fracture analyses conducted as part of a separate DOE project to characterize fracture permeability in the Glass Mountain geothermal system (Clausen et al., 2006). The EGI analysis of permeability in geothermal systems based on the Glass Mountain rock properties data sets is an ongoing project that is expected to benefit from the 3D resistivity study reported here (Moore, 2006).

3.1.5.2 Wireline Induction Resistivity Log

CalEnergy, Inc. acquired a wire line induction resistivity log in well 17A-6. In order to more directly evaluate the performance of surface resistivity methods, the well log data set was reprocessed by Nordquist (1985) into a plot showing resistivity computed with a 100’ (30 m) moving average. This plot was released by Calpine and the data was digitized into an Excel spreadsheet that was used to support the analyses of this project.

3.1.5.3 General Well Data

Calpine released a variety of other well data to support the project including well locations and well courses. As Calpine agreed in its initial letter of support, some data sets were made available only in abstracted form; for example, natural-state isotherm plots, permeable entry locations, and general well productivity information were provided as interpreted cross-sections.

3.1.6 Legacy MT and TDEM Data Analysis

The legacy MT and TDEM data released by Calpine was initially analyzed with three objectives: 1) validate the import of the legacy MT and TDEM data into a modern analysis format; 2) provide test data for the 3D MT inversion software; and 3) analyze shortcomings in the earlier resistivity imaging and its implications for the new MT and TDEM surveys.

3.1.6.1 Data recovery quality assurance

Importing the legacy TDEM data involved the relatively straightforward task of entering the conventional resistivity models into a data base by hand. The principal control on the reliability of the data was consistency between neighboring TDEM stations and comparisons to MT. The comparisons to MT seemed to indicate some of the TDEM stations were probably biased to relatively high values, particularly TDEM stations that were acquired on a thick high resistivity zone over a relatively deep clay cap. That is, TDEM stations that were more resistive than others had their already high resistivity biased to even higher values. The processing notes dealing with the correlation of MT with TDEM has noted examples of this in Appendix A. This pattern of distortion was convenient in that it did not create misleading features in TDEM interpretation maps. However, it could have distorted MT statics estimates in areas where a clay cap was unusually deep. This tentative conclusion was to be confirmed by the new MT and TDEM survey.

The legacy MT data recovered in this study were recorded before format standards and, in some cases, before even parameter definition standards were widely accepted in the MT industry. Therefore, the analysis involved checking the internal consistency of the data as well as producing resistivity images of the subsurface. As detailed earlier, of the 105 legacy MT stations released by Calpine and incorporated into this study, 88 were translated to the standard MT EDI format and 17 were digitized as tab-delimited text files. Several iterations were required to resolve inconsistencies among the data sets. For example, the translation did not initially rotate the east-orientation of the Unocal MT format x-axis to the north-orientation of the EDI standard x-axis. The best indication that the final translation of the legacy MT data is consistent with modern standards is the consistency between the new and old MT data sets and between 3D MT resistivity images and the well data.

3.1.6.2 Preliminary Resistivity Imaging

Basic 1D and 2D MT processing and imaging and 3D resistivity visualization were completed using WinGlink® Geosystem, a geophysical processing and interpretation software system widely used for academic and industry MT and TDEM applications. The initial resistivity analysis based on the MT and TDEM was generally consistent with the earlier results and outlined the same prospective zones shown in Figure 2.

Figure 10: TDEM Conductance to 300 m (984 ft) Depth Using Legacy TDEM Stations

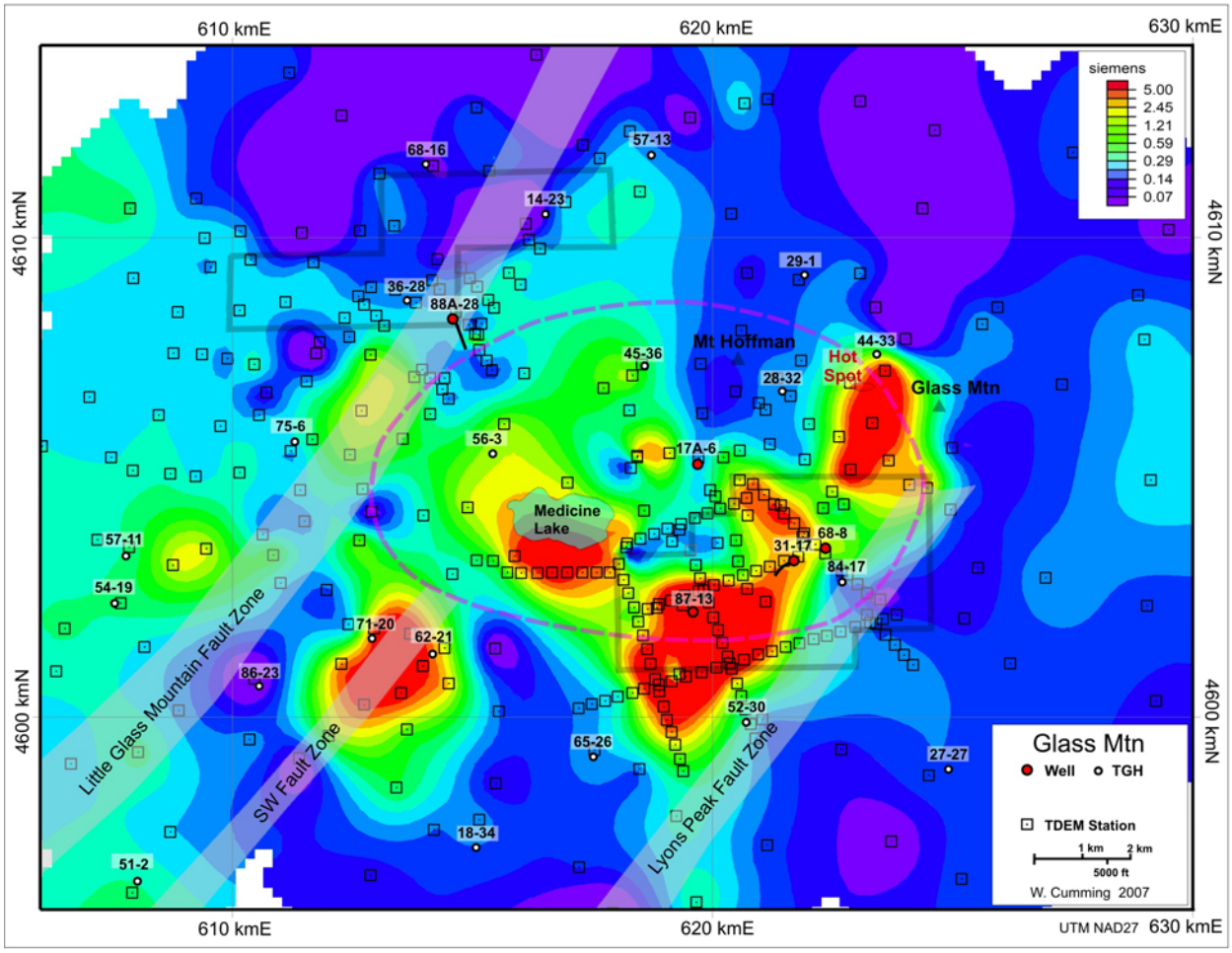

For example Figure 10 shows conductance to a depth of 300 m (984 ft) based on the legacy TDEM data. High conductance implies low resistivity over a particular depth interval. Therefore, the red and yellow shading highlights areas of particularly intense hydrothermal smectite alteration averaged from the surface to 300 m (984 ft) depth. Given the relatively large TDEM transmitter used with 300 m (984 ft) loops, it is likely that the resistivity inversions of the legacy TDEM data sets are reliable to a depth of 300 m (984 ft). Although these particular TDEM stations tended to estimate resistivity too high where no low resistivity zone was encountered, this would probably not create a misleading geothermal interpretation because it would just make a high resistivity zone slightly higher.

The alteration resolved in the map of TDEM conductance to 300 m (984 ft) depth in Figure 10 is very shallow relative to the expected reservoir depth. In higher elevation areas, where the water table is below 300 m depth, intense clay alteration above the water table may indicate boiling in the underlying reservoir. This would be consistent with the Lutz et al. (2003) interpretation of well 31-17.

Figure 11: TDEM Conductance to 600 m (1969 ft) Depth Using Legacy TDEM Stations

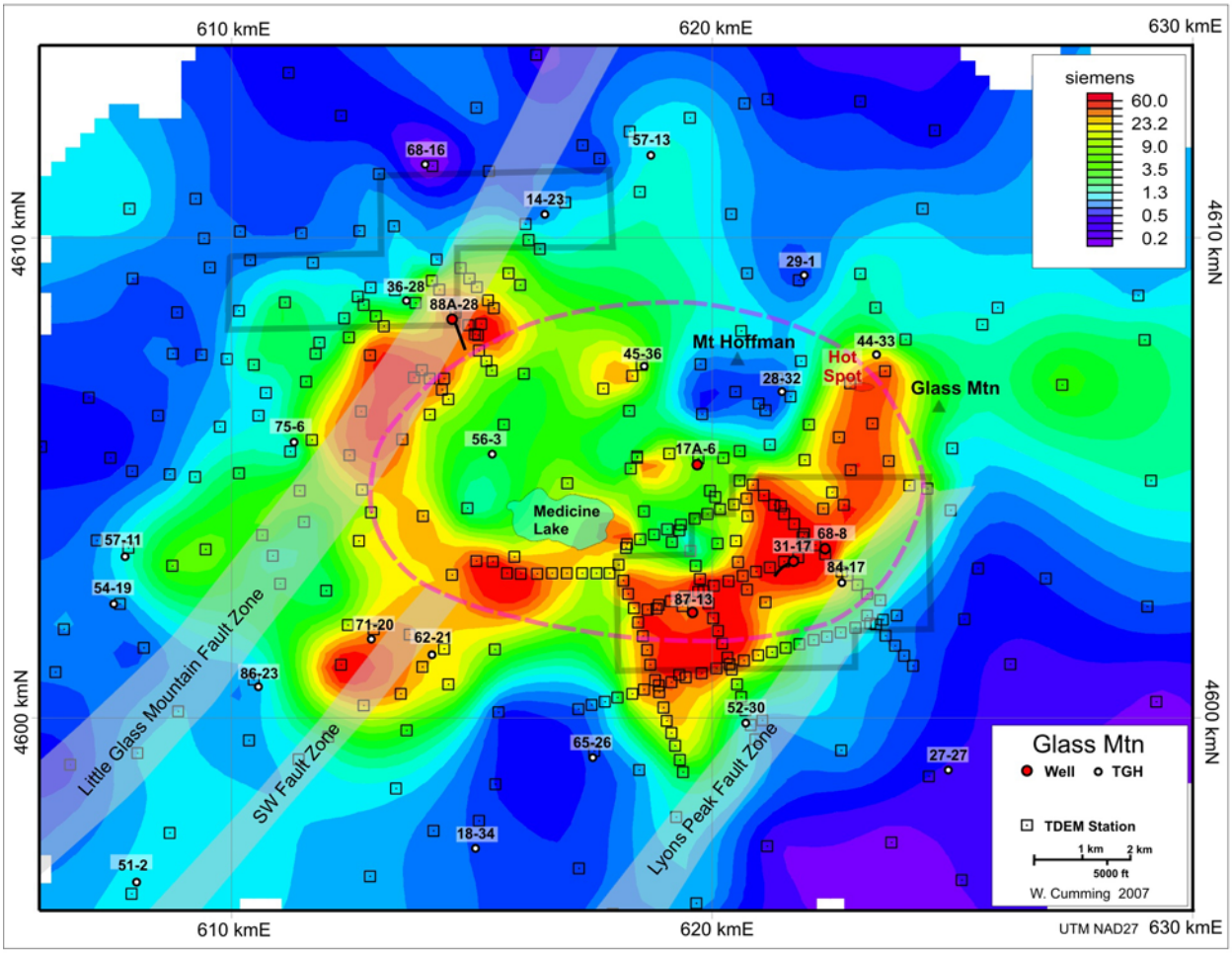

In the case of the exploration program for well 88A-28, the TDEM was stretched to resolve resistivity at depths exceeding 600 m (1969 ft) (Calpine-Siskiyou Geothermal Partners L.P. 2004). This produced results like the map of conductance to 600 m (1969 ft) depth in Figure 11. The area that was targeted southeast of the 88A-28 surface location looked much more prospective in Figure 11 than in Figure 10. Although a reasonable target, this pushed the TDEM to its limits of reliable resolution. Because such maps did not reliably show patterns of alteration intensity deeper than 300 m (984 ft) or illustrate how the 3D resistivity geometry of the base of the clay cap and upper reservoir constrained the geothermal conceptual model, they did not fully utilize the capability of resistivity methods, particularly MT, in reducing geothermal well targeting risk.

3.2 New MT and TDEM Data Acquisition

The project proposal included the acquisition of 50 standard MT stations, 40 reduced bandwidth MT stations and 40 TDEM stations. The proposal did not include a specific plan for the locations of these stations because this would depend on the results of well 88A-28 and the initial processing of the legacy data. In addition it was expected that some proposed locations would prove to be inaccessible because of difficult terrain or archeological sensitivity. Although the permitting process took over two years longer than expected, delaying the start of fieldwork well into the funding term of the grant, 91 new MT and TDEM stations were collected in October 2005.

3.2.1 Survey Location, Permitting and Design

The final surveyed station locations generally covered the same area as the project proposal but with differences in emphasis. The proposal assumed that the survey would primarily fill in gaps in the legacy MT coverage in the Fourmile Hill area, on Mt. Hoffman and in the Pumice Mine area near well 44-33. However, specific station locations would depend on the analysis of the 88A-28 well test and the initial review of the legacy data. In consultation with Calpine regarding the most likely drilling targets that might follow up the disappointing 88A-28 test, a set of 208 candidate MT station locations for 90 survey sites were prepared for permitting in April 2003. These reduced the earlier focus on Fourmile Hill and Mt. Hoffman and included more stations at Telephone Flat and in the southwest part of the volcanic rim. A large number of candidate sites were included in the permit application to provide flexibility.

3.2.1.1 Permitting

Getting regulatory permission to do the work was much more challenging than was initially expected based on earlier experience getting permits for similar surveys on geothermal leases managed by the Bureau of Land Management (BLM) or on land managed by the United States Department of Agriculture Forest Service (USFS). As recently as 2002, Calpine obtained permission to run a TDEM survey near Fourmile Hill in a few weeks. As noted in the descriptions of the methods, the survey impact was low and the locations flexible so permitting seemed straightforward. However, arranging permitting required an unexpectedly large investment in time by the participants in the project and delayed most of the project milestones.

Uncertainty regarding the standards for permitting survey activities on federally managed lands was the most serious survey issue. In particular, the standards for mitigating or addressing cultural issues on USFS-managed lands were unclear. After almost two years of effort, it seemed likely that a resolution of the permitting questions on lands managed by the USFS in the Glass Mountain KGRA would depend on resolving larger questions of public policy, a process likely to take much longer than the span of the project contract. Therefore, the survey was redesigned to avoid areas administered by the USFS and focus on 120 candidate station locations on Calpine lease blocks administered by the BLM. Because of the large number of candidate stations initially proposed, this restriction did not too seriously impact the survey coverage. Survey descriptions had already been developed for the USFS so these were further elaborated and provided to the BLM. On the basis of the descriptions, the BLM declared the

surveys to be a casual use activity consistent with the conditions of Calpine's geothermal leases. After the survey was completed, the BLM sent a notice indicating that no further work could be conducted under the existing letter approving the survey as casual use.

The conditions that the BLM specified for the survey at Glass Mountain to proceed as casual use were typical of those required in other BLM managed areas. At the time the survey commenced, the local office of the USFS was contacted to review whether any temporary restrictions in local areas were required, for example to avoid nesting birds. An archaeologist conducted a reconnaissance for historically or culturally important artifacts in advance of the crew. There were sufficient spare station locations to allow a move of any site that proved to be sensitive. Although no specific cultural resources were identified, two stations were moved 100 to 200 m (300 to 600 ft) to avoid areas with a higher probability of encountering cultural resources.

3.2.1.2 TDEM Survey Design

The permitting issues significantly affected the conduct of the TDEM survey. The project proposal specified that 40 TDEM stations would be recorded at new MT stations that were not near legacy TDEM stations. The initial permit application included the option of using a separate crew to collect the TDEM using a generator-powered transmitter. However, the final survey design further minimized the impact of the TDEM by having the MT crews collect the TDEM using noiseless battery-powered equipment at the same time that the MT station was acquired. Because a battery-powered Sirotem-3 system was carried by each MT crew for this purpose, a TDEM station was recorded at all 91 MT stations.

3.2.1.3MT Survey Design

The project proposal specified that 40 of the 90 MT stations be recorded as narrow-band or telluric-only recordings that would be quicker and less expensive to acquire. However, Calpine's change in focus to a larger area of coverage led to a station spacing of 500 to 2000 m, much farther apart than the 100 to 1500 m that was initially planned. In addition, the initial analysis of the legacy data showed that the desirable bandwidth extended to below 0.1 Hz, which could not be reliably recorded in less than several hours. As a result of the wider spacing and longer recording times, station moves could not occur fast enough to achieve a cost reduction using narrow-band or telluric-only stations. Therefore, all 91 MT stations in the 2005 survey were recorded as full-bandwidth, five-component MT stations.

3.2.2 MT and TDEM Field Survey

Following the completion of the scouting and the archeological review of station locations in late-September 2005, GSY-USA geophysical crews acquired 91 MT and TDEM stations during October 2005. The results of this survey are detailed in the survey field operations report (GSY-USA, Inc., 2005), a separate document designated as Appendix B to this report. Although the interpretation could be largely reconstituted from the parameter plots included in the operations report, the MT data have also been made available as standard MT EDI files (Wight, 1991) compatible with the files released for the legacy MT data. The TDEM data are available in the native format of the acquisition system and as text files with the extension TEM that include the edited time series data in a format readable in any word processor.

3.2.2.1 Changes to Station Locations During the Survey

In consultation with Calpine, the list of 120 permitted candidate locations was narrowed to 98 preferred locations, with field logistics dictating the final subset of recorded sites. As had been anticipated based on difficulties reported by previous surveyors, eight locations on the Glass Mountain rhyolite lava flow proved to have very dangerous access over blocky lava. Moreover, the large dry voids in the top of the lava flow made the MT electric field measurement problematic. Eight stations were dropped from the program and one was moved to location n200, as approved by the archeologist. Candidate site n102 was on a slope too steep for reliable MT measurement and so, with the approval of the archeologist in the field, the Party Chief moved it 600 m (1970') southeast. Unfortunately, that inadvertently duplicated a legacy station and left a gap in the coverage. An alternative location was recorded as station n202, after a review by the archeologist. Because both stations n102 and n202 were recorded, a total of 91 instead of the contracted 90 MT and TDEM stations were delivered. The average offset of the centers of the measured locations from the planned locations was 37 m, small for surveys in mountainous terrain like Glass Mountain. Except for the stations on Glass Mountain that were dropped, the moves did not have a significant effect on the survey coverage.

3.2.2.2 Data Set Characteristics

Because modern MT robust time series processing (Larsen et al. 1996) more effectively attenuates noise, the 2005 MT data were generally better quality than the legacy MT data sets. For example, trees waving in the wind disturbed earlier magnetic measurements from 0.1 to 1 Hz much more than for the 2005 survey, although this was still a serious issue on windy days. Similarly, local lightning, logging activity, traffic noise and 60 Hz noise from the major power transmission corridor 30 km (20 miles) to the east were better attenuated, although not always eliminated. Because the 2005 survey was a fill-in survey, the most serious noise problems were encountered at locations that had been avoided by the earlier surveys because conditions were known to be problematic, for example, on resistive rocks like lava flows that would have very high contact resistance. The Woodward-Clyde (1981) survey achieved reliability similar to the 2005 survey by occupying only the most promising sites near roads. The quality of the Phoenix Geosciences (1986 and 1989) and CGG (1982) MT surveys was poorer than that of the 2005 survey. Fewer than 10 percent of the 2005 MT stations were affected by noise in a manner that seriously impacted their resolution of the top of the reservoir.

Because the TDEM stations in 2005 were recorded using a battery-powered transmitter, data quality was expected to be troublesome in areas where the top of the conductive clay cap was too deep to detect using a small portable system. Apparently usable time series were recorded for all stations and most of the inversions produced models that conformed to the collocated MT. However, this proved to be misleading and many of the 2005 TDEM data were not used. However, because twice as many TDEM stations were recorded than were planned for this project and a much higher than expected number of legacy TDEM stations were released by Calpine, most MT stations had adequate TDEM constraints to correct static distortion.

3.3 MT and TDEM Interpretation Data Processing

Following the acquisition of new data in 2005, the interpretation data processing was repeated for the legacy data in the context of the complete data set. The field processing detailed in the operations reports for each survey produced MT apparent resistivity and phase plots like those shown in Figure 12. Interpretation processing took the results of the field processing shown in Figure 12 and turned them into cross-section and map images of subsurface.

The MT data recorded by GSY-USA, Inc. are compared to the legacy MT data in Figure 12, which shows apparent resistivity and phase spectra from representative stations near the Telephone Flat area, analogous to the plots shown in Figure 4. The first task in the interpretation processing is editing these curves to eliminate unusable data, leaving the gaps between points shown in Figure 12

As indicated by the plots in Figure 12, the Phoenix Geosciences (1986 and 1989) and CGG (1982) surveys presented the most challenges in editing and weighting data in the interpretation. The GSY-USA, Inc. (2005) data had two populations; one group of very easy to evaluate stations like n090 shown in Figure 12, and a few more problematic stations located in noise-prone areas. Because of the greater density of points and the generally high quality of the 2005 survey, data from this survey were emphasized in the inversion and imaging.

Figure 12: MT xy (Red) and yx (Blue) Data Recorded in 1981, 1982, 1989 and 2005

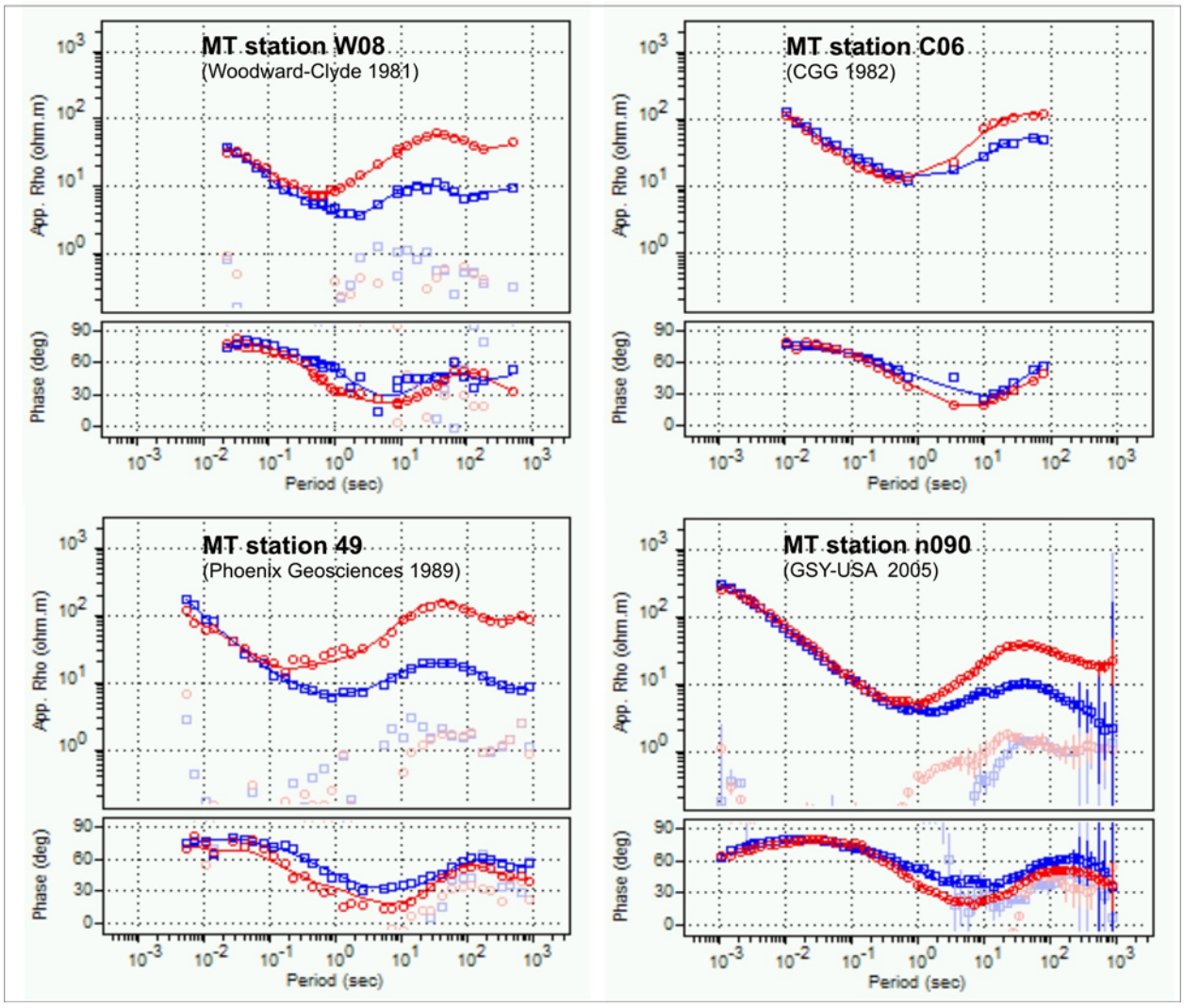

3.3.1 Initial Processing

The general progress of the MT and TDEM interpretation processing involved taking several passes at successively more aggressive editing to reduce the effect of noise on the resistivity imaging. The processing used the basic tools of the WinGlink® Geosystem processing software with some adjustments to address 3D MT inversion issues that are less routinely encountered. All of the digital MT data, including the 105 legacy stations and the 91 newly acquired stations, were reviewed using the following procedures.

The digital MT data were imported into WinGlink as standard EDI files, except for the CGG data which were imported as parameter tables. All of the legacy TDEM data were imported as 1D models except the Quantech (2002) data that were imported as both time series and models in the TEX format used by the contractor's TEMIX® Interpex software. The TDEM from the 2005 survey was imported as time series in the contractor's TEM format and, for a few stations, in the

native format of the recording systems. The impact of the TDEM results on the subsequent MT interpretation processing was summarized for each station in Appendix A.

As illustrated in Figures 4 and 12, the MT data were reviewed as apparent resistivity and phase plots of the two resistivity modes. The xy apparent resistivity in red in Figure 12 was calculated from the ratio of the electric field along the x-axis set of electrodes and the magnetic field along the y-axis magnetometer. The yx apparent resistivity in blue was calculated from the orthogonal set of axes. The curves in very light shades of red and blue were the xx and yy modes that would be zero if the MT responses were compatible with a 1D resistivity geometry, or a 2D geometry in this view of the data, making them useful measures of the validity of 1D or 2D assumptions.

3.3.1.1 Rotation to Geological Strike

The x- and y-axes could have been left in the orientation in which they were measured in the field but, for this analysis, the axes of the MT apparent resistivity and phase curves were mathematically rotated to orient the data with respect to the resistivity geometry of the underlying geology rather than with respect to the field layout. Therefore, the basic processing began with a mathematical rotation of the MT data to x- and y-axes rotated to a Principal Axes (PA) direction. The PA orientation made the two orthogonal apparent resistivity modes the most different, usually the maximum and minimum values. In a 1D geology, the two apparent resistivity modes in PA rotation would have overlain each other or would have been separated by a constant static offset. If the data were 2D, one mode would have been a maximum and the other a minimum and the xx and yy modes would have been zero. The PA rotation has many virtues: it is an established standard; it is used for the apparent resistivity and phase plots in the contractors' reports; it minimizes apparent resistivity and phase noise distortion when data are computed using the robust code of Larsen (1996); it makes static distortion more consistently recognizable; it illustrates geometric distortion in a relatively simple way; and more elaborate approaches designed to make 2D imaging effective are not necessary when 3D inversions are used.

3.3.1.2 Data Editing

Following rotation, the data were edited using interactive screen plots of apparent resistivity and phase like those in Figure 12. The D^+ procedure of Beamish and Travassos (1992) illustrated what physically valid smooth curves would most easily fit the observed data and outlier points, and inconsistent bands of data were eliminated from subsequent computations. Depending on relative levels of noise, phase was given more or less weight than apparent resistivity in producing the smooth curves. The resulting smoothed apparent resistivity and phase curves, not the actual data, were used to compute all subsequent 1D and 2D inversions.

3.3.2 TDEM Inversion and MT Static Correction

The most obvious assessment of static distortion is the offset between the two MT apparent resistivity modes at high frequency, as illustrated in Figure 4. This is quantified in the table in Appendix A which has a column showing the ratio of the apparent resistivity of the higher resistivity mode to the lower mode for all of the MT stations. A ratio of 1 is not an infallible

indication of a lack of static distortion because it is possible that both modes may be shifted in the same direction, but higher ratios do indicate an obvious static problem.

Statics in the Glass Mountain data sets are relatively low, with most ratios below 2.0. Resistivity images can become noticeably distorted if the average static offset for a station is a factor of 2.0 but, if the offsets are generally smaller than 2 and symmetrical, then 3D inversions of MT for geothermal applications are unlikely to be significantly affected. The 2D and 3D inversion algorithms include options for static correction but they tend to smooth shallow structure more than is desirable, especially in areas like Glass Mountain where resistive shallow lavas vary in thickness significantly. The most common approach to resolving MT static ambiguity is to constrain the MT using measurements made with an auxiliary resistivity method like TDEM that is purely inductive and is not affected by static distortion (Pellerin and Hohmann, 1990).

Figure 13: TDEM Static Correction of MT Station n083

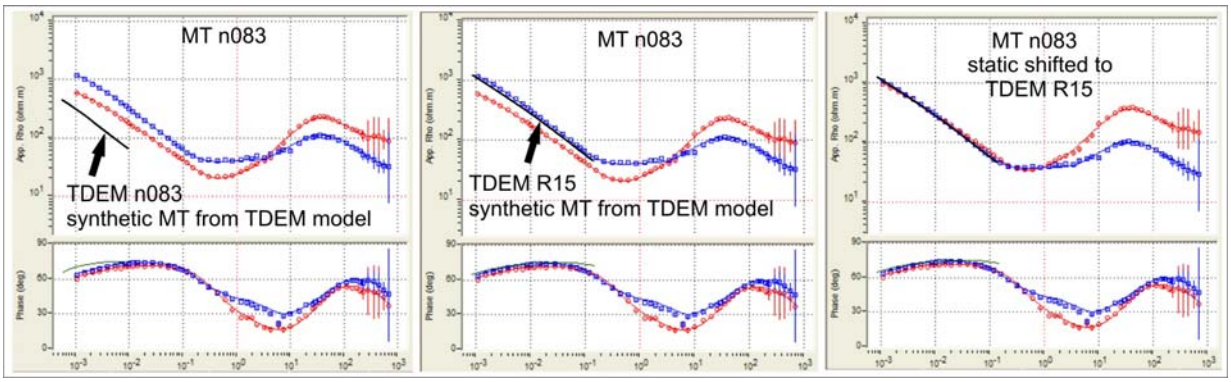

This Glass Mountain study highlighted a significant limitation in the TDEM approach to correcting MT statics. No specific problems were apparent when reviewing the time series processing for either the legacy or the 2005 data. However, when comparing synthetic 1D MT responses derived from the TDEM models to the measured MT responses as shown in Figure 13, the synthetic MT curves from the Sirotem recorded in 2005, like station n083, commonly had much lower apparent resistivity than both of the MT modes and the synthetic phase seldom fit the MT well. Synthetic MT derived from the 1980's TDEM that used a generator and 300 m loops like station R15, often fit the MT modes better, although usually closer to the higher resistivity mode. The descriptions in Appendix A summarize how well the MT stations fit nearby TDEM stations and point out particularly problematic misfits.

Further analysis of the Glass Mountain TDEM indicates that TDEM inversion models can be unreliable over thick resistive surface material in a more subtle manner than had been appreciated earlier. The schematic in Figure 5 attributes the TDEM signal to "smoke rings" of current that progressed to greater depth with time. If the local geologic section is resistive to great depth, no currents would be induced by the time the inducing fields decay to the noise level. Larger loops and more powerful transmitters could extend this maximum depth but would not eliminate the problem.

Different types of TDEM systems respond to a thick surface resistor in different ways. The small Sirotem system produces a short time series and a 1D inversion model with unrealistically low resistivity, typically too low by a factor of 0.2 to 0.7. The Geonics systems produce longer time series and resistivity models that are sometimes unrealistically high in resistivity by a small ratio. Both of these distorted results would be unsuitable for MT static corrections but the too-high resistivity Geonics models would not affect the overall pattern of TDEM conductance maps as seriously as the too-low resistivity Sirotem models. As a result, the Sirotem data was not integrated into the TDEM conductance maps like Figure 10. As detailed in Appendix A, the TDEM was used as a guideline for static corrections but not as reliable data to which the MT should always be adjusted.

Because MT statics were generally small and symmetrical at Glass Mountain, using average resistivity for 1D inversion and the internal smoothing of the 3D inversion seemed effective. The potential for problems with using TDEM at other prospects may be mitigated by the tendency of statics to be small in resistive areas where the TDEM is less reliable. Surface patches of low resistivity hydrothermal alteration can cause very large static distortion, but in these cases the TDEM is likely to work well because there would be no thick surface resistive layer to distort the TDEM results. Therefore, this problem implies greater care when correcting statics with TDEM and implies that TDEM should not necessarily be acquired at every geothermal prospect that could benefit from an MT survey. In any case, the static correction approach taken at Glass Mountain was apparently effective, because most of the 1D cross-sections did not exhibit the improbable lateral discontinuities characteristic of statics, and the 2D and 3D inversions were even smoother.

3.3.3 MT Dimensional Assessment and Inversion

To assess the range of frequencies over which the 1D, 2D and 3D inversions would be valid, a wide variety of dimensional indicators available in MT analysis were reviewed. A separation in the apparent resistivity modes that did not look like a constant static offset at high frequency was an obvious indication that the MT was no longer 1D. MT dimensional parameters such as skew and ellipticity (Vosoff 1991) were considered for their general indication of resistivity trends. As mentioned earlier, when the amplitude of the Principal Axes xx and yy mode apparent resistivity (the light blue and red data in Figure 12) became significant, the data were likely to be affected either by noise or by 3D resistivity geometry, a pattern that occurred at most stations at Glass Mountain between 0.1 and 1.0 Hz, as illustrated in Figure 12.

The map in Figure 14 shows, for the GSY-USA MT stations, xy (black) and xx (red) impedance polar diagrams and the directional parameters derived from the magnetic field data. The magnetic data include tipper strike (pointing along resistivity strike) and induction arrow (pointing toward a dominant conductor) in a range of frequencies around 0.01 Hz. Static effects have been removed from these polar diagrams using a static stripping process, so that statics does not distort the diagrams. The diameter of an xy impedance polar diagram along any direction is proportional to the amplitude of the apparent resistivity in that direction. The xx polar diagram is more difficult to interpret except to note that, in general, at stations where the xx amplitude is larger, the data are more affected by 3D resistivity geometry. Along with TDEM

and MT 1D conductance maps, diagrams like those in Figure 14 were the main tools used to review strike for 2D inversions and to choose a frequency range for 3D inversion.

Figure 14: MT Impedance Polar Diagrams at 0.01 Hz with Tipper Strike and Induction Arrows

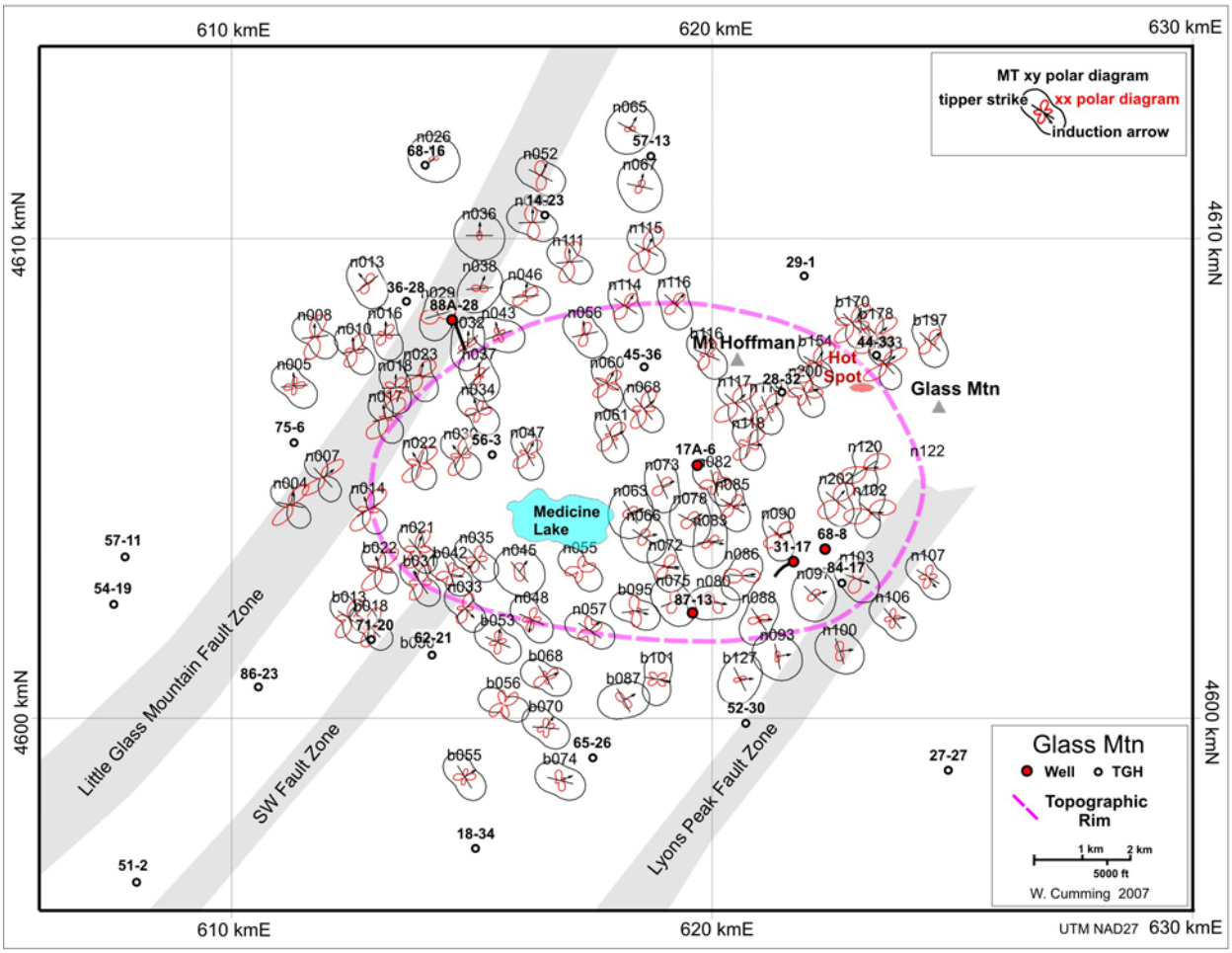

A series of plots like Figure 14 showed that most of the MT stations were strongly polarized with a maximum resistivity axis aligned with tipper strike in a NW or NNW direction. Based on induction arrows and tipper strike, the 0.01 Hz polar diagrams seemed to be responding to a NW trending regional conductor east of the Medicine Lake Highland. However, the high xx amplitudes indicated that 3D effects were also prominent. Some areas, like part of the Telephone Flat area, seemed to follow a more local resistivity pattern at 0.01 Hz. Ideally, polar diagrams at higher frequencies more sensitive to local variations in resistivity would be used to assess dimensionality for 2D inversions of a geothermal clay cap. However, data from 0.1 to 1 Hz were generally too noisy and most of the data above 1 Hz was not highly polarized. Therefore, 1D TDEM and MT conductance maps were emphasized in assessing resistivity strike for 2D inversions and the regional resistivity geometry was considered in assessing the frequency range of the data to be inverted, generally greater than 0.1 Hz. The compromises needed to choose an appropriate strike in 2D inversions were largely avoided by using 1D MT

and TDEM inversion for quality assurance and the 3D MT imaging for most of the interpretation.

A significant proportion of the MT stations, as noted in Appendix A, show ambiguous evidence of coherent noise at frequencies lower than 0.1 Hz. For example, apparent resistivity curves with a rising slope greater than 45° on a log-log plot are often characteristic of coherent noise sources and appear on many Glass Mountain MT stations. The Pacific Intertie high voltage direct current (HVDC) power lines that connect Oregon to southern California are oriented NNW where they pass about 120 km (75 miles) to the east (Figure 1), consistent with the Glass Mountain MT polarization at 0.01 Hz.

Wannamaker et al. (2005) more thoroughly investigated much more severe coherent noise at the Coso Geothermal Field, which is located less than 30 km (19 miles) from the Pacific Intertie HVDC power lines. That study also reported significant HVDC signal at a remote reference site located 110 km (68 miles) from the power lines. Wannamaker et al. (2005) noted that at such a distance, the HVDC signal would probably be planar at 1 Hz and could be treated as conventional MT data. This is consistent with the Glass Mountain MT which shows no distortion at 1 Hz but, even at a 120 km (75 mile) distance, HVDC noise might distort MT data at frequencies below 0.1 Hz.

3.3.3.1 1D MT Inversion

Experience at many geothermal fields indicates that 1D inversion usually works well enough to characterize the overall resistivity geometry of a tabular geothermal clay cap, although probably not abrupt edges of the cap or variations in resistivity below it. This is the case even when the apparent resistivity modes at MT stations show some non-1D separation at frequencies higher than the upturn in apparent resistivity that corresponds to the base of the clay cap (Anderson et al. 2000). As a result, most MT data in geothermal fields can be interpreted in a 1D context, except near areas with significant lateral variation in conductance at depths shallower than the top of the reservoir. Unfortunately this corresponds to the field edges, a conceptual part of the reservoir where more reliable resolution is likely to have value.

In the present study, the smooth 1D MT inversions at Glass Mountain were computed from the average of the two MT modes. This made the choice of mode simple and predictable and avoided imposing arbitrary static corrections on stations that lacked reliable TDEM. The suitability of this choice was established by the close match of 1D MT inversions to borehole resistivity data to the top of the reservoir. When plotting maps and cross-sections based on the 1D inversions, data from each station affects the contouring independently, making it easier to identify problems with particular stations. Because 1D inversions can be assembled into cross-sections without regard for 2D strike, it is easy to generate a 1D comparison to any 3D cross-section. Providing that the limitations of 1D MT inversion are understood, such as being careful about interpretations below the base of the clay cap or near the boundaries of conductors, 1D MT inversion can support an effective quality assurance and interpretation process.

3.3.3.2 2D MT Inversion

To prepare the MT data for 2D inversion, assumptions must be made about how to orient the two MT modes relative to the strike of the profile. Unless the data is strongly 2D, all choices are compromises. A variety of approaches were used to assess 2D strike including using resistivity polarization diagrams, patterns of 1D conductance and, most importantly, goodness of fit to both modes in the 2D inversions. Alternatives to the data rotation like that of Smith (1995) were also tested. A common remedy, fitting only the TM mode, was preferable to fitting TE mode data that were incompatible with a 2D assumption but implied greater uncertainty. Because 2D inversion proved to have few conceptual advantages with respect to 3D inversion, 2D inversions were mainly used early in the interpretation process to check the progress of 3D inversions.

The most common interpretation pitfalls encountered in published 2D MT inversions at geothermal fields include making inappropriate statics assumptions, failing to edit noise before inverting the MT data, distorting spatial relationships when projecting stations onto a profile, orienting the profile in a manner inconsistent with the strike of the MT data, and including MT data that are inconsistent with a 2D resistivity model. Although these issues are addressed in several Glass Mountain 2D inversions, none are superior to the 3D inversion results presented in this report.

This is not to say that 2D inversion would not have been more appropriate in other circumstances. For example, if a profile could be found along which the MT station data were consistent with the 2D resistivity strike implied by the profile azimuth, then 2D inversion might provide a higher resolution representation of the resistivity pattern because of the courser grid blocks currently feasible in 3D inversion. At Glass Mountain, the MT data set was used to develop the 3D inversion at relatively low cost to the project. Reliable 3D MT inversion is likely to cost less than reliable 2D inversion within a few years because sorting out effective orientation compromises for a 2D inversion will remain a time-consuming process while the cost of computing a 3D MT inversion is likely to decrease. However, at present 3D inversion remains expensive. Regardless of expected decline in cost of the inversion computation, 3D MT inversion requires an expensive grid of MT stations whereas 2D inversion requires only a line of stations oriented perpendicular to resistivity strike.

3.3.3.3 3D MT Data Set Preparation

This experience of this project suggests that the 3D MT inversion used is less forgiving of poor data than 1D and 2D inversion and so the input data set requires more careful pre-processing. In this particular case, the impedance data requires more conservative editing because the 3D inversions are computed from observed impedances, not smoothed apparent resistivity and phase curves. However, it is likely that more careful editing will be required in any reliable 3D MT inversion. The much larger number of elements in a 3D model that must be constrained by the same MT data set implies that there is more opportunity for a 3D inversion to produce unrealistic results if misleading data are included.

The editing procedure began with a comparison of the observed data to smooth apparent resistivity and phase curves computed using D^+ smoothing of Beamish and Travassos (1992). The D^+ smoothed curves fit the observed data as closely as was consistent with physical validity. Outliers and inconsistent bands of observed data were interactively marked for probable suppression and, after checks were completed with respect to the consistency of these choices with nearby stations, the corresponding impedance data were edited. A few MT stations that were dominated by noise were omitted from the 3D inversion and, if two stations were over the same inversion block, the noisier station was omitted. The effect of editing on the contribution of each MT station to the 3D inversion was summarized in Appendix A.

Although MT magnetic parameters were also edited to obtain consistent values, including even the edited data produced unrealistic patterns in the 3D resistivity models without fitting the vertical magnetic data well. Effective use of vertical magnetic data in 3D inversion may require the development of more sophisticated tools for testing reliability, especially for older MT data. For this project, the 3D inversion was not constrained by the vertical magnetic data.

The effective depth of investigation of the 3D inversion is not limited by the geometric assumptions of the 3D inversion algorithm, as is the case with 1D and 2D inversion, but by the average resistivity of the model, the frequency range of the reliable data and the MT station coverage. Because of the possibility that the MT data at frequencies less than 0.1 Hz might be distorted by non-planar HVDC signals and given the lack of reliable regional MT coverage to better constrain the large scale resistivity pattern, the data at frequencies lower than 0.1 Hz seemed likely to increase uncertainty in the 3D inversion results. Moreover, restricting the MT data set used in the 3D inversion to frequencies greater than 0.1 Hz allowed for a greater number of frequencies from 0.1 and 300 Hz to be included in the 3D MT inversion, improving the resolution of finer details in the clay cap and upper reservoir to a depth of at least 4000 m (13,000 ft).

CHAPTER 4:
Developments in 3D MT Resistivity Imaging

4.1 Interpretation Approach

Most recently published MT interpretations are based on the results of 2D imaging algorithms (Rodi and Mackie 2001). Because of the nature of its target and numerous successful case histories, 1D imaging is still popular in the geothermal industry, although its limitations are appreciated. While these algorithms have proven to be useful and effective for interpreting MT data, it is rare to find MT data that is 1D or truly 2D. Most MT data show some evidence of 3D structure, especially at lower frequencies. Elaborate manipulation of MT data to better fit the assumptions of 2D inversion often increases the uncertainty in the resulting images. Rather than interpreting MT results in terms of 2D resistivity images obtained along linear profiles, or coping with the artifacts in stitched cross-sections and maps derived from 1D MT inversions, it would be preferable to obtain 3D models of the subsurface resistivity directly from the entire grid of MT stations.

In the 1980's and 1990's, the tool available for fully 3D MT interpretation was trial-and-error forward modeling. This approach had been used for interpreting field data with some success, but it was extremely laborious and time-consuming, failed to image many of the most important details in the data set, and often failed to detect unexpected patterns of resistivity. One difficulty was the size of the problem: multi-station/multi-frequency 3D data sets typically comprised thousands of MT measurements, and a large number of model parameters were needed to fit the data. Additionally, the non-linearity of the forward problem made it very difficult to predict the parameter changes needed to fit data and to account for the complicated trade-offs among parameters. These difficulties were severely compounded by the computational intensity of 3D MT forward modeling. As a result, although the geothermal industry understood the potential value of 3D MT modeling and inversion, after a few experiments in the 1980's and 1990's it was dismissed as being impractical for the detailed models of large data sets used in well targeting and resource assessment.

The need for an automated way of deriving 3D models from a grid of MT stations has led to the development of a proprietary 3D algorithm by GSY-USA, Inc. This algorithm is a 3D MT imaging (inversion) algorithm that iteratively finds a smooth 3D resistivity model that fits the observed data. This fully automates the process of fitting MT data to 3D earth models in a rapid and robust inversion process.

The standard approach to nonlinear inverse problems in geophysics has been iterative, linearized inversion. When run to convergence, this algorithm minimizes an objective function, a measure of both misfit and smoothness, over all allowed models and, in this sense, produces an optimal solution of the nonlinear inverse problem. However, the practicality of iterative, linearized inversion algorithms is greatly limited in 3D electromagnetic applications by the need to compute a Jacobian (partial derivative matrix) of the forward problem, and solve a non-sparse, linear system of equations over the entire model at each inversion iteration. In its

development of a 3D MT inversion algorithm, GSY-USA adopts the method of nonlinear conjugate gradients (NLCG) in lieu of iterative, linearized inversion.

4.1.1 3D Forward Modeling

A magnetotelluric measurement of naturally occurring electric and magnetic fields at Earth's surface will comprise a 3D magnetotelluric data set. A typical 3D MT data set includes as many as six complex quantities as a function of receiver position and temporal frequency for a large array of positions. These are defined by the relation:

$$\begin{bmatrix} E_x \\ E_y \\ H_z \end{bmatrix} = \begin{bmatrix} Z_{xx} & Z_{xy} \\ Z_{yx} & Z_{yy} \\ T_x & T_y \end{bmatrix} \begin{bmatrix} H_x \\ H_y \end{bmatrix}$$

Where subscripted E and H are components of the electric and magnetic induction fields, respectively; the vertical electric field is negligible at Earth's surface because of the nearly infinite conductivity contrast between the atmosphere and ground. The six quantities observed in 3D MT, then, are the four components of an impedance tensor Z and two components of the vertical magnetic transfer function T.

Modeling the impedance tensor and vertical magnetic transfer function requires solving Maxwell's equations in the solid Earth and atmosphere using a horizontal current source in the atmosphere to represent ionospheric and magnetospheric MT signal sources. At the frequencies involved in MT exploration, conduction currents dominate over displacement currents and the latter can be ignored. In the forward modeling algorithm, the earth and atmosphere are divided into rectangular blocks with the magnetic fields defined along the block edges and the electric fields defined at right angles to the block faces. This is equivalent to the staggered grid formulation (Yee 1966). Finite difference equations can be easily derived using this formulation. When the electric fields are eliminated from the difference equations, a second-order set of equations in the magnetic field, H, results, and these can be grouped together in the form Kv=b, where b contains the terms associated with the known boundary values and source field, v contains the unknown magnetic fields, and K contains the coefficients from the second-order difference equations (Mackie et al. 1994). This system of equations is sparse and symmetric with mostly real elements except for the complex diagonal elements. The solution is obtained by using a biconjugate gradients stabilized algorithm. Convergence is improved by using a preconditioner that is the incomplete Cholesky decomposition of the diagonal sub-blocks of the coefficient matrix that also includes a correction for the divergence of the magnetic field. Once the electric and magnetic fields have been determined for two linearly-independent source polarizations, the impedance tensor and vertical magnetic transfer function can be computed.

4.1.2 3D Inversion

The approach to solving the 3D MT inverse problem is based on the framework of Tikhonov regularization (Tikhonov and Arsenin 1977). Following many previous workers in MT inversion (Constable et al. 1987, Smith and Booker 1991) a smooth, or ‘minimum-structure’,

resistivity model is sought that gives acceptable fits to the observed data. Such models minimize an objective function defined by

$$\psi(m) = \left(d - F(m)\right)^T V^{-1}\left(d - F(m)\right) + \lambda m^T L^T L m$$

The regularization parameter, λ, is a positive number. The positive-definite matrix V plays the role of a variance-covariance matrix of the error vector. The second term defines a stabilizing functional on the model space. The matrix L is chosen as a simple, second-difference operator approximating the Laplacian operator on the model grid. Thus, solutions are models with minimum spatial variability, or roughness.

This algorithm is based on earlier work on a NLCG algorithm for 2D magnetotellurics (Rodi and Mackie, 2001). The key features of the algorithm include avoiding the solution of a linear system of equations for the entire model, replacing computation of the full Jacobian matrix with operations that are much more efficient, and embedding these features in the context of NLCG. A variety of computational techniques that exploit the structure of the MT problem such as line-search and preconditioning make this implementation of the NLCG algorithm rapid, robust and fully nonlinear without approximations.

4.1.3 Advances in 3D MT Inversion during this Project

The original 3D inversion code developed for a desktop workstation was optimized during the course of this project to run more efficiently using massively parallel processing on clusters of computers. This allowed successive 3D inversions of the Glass Mountain MT data to match more frequencies, resolving finer details in larger and much more finely sampled resistivity models. Following the initial test inversions with only a few frequencies, early models run for this study included 8 frequency data points for each station and 88,000 model elements, with no topography. The model inversion presented in this study included over 300,000 elements and topography was modeled in vertical increments less than 50 m (160 ft) while the lateral dimensions of the model elements within the perimeter of the MT stations are less than 400 m (1300 ft). Although the general resistivity outline of Glass Mountain was imaged using the initial coarse grid without topography, the more finely sampled model including topography matched the well data much better.

Since the completion of the work for this study, typical commercial MT model sizes have increased to 1,000,000 elements and, within a few years, more detailed models are likely to significantly improve the handling of issues like static distortion due to topography.

Stabilizing functions have been steadily improved so that the 3D inversion is now less likely to put resistivity variations in the model where there is less data, for example, outside the perimeter of the stations or in gaps between stations, especially at greater depth. A related development is the smoothing optimization that reduced the correlation between the inverted resistivity pattern and the distribution of stations. As a result, the resulting 3D resistivity models continue to improve and are more realistic than when this project started.

The 3D inversion code now has an option to invert for static shift effects based on smoothness of the shallow model, independent of outside data like TDEM. This project showed that, although this option does reduce the distortion caused by stations with large statics, the effectiveness of the current approach depends on the geological environment. This approach has proved to be effective in sedimentary basins but, for geothermal exploration on volcanic highlands like the Glass Mountain area, it tends to smooth geological elements that are important to the conceptual interpretation. Future development of this capability may include customization to adapt the smoothing to the geological environment. A more promising option for mitigating static distortion in rugged volcanic areas is to more closely model the topography. Statics may be much less problematic when it becomes computationally practical to invert large models that have vertical element dimensions of 10 m and horizontal dimensions of 100 m, perhaps in a few years.

Because MT error statistics are often overly optimistic about the reliability of impedance data, several methods were tested to make the inversion less sensitive to noise. Modern robust processing algorithms like that of Larsen et al (1996) are particularly prone to underestimating errors in MT impedances. When such behavior is suspected, a procedural change in the inversion can be adopted, optionally employing user-determined error estimates instead of the computed errors. An L1 norm was implemented in the 3D inversion to avoid over-fitting the noisiest data points.

It was hoped that using smoothing and L1 norm statistics would allow the 3D inversion to be used with a minimum of prior MT data editing. However, experience has shown that excluding unreliable data is an important step in 3D inversion, especially when a group of neighboring stations have data biased by noise in a similar way. For example, access issues sometimes require that a group of neighboring stations be recorded on the same day. If many of these stations are among trees and the day is windy, they may all exhibit a noise bias to lower resistivity at about 0.1 to 0.5 Hz. Although the original field reports for the survey are not available, this type of noise may have affected part of the Glass Mountain MT data set collected by Phoenix. If not edited, the apparent consistency of this response among several stations causes the 3D inversion to produce a zone of unrealistically low resistivity below 3000 m depth. Similar patterns are commonly observed where geothermal power plant facilities create a high electrical noise environment. (In fact, operators might consider acquiring additional MT immediately before beginning construction of a first power plant if the additional information is reasonably likely to aid make-up and injection well targeting.) This project showed that, as 3D MT inversion becomes more efficient and makes interactive 3D MT inversion feasible, an interpreter will be able to more effectively edit and optimize the data sets to improve the resistivity imaging.

In a few years, it is likely that a mass market computer built for applications like home-video editing will provide performance equivalent to the clusters used for the 3D MT inversions of this study. By that time, customized clusters might make interactive 3D MT inversion feasible. Before then, 3D inversion is likely to become a routine standard for commercial MT imaging.

Before this project began, the 3D MT inversion algorithm had been validated using synthetic data and had been tested on a few real data sets. Since then it has probably been applied to over 100 real data sets collected in a variety of exploration environments including mining, geothermal, and oil and gas targets. Many of these targets had well logs available to validate the results. The current study is the first 3D MT inversion at a geothermal field in California that has been checked by direct comparison to a resistivity well log extending from above the low resistivity smectite clay zone to a depth more than 1000 m (3300 ft) into the reservoir.

4.1.4 3D MT Inversion Resolution and Uncertainty

The 3D MT inversion algorithm computes performance parameters that are important to assessing the inversion computation but these parameters are less reliable as indicators of how realistic the resistivity images are. The misfit statistic summarizes the difference between the observed MT data and the MT predicted from the model. Roughness illustrates how rapidly resistivity varies between each block and its neighbors. A resistivity model that compromises between the least misfit and the least roughness is the objective of the inversion. To improve resolution, it is tempting to reduce the misfit if the overall roughness does not change much. Unfortunately, this can lead to the common pitfall of over-fitting noise. Other performance parameters like model sensitivity, the change in the misfit caused by a given change in each model element, help characterize the reliability of details in the model. However, the interpretation of all such inversion statistics ultimately relies on an interpreter's judgment of what is realistic. Because a resistivity well log and other borehole data are available to the depths of greatest interest for geothermal exploration at Glass Mountain and are more intuitively appealing to geoscientists who are not experts in electromagnetic inversion, these will be emphasized in the assessment of resolution and uncertainty of the 3D resistivity images.

CHAPTER 5:
Resistivity Interpretation of the Geothermal Resource

As detailed in Section 2, the plan for the characterization of the Glass Mountain geothermal resource properties using the MT and TDEM resistivity images was based on a chain of inference involving the interpretation of the resistivity in terms of clay alteration and then the inference of temperature and permeability patterns in the resource from the geometry and intensity of the clay alteration. An important component of the proposal was the confirmation of the applicability of this interpretation approach to the Glass Mountain prospect using alteration, temperature and resistivity data from geothermal wells.

5.1 Confirmation of Clay-Oriented Resistivity Interpretation

To confirm that a clay-oriented approach was applicable to the interpretation of the Glass Mountain MT and TDEM resistivity images, EGI compiled and reinterpreted voluminous petrographic data released by Calpine in support of the project. The conceptual interpretation of the alteration relative to the fracture permeability is summarized in Clausen at al. (2006) and Moore (2006). The petrography results and alteration interpretation compiled by EGI are compared to the MT in detail for two wells, 88A-28 and 17A-6. The larger scale alteration patterns are compared to the MT data in two cross-sections that show the setting of all five exploration wells drilled at Glass Mountain. The cross-section interpretations correlate the alteration zones with the MT resistivity, the isotherms from the measured well temperatures, and the permeable zones in the wells.

5.1.1 Well 88A-28

Figure 15 illustrates the relationship between MT resistivity and the geology, alteration, temperature and permeability in well 88A-28. Most of the well data in Figure 15 is taken from a similar figure from Calpine-Siskiyou Geothermal Partners L.P. (2004). The methylene-blue (MeB) log digitized by EGI from the well mud log provides a semi-quantitative relative indication of the amount of smectite clay in the cuttings (Gunderson et al. 2000). The scale of the MeB curve at the top of the plot is reversed so smectite increases to the left, in the direction it would be expected to correlate with decreases in MT resistivity plotted using the logarithmic resistivity axis at the bottom of the plot. To compare the MT to the well data, 1D MT resistivity curves from the two closest MT stations, n029 and n032, are plotted with the MeB smectite clay curve, along with resistivity from two 3D inversion models, one with static corrections (red squares) and one without statics (orange-black diamonds).

Well 88A-28 did not encounter production at a currently commercial rate, although the interpreted maximum temperature of 238°C (460°F) at an elevation of 1200 meters above sea level (masl) or 3337 feet above sea level (fasl) in the upper part of the mafic volcanics imply that a nearby reservoir upflow zone heats the well (Calpine-Siskiyou Geothermal Partners L.P. 2004). Fluid produced from the 211°C (411°F) permeable zone at 1938 m (6360 ft) depth (182 masl, 597 fasl) had geothermometry as high as 249°C (480°F). Because this geothermometry was from a non-commercial permeable zone below the temperature maximum of the well, it may be

unreliable but probably provides a reasonable minimum for the temperature of a nearby permeable upflow source

Figure 15: MT Resistivity and Well 88A-28 Geology, Alteration, Temperature and Permeability

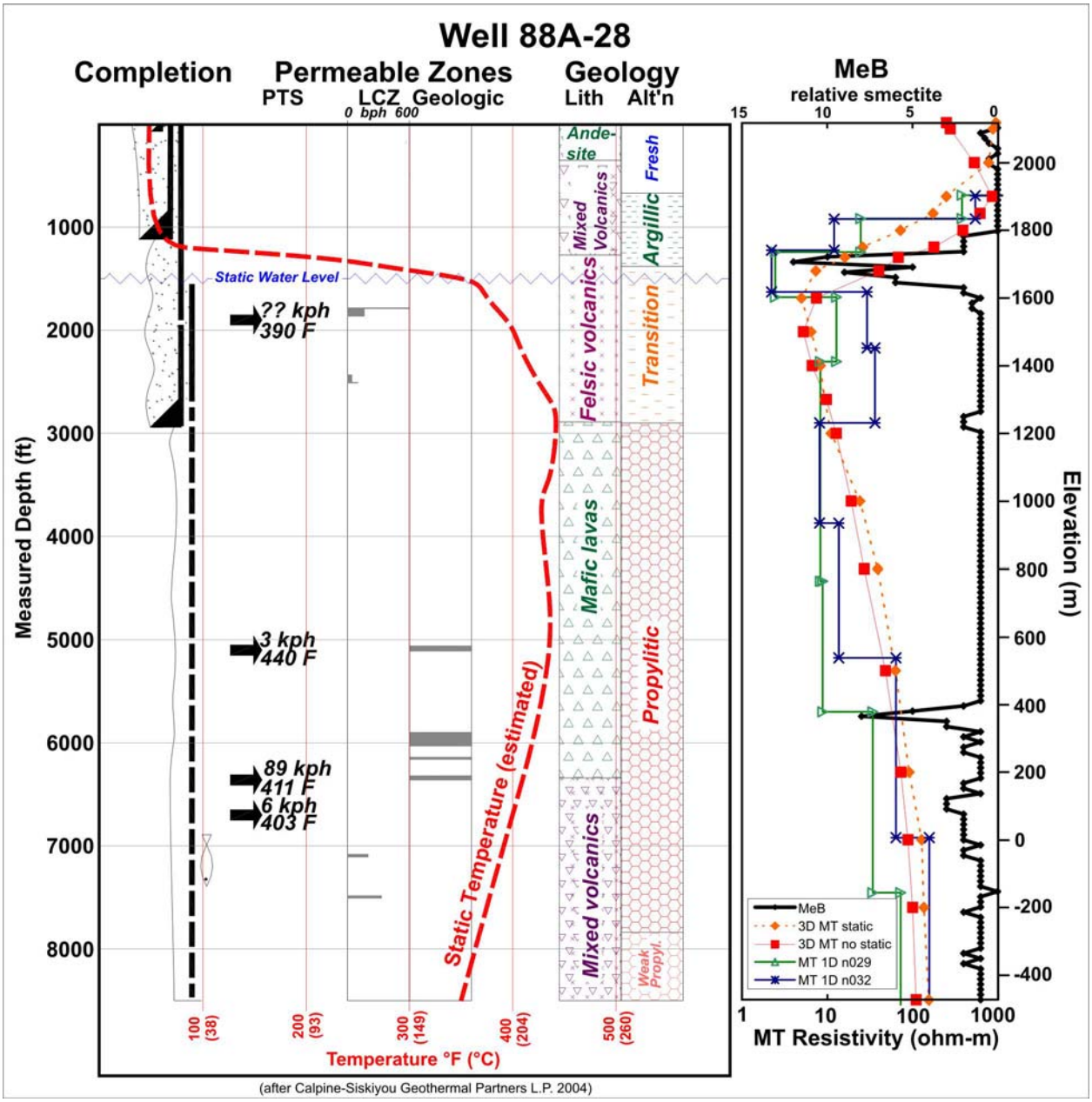

The 88A-28 well demonstrates an important conceptual aspect of the clay cap. The highest concentrations of smectite clay, and as a result, the lowest resistivity, occur just above and below the static water level. Therefore, a flat lying low resistivity zone detected near elevation 1700 masl (5578 fasl) in the Glass Mountain KGRA is probably constrained by the deep water table.

The very steep increase in temperature from less than 40°C (100°F) at 366 m (1200 ft) depth (1750 masl, 5742 fasl) to over 177°C (350°F) at 450 m (1500 ft) depth (1660 masl, 5446 fasl) implies that this interval has very low permeability. This also correlates with the highest relative values of MeB smectite in the argillic alteration zone and the underlying transition from smectite to higher temperature minerals. The smectite component of the mixed layer smectite-illite clay characteristic of the transition zone is seldom detected using the MeB method and so XRD is used instead. As expected, smectite rapidly decreases in the transition zone, as temperature rises above 180°C (380°F) and smectite is progressively converted to illite. The propylitic alteration zone that typically corresponds to the top of the geothermal reservoir is encountered at the interpreted maximum temperature of 238°C (460°F) at 1200 masl (3937 fasl) (914 m, 3000 ft depth).

The pattern of alteration at 88A-28 is generally consistent with the pattern expected in a well adjacent to a >238°C (460°F) geothermal reservoir. That is, a low permeability smectite clay zone caps the high temperature geothermal system and smectite decreases as temperature increases over 180°C (380°F) and then smectite reappears in the underlying cooler zone. The entry zones in the well are small and, based on the measured temperatures that are cooler than the maximum temperature, these entries are probably not representative of permeability in the nearby reservoir. The peaks in smectite content below 400 masl (1312 fasl) where temperature is over 216°C (420°F) may be related to dehydrated smectite found in low permeability zones or to increasing smectite stability due to the decrease in temperature below 600 masl (1969 fasl), probably both. The weak alteration at greater depth reported by Clausen et al. (2006) also indicates generally low permeability below 400 masl (1312 fasl).

The MT resistivity at well 88A-28 is consistent with a conventional geothermal reservoir pattern. The lowest resistivity correlates with the most intense smectite alteration at the top of the reservoir and, as smectite decreases, resistivity increases within the high temperature reservoir. The MT resistivity curves do not follow the smectite curve in the alteration transition zone because the MeB method is less sensitive to the mixed-layer smectite-illite clay in that zone. The XRD detection of smectite in the transition is more reliable. The almost constant resistivity and higher smectite found below 400 masl (1312 fasl) has two potential interpretations. At temperatures over 200°C (400°F), smectite is sometimes dehydrated and resistive. However, it is more likely that the increase in smectite is related to the reversal of the temperature gradient marked by the steady decrease in temperature from 600 masl (1969 fasl) to the bottom of the well. The intensity of alteration also decreases, consistent with the interpretation that the well exited a zone heated by a nearby upflow and entered a cooler underlying zone (Calpine-Siskiyou Geothermal Partners L.P., 2004). When the 3D resistivity model is viewed in cross-section and map view, the trends in resistivity near the bottom of well 88A-28 decreases slightly, consistent with the same interpretation. In any case, the alteration pattern in well 88A-28 is consistent with the smectite-illite model for MT resistivity interpretation at Glass Mountain. The low resistivity detected by MT matches the smectite clay zone capping the high temperature geothermal reservoir and a map of the elevation of the base

of the low resistivity zone, in this case at about 1200 masl, (3940 fasl) conforms to the top of the high temperature reservoir to within the expected resolution of the MT.

Figure 16: MT Resistivity and Well 17A-6 Resistivity Log, Alteration and Temperature

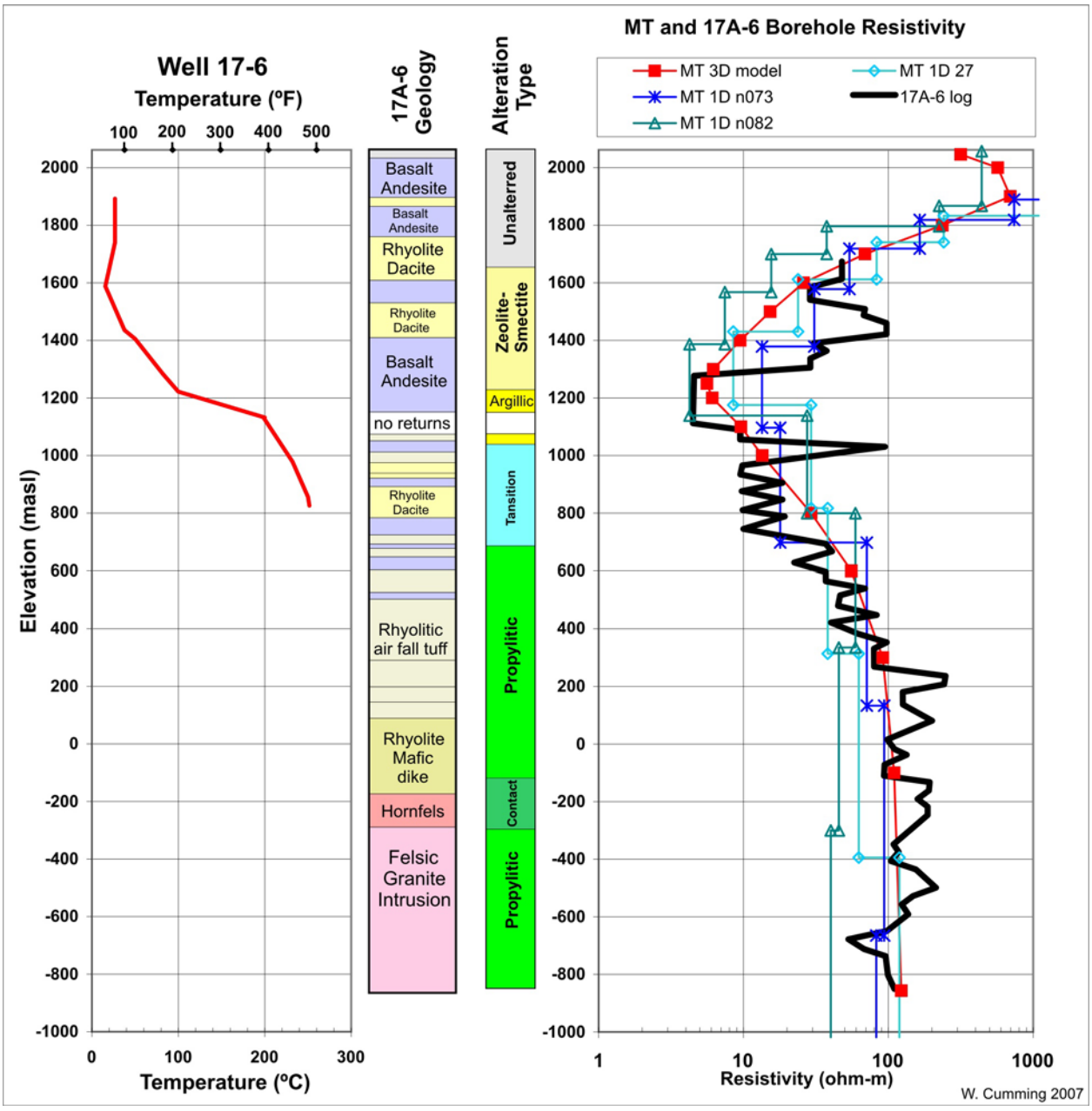

The MT plots in Figure 15 show the performance of different approaches to MT inversion and static correction. MT stations n029 and n032 are located about 250 m and 500 m from the surface location of 88A-28, respectively. Although n029 is closer to the well and has lower noise than n032, they fit the MeB peak equally well. However, if TDEM static shifts are used, n032 fits the MeB slightly better because it has a symmetrical static shift, the lower mode was shifted up and

the higher one down. Both modes at n029 would be shifted up to match the TDEM, resulting in a poorer fit to the MeB. Although the difference is minor, it confirms that TDEM at Glass Mountain should be reviewed skeptically if it implies an asymmetrical MT static correction. The 3D inversion curves have a slightly deeper minimum resistivity than the top of the clay cap from MeB would suggest, although a version that attempts to allow for statics by lateral smoothing is closer. However, all of these variations in the fit of the MT resistivity to the MeB clay pattern are minor and would not distort the interpretation.

5.1.2 Well 17A-6

The induction resistivity log from well 17A-6 shown in Figure 16 provides a direct confirmation of the relative effectiveness of the 1D and 3D MT resistivity imaging and, when combined with the alteration data from EGI, also confirms the applicability of the smectite-illite approach to geothermal resistivity interpretation at Glass Mountain.

The correlations between alteration, temperature and resistivity in well 17A-6 are similar to those of 88A-28. In well 17A-6, the resistivity minimum is located at the same elevation as the argillic alteration cap near 1200 masl (3837 fasl). Because well 17A-6 had mechanical problems and was abandoned before it was tested, no stable temperature log or water level is available so temperatures are plotted for the neighboring TGH, 17-6. In both 17-6 and 88A-28, the maximum temperature gradient coincides with the resistivity minimum and the argillic alteration zone. The increase in resistivity below this zone corresponds to the transition from smectite clay in the argillic zone to illite clay in the propylitic alteration zone.

Wells 17A-6 and 88A-28 differ in their conceptual relationship to the geothermal reservoir. At 17A-6, the low resistivity argillic zone capping the high temperature reservoir is centered at 1200 masl (3837 fasl), about 500 m (1641 ft) deeper than similar correlations at about 1700 masl (5578 fasl) in well 88A-28. Another significant difference between the wells is that well 17-6 is hotter, reaching 252°C (485°F) at 826 masl (2710 fasl) with no indication of a reversal to lower temperature at greater depth. No entries or other indications of reservoir permeability are reported for well 17A-6 and the low intensity of alteration is consistent with this. Well 17A-6 appears to be located on a low permeability margin of a geothermal upflow but at greater depth and higher temperature than well 88A-28. These conceptual differences probably account for the different temperatures at which the smectite to illite transition occurs, about 210°C (410°F) in well 17A-6 versus about 180°C (380°F) in well 88A-28. Despite these conceptual differences, the very similar correlations between resistivity minima, temperature gradient maxima and argillic alteration in wells 17A-6 and 88A-28 imply that the smectite-illite approach to MT interpretation is robust and likely to work in widely varying conceptual situations at Glass Mountain.

A detailed comparison of the MT resistivity to the 17A-6 induction well log illustrates the reliability of the different MT inversions and their resistivity images. The 1D inversions of MT stations n073, n082 and 27 are generally consistent in elevation and a combination of lateral variations in resistivity and statics are consistent with the differences in resistivity values. The station that has the poorest match to the lowest resistivity in the induction log, MT station n073,

is farthest from the well, almost 1000 m (3281 ft) to the southwest, a direction where the 3D inversion also images a higher resistivity and presumably less intensely altered argillic alteration zone. The reliability of the 1D inversion to the base of the clay cap is surprisingly good, although its performance is poorer at greater depth. The 3D inversion matches the well log closely, much more closely below the top of the clay cap than the 1D inversions, as would be expected. The only significant mismatch of the 3D MT to the induction well log is at 1450 masl (4757 ft) where a rhyolite-dacite lava of probably limited lateral dimensions produces a much higher resistivity in the induction log than the 3D MT detects. This may also reflect differences in the physics of the measurements because the well log measures resistivity at a much smaller scale. All of the 1D and 3D inversions shown in Figure 16 match the induction log closely enough that they will conform to the overall geometry of the clay cap near well 17A-6.

An important geological and conceptual feature of well 17A-6 is the felsic granite intrusion below -300 m (984 ft) elevation. By analogy to the petrographically similar granite dike in well 31-17, this is likely to be part of a large, perhaps 6 km diameter, granite intrusion at shallow depths with an age of about 320 ka (Lowenstern et al. 2003).This would fit with the Finn and Williams (1984) gravity model but, given its age, its importance to the current system will be mainly related to whether its properties favor the development of permeable joints and fractures and perhaps to its pore storage if the geothermal system is close to the boiling point and might form a deep steam zone. If the granite is likely to host a productive reservoir zone, then further study might usefully address whether it is more like the Coso, California main field granite reservoir or the lower permeability Coso east flank (Adams et al. 2000) or perhaps like the >216°C (>420°F) part of the Steamboat Springs, Nevada granite reservoir (Johnson and Hulen 2006).

5.2 MT Maps Illustrating Overall Clay Cap Geometry

Three types of maps are used in this report to display and interpret the patterns of MT resistivity: (1) conductance to 600 m (1969 ft); (2) elevation of the base of the low resistivity clay cap; and (3) maps of the 3D resistivity model sliced at several representative elevations. A map of MT 3D conductance to 600 m (1969 ft) depth provides a direct comparison to the TDEM map in Figure 11 and illustrates the distribution of shallow clay alteration. A standard part of many geothermal MT interpretations is a map of the elevation of the base of the low resistivity zone. Because it matches the smectite-illite alteration transition that typically occurs close to >200°C (392°F), it usually conforms to the top of >200°C (392°F) geothermal reservoirs. A map of resistivity at a particular elevation in a 3D inversion model (sometimes called a horizontal slice through the model) provides a direct map-view comparison to resistivity patterns shown in cross-sections. However, because the resistivity cross-sections more easily illustrate the conceptual relationship of the resistivity patterns to well data, the maps of conductance and elevation of the base of the clay are used here to introduce the seven cross-section profiles that, in turn, introduce the maps of resistivity at a particular elevation.

5.2.1 Map of 3D MT Conductance to 600 m (1969 ft) Depth

In studies of high temperature geothermal fields, maps of conductance are often used as a surrogate estimate of total hydrothermal smectite clay content over a particular depth interval. Maps of conductance are particularly useful for mapping the results from 1D layered resistivity inversions like those used to produce the TDEM conductance plots in Figures 10 and 11. Maps of 1D layered resistivity at a particular elevation tend to display unrealistically abrupt changes in value. Because conductance maps illustrate an average over a depth interval, they are less prone to such distortion. Although the type of 3D MT inversion presented in this report is inherently smooth and experience shows that realistic resistivity slices can be made through the model at a particular elevation, the 3D MT conductance to 600 m (1969 ft) in Figure 17 is provided as a direct comparison to the TDEM conductance to 600 m in Figure 11. Also, it is inherent to all MT and TDEM inversions that the total conductance of a very conductive layer is better resolved than its thickness or its conductivity, so this is the most reliable parameter to display in a map, especially when comparing results from different methods or different types of inversions of a single method.

Figure 17: MT Conductance to 600 m (1969 ft) from 3D Inversion with Cross-Sections

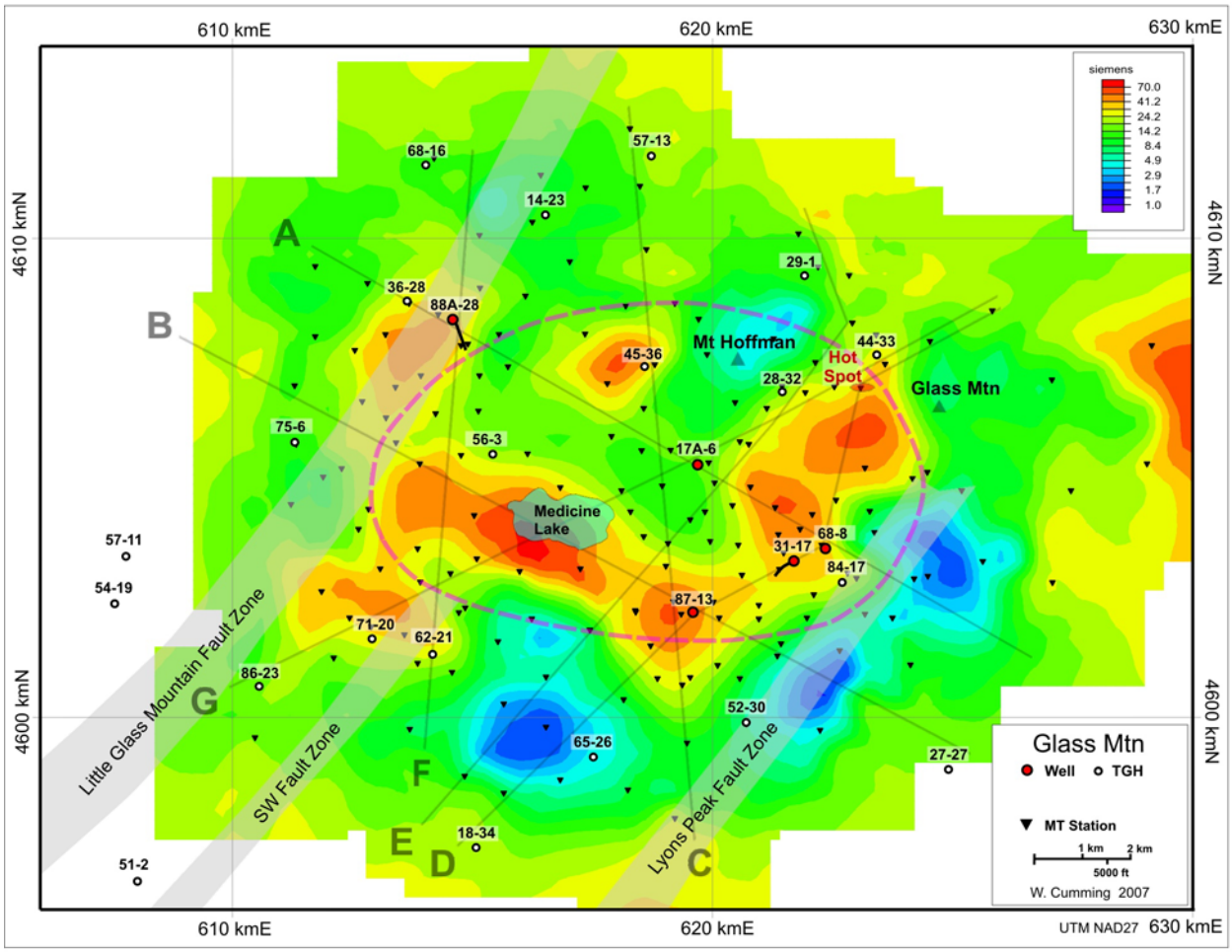

The pattern of MT conductance to 600 m (1969 ft) in Figure 17 is generally consistent with the TDEM conductance in Figure 11. The TDEM sometimes produces an unrealistically high

conductance if the base of the conductive clay cap is shallower than 600 m (1969 ft) and the TDEM fails to detect it. However, in general, the TDEM conductance to 600 m (1969 ft) in Figure 11 seems more reliable than the MT conductance to 600 m (1969 ft) in Figure 17. Figure 11 shows much more intense alteration to the southeast of well 88A-28 than in Figure 17. This pattern is consistent with the Figure 15 comparison of the 3D MT resistivity, 1D MT resistivity, and MeB smectite content in well 88A-28. The 1D MT resistivity curves (that were matched to the TDEM in the static correction) show a minimum resistivity at the MeB smectite maximum but the 3D MT is too deep by over 100 m (328 ft). This misfit results in the lower conductance in Figure 17.

Therefore, such intricate details of the shallow alteration may be better illustrated by TDEM. The map of MT conductance to 600 m (1969 ft) illustrates another potential pitfall in the interpretation of the 3D MT inversion. At data gaps, the 3D inversion determines the resistivity of the underlying model elements based on maintaining smooth resistivity variation and consistency with the dimensional MT implications of the adjacent MT stations. However, to obtain high resolution where the stations are closely spaced, the smoothing of the 3D inversion is relaxed for the entire model and local conductance concentrations sometimes appear between stations. For example, Figure 17 shows a local conductor in a gap to the west of Glass Mountain where a lava flow prevented stations from being acquired. Another conductor is located in gap southwest of 88A-28. Changes made to the smoothing suppressed this tendency and a comparison to the independent coverage of the TDEM in Figures 10 and 11 shows that the 3D inversion results are generally realistic, even at significant data gaps. However, there is a trade-off between smoothing and resolution that is manifested in the slight depth mismatches between the 3D MT inversion and the clay cap in the wells shown in Figures 15 and 16.
The resistivity cross-sections shown in Figure 17 are selected from a much larger number reviewed during the course of the project. The cross-section alignment is based on both conceptual and practical issues. Sections A and D each cross three exploration test wells and, together, they tie all five wells. The other sections are generally aligned to cross the low resistivity features of the map close to MT stations where the 3D inversion model is better constrained by data, although F and G are also directed at tying particular wells.

The color schemes for conductance and resistivity are designed to be conceptually consistent, that is, low resistivity and high conductance are red whereas high resistivity and low conductance are blue. At shallow depth, red tones may indicate shallow smectite alteration over a reservoir. At depths below the expected top of the reservoir, red tones indicate smectite alteration over a deep reservoir or a low permeability area adjacent to a reservoir. Although local variations may be due to imaging artifacts related to MT statics, noise or dimensional distortion, the conceptual consistency of the cross-sections indicate that most of the resistivity patterns in the maps are consistent with the geology.

5.2.2 Maps of Elevation of the Base of the Clay Cap

An important part of most geothermal MT interpretations is a map of the elevation of the base of the low resistivity smectite clay zone because this zone typically conforms to the top of the reservoir (Ussher at al. 2000, Cumming et al. 2000; Uchida, 2005). An apex in the top of a geothermal reservoir is associated with a locus of shallow high permeability and this will

usually correspond to a high point in the base of the clay cap. However, a high point in the base of the clay cap can have other interpretations, such as a change in lithology. Two maps of the base of the clay cap are presented, one based on the 3D inversion and the other on a 1D approach that has been widely used in the geothermal industry (Anderson et al. 2000).

Figure 18: Map of Elevation of the Base of the Clay Cap Based on 3D MT Inversion

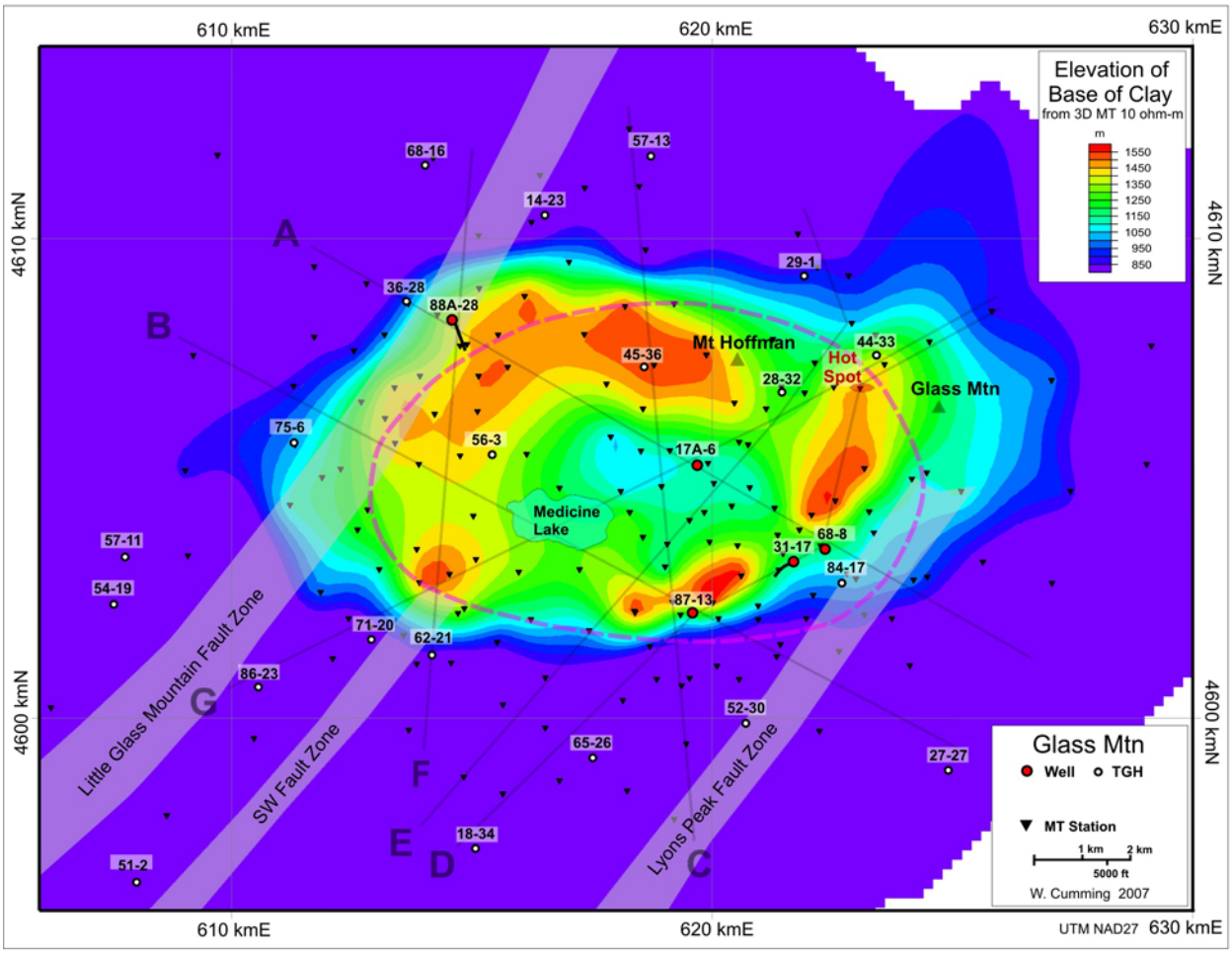

5.2.2.1 Elevation of the Base of the Clay Cap Based on 3D MT Inversion

The map of the elevation of the base of the conductive clay cap based on the 3D inversion in Figure 18 is constructed by measuring the elevation at which the 3D model increases to 10 ohm-m below the low resistivity zone. The measurement is made at the MT stations because the 3D inversion is better constrained there. The map shows a rim of high elevation in the base of the clay cap, located about 500 to 1500 m (1641 to 4922 ft) inside the topographic rim of the Medicine Lake Volcano. Four high areas are highlighted as red and orange zones at elevations of about 1450 to 1550 masl (1450 to 5086 fasl). These correspond to parts of the clay cap that are close to the elevation of the water table. This map does not consider the intensity or quantity of clay alteration, only the elevation of its base. Thus, a comparison to the conductance map

highlights the likely importance of each of the high points in the base of the clay cap. The conceptual implications of this map are best understood by reviewing the MT images in cross-section.

5.2.2.2 Elevation of the Base of the Clay Cap Based on 1D MT Inversion

The map of the base of the low resistivity clay cap derived from 1D inversions shown in Figure 19 might be compared to a photographic imaging method that maximizes contrast at the expense of increased noise. The map in Figure 19 is based on using the average of the static corrected MT resistivity modes to compute a simple 1D model with a few layers, often just a high-low-high resistivity pattern. The depth to the base of the low resistivity layer roughly corresponds to the base of the smectite-rich argillic alteration zone. When the clay cap becomes either less well developed or thicker, the layered model approach tends to make it appear much thicker, providing the high contrast appearance. This approach highlights the area northwest of well 68-8 and detects most of the other areas resolved by the 3D map. It does not resolve a continuous trend from Mt. Hoffman to the southwest past well 88A-28, mainly because the resistivity is relatively high in the gap and the alteration less well developed. The 1D approach did highlight the area southwest of well 88A-28 that coincides with the Little Glass Mountain Fault Zone. The 3D MT conductance in Figure 17 highlighted a similar trend but the 3D MT elevation of the base of the cap only hinted that the area was relatively high in elevation.

The simple 1D approach to mapping the base of the clay cap illustrated by Figure 19 has become a standard for interpreting MT in a geothermal context (Anderson et al. 2000). However, too much emphasis on this particular parameter in both 1D and 3D has conceptual pitfalls. For example, at geothermal fields where a deep developable reservoir flows at an angle upward, a lower temperature reservoir will usually be better resolved than the deeper, higher temperature (and possibly higher value) resource located on its margin. Upflows can be entirely obscured by higher elevation outflows like that illustrated in Figure 3. Such pitfalls can be resolved by considering the implications of such maps for a resource conceptual model based on an integrated interpretation of resistivity cross-sections (Gunderson et al. 2000). Because a 3D MT inversion is available at Glass Mountain and has been integrated with well data, the classic 1D MT base- of- clay map in Figure 19 mainly provides an interpretive benchmark with respect to published geothermal resistivity case histories.

Figure 19: Map of Elevation of the Base of the Clay Cap Based on 1D MT Inversion

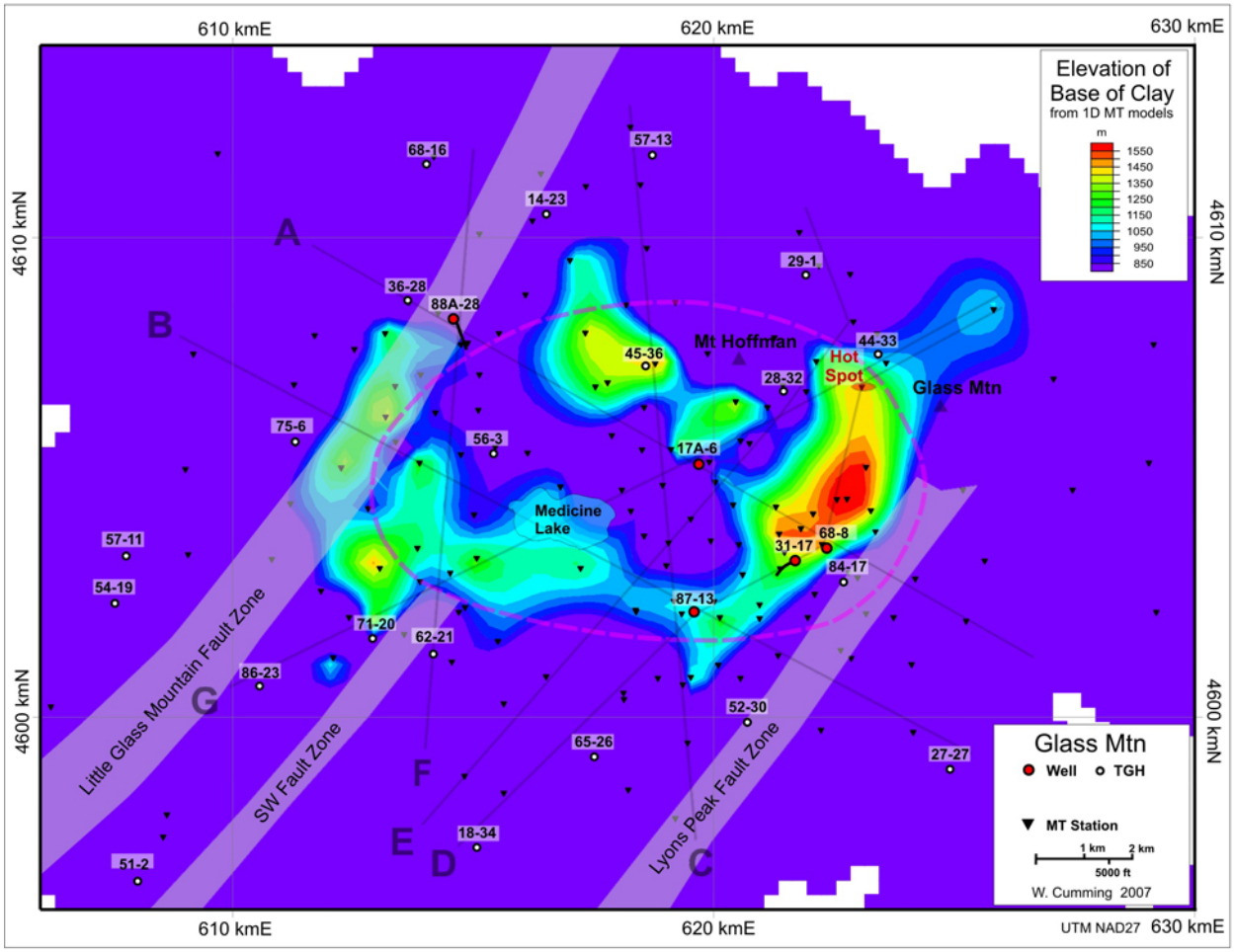

The differences between the 1D and 3D MT approaches to mapping the base of the clay cap are most significant southeast and southwest of well 88A-28 and near well 87-13. In Figure 19, the very low elevation of the 1D base of the cap in the area southeast of well 88A-28 probably reflects relatively high resistivity of clay alteration shown by the conductance map in Figure 17. In the 3D MT elevation map of the base of the cap in Figure 18, well 87-13 is southeast of a high trend in base of the clay cap whereas in the 1D version in Figure 19, it is to the northwest. This is, however, consistent with the approaches used; the 1D MT inversions tends to exaggerate changes near discontinuities.

5.3 MT Resistivity Cross-Sections

Cross-sections usually provide the most effective illustration of the conceptual properties of geothermal systems and of the implications of MT resistivity data for those properties. Cross-sections are particularly effective in integrating MT resistivity and well data into a consistent conceptual model. Two cross-sections are given special attention in this report because they tie the five exploration wells. Detailed parts of these sections are first analyzed with respect to the wells. Extended versions of these two sections and five additional cross-sections with profiles

shown in the maps in Figures 17 to 19 are reviewed with respect to their implications for the geothermal conceptual model at Glass Mountain. The cross-section resistivity data are all derived from the same 3D MT inversion used to prepare the 3D MT resistivity maps.

5.3.1 MT Resistivity Cross-Sections Correlated with Wells

The two cross-sections through the exploration wells, A and D, show the 3D resistivity as a background for temperature, alteration and production data. The temperatures, lithology and alteration data are derived from a variety of sources, primarily EGI's compilations. However, follow-up reviews continue to clarify the details of the temperature interpretation. Improving the consistency of the alteration interpretations of a variety of geologists over a 20 year period is an ongoing project. However, although numerous details and adjustments are likely, the overall pattern of the isotherms shown as solid lines in the figures is representative. The dashed isotherm lines are inferred mainly from the resistivity data. Through their pattern, the isotherms imply a distribution of permeability and, thereby, well targets.

5.3.1.1 MT Cross-Section through Wells 17A-6 and 68-8

The cross-section in Figure 20 extends the correlation of the MT resistivity with well 17A-6 as detailed in Figure 16 to well 68-8. The expected correlation between <5 ohm-m (red) resistivity and the argillic alteration zone is consistent in both wells. The propylitic alteration zone at the top of the 500°F (260°C) reservoir correlates with resistivities of 15 ohm-m (green) at 1200 masl (3937 fasl) and 50 ohm-m (blue) at 800 masl (2625 fasl). This is consistent with the pattern at most geothermal reservoirs, where resistivity corresponding to a particular temperature within a single alteration type tends to increase with depth of burial. The only significant permeable zone is in 68-8 below the >100 ohm-m contour. The relatively low deliverability of well 68-8 may have been caused by the well completion process that involved injecting all of the drill cuttings into the permeable zone in order to dispose of them. The increase in resistivity and thinning of the low resistivity zone over 17A-6 is consistent with the general lack of permeability and alteration observed in this well. The granite in 17A-6 is not resolved by the resistivity, a common pattern where adjacent rocks are compacted and altered at depths over 2000 m and temperatures over 290°C (550°F).

Figure 20: MT Resistivity Detailed Cross-Section A' through Wells 17A-6 and 68-8

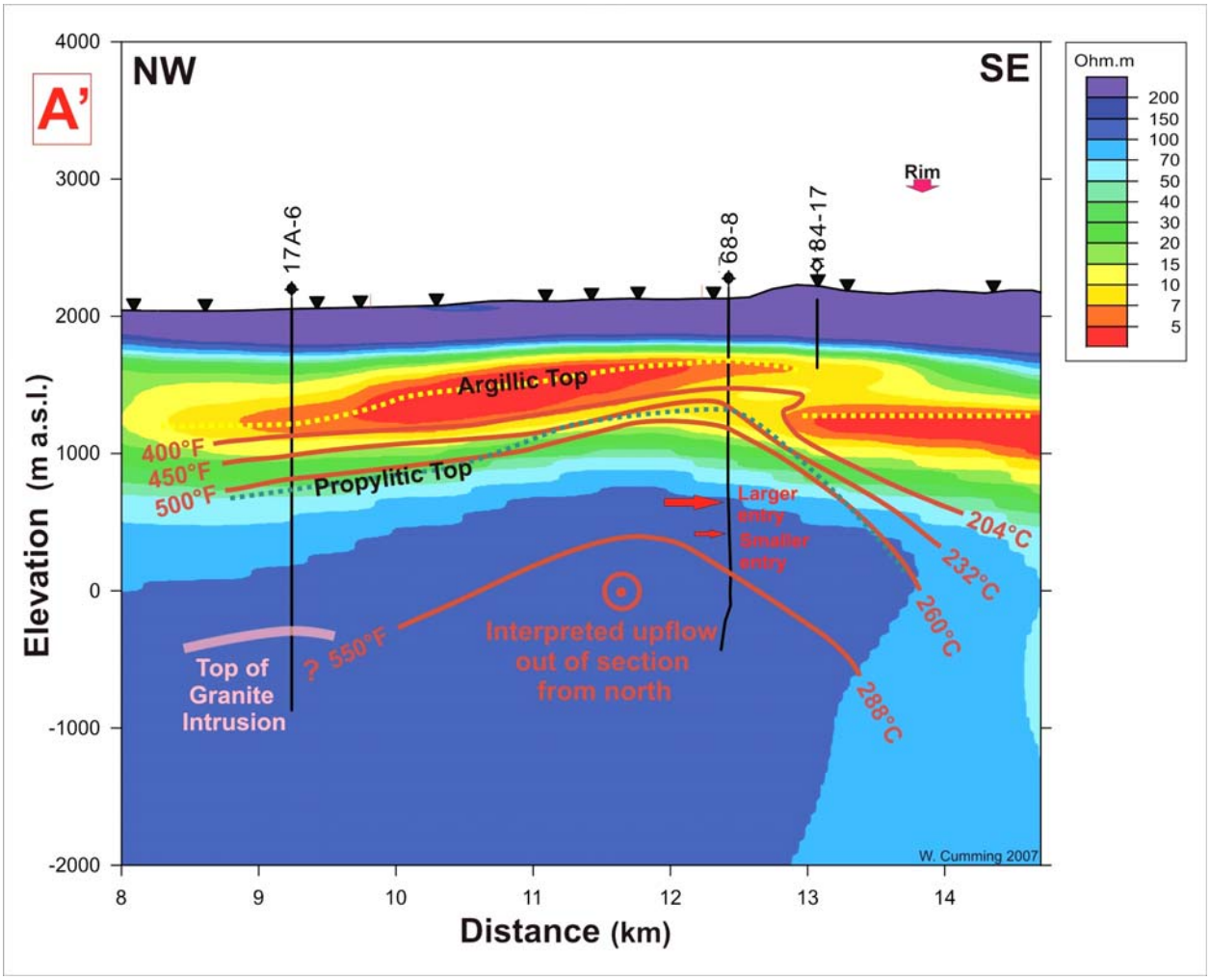

The apex in the 70 ohm-m contour (light blue) about 700 m (2297 ft) northwest of well 68-8 (left of 68-8 on A' in Figure 20) indicates that reservoir permeability is probably higher in this zone. This fits with the very low resistivity in the overlying argillic alteration zone between wells 17A-6 and 68-8, consistent with particularly intense alteration over a more permeable part of the geothermal reservoir. Based on correlations with other maps and sections, it seems likely that this zone is an extension of an upflow that lies north or northwest of the apex in this section.

The <5 ohm-m (red) zone with high clay content is segmented at TGH 84-17. To the northwest, it is correlated with hydrothermal clay alteration. To the southeast, it has the flat lying appearance of a volcanic sediment, probably also hydrothermally altered. A 10 ohm-m (yellow and orange) intermediate resistivity zone at TGH 84-17 marks the overlap of the two low resistivity zones. Similar features are imaged by the 3D inversion in two other areas where the deep and shallow resistivity zones meet. However, it is detected by only one or two stations and does not appear in 1D and 2D inversions, so it may be an artifact of the inversion. The sensitivity of the 3D inversion is dominated by the much more significant discontinuity

between the shallow and deep low resistivity (red) zones near well 84-17 that is unambiguously resolved and marks a significant structure. Additional MT stations with low noise and static distortion would be needed to reliably resolve the more subtle 10 ohm-m transitional feature that might be important to understanding permeability related to the larger structure.

The overall pattern of the resistivity and isotherms indicate that the Lyon's Peak Fault Zone and the Medicine Lake Volcano rim are boundaries to deep flow and are unlikely to be permeable at elevations below 1000 masl (3281 fasl). Both wells 17A-6 and 68-8 appear to be on the margins of a reservoir upflow that, based on the map of conductance and maps of the elevation of the base of the clay cap, probably lies to the north or northwest of cross-section A'. The interpretation in Figure 20 concludes that, with the highest temperature upflow to the north of this section, the hot water flows at about 290°C (550°F) in a southwest trending zone of permeability.

Figure 21: MT Resistivity Detailed Cross-Section D' through Wells 87-13, 31-17 and 68-8

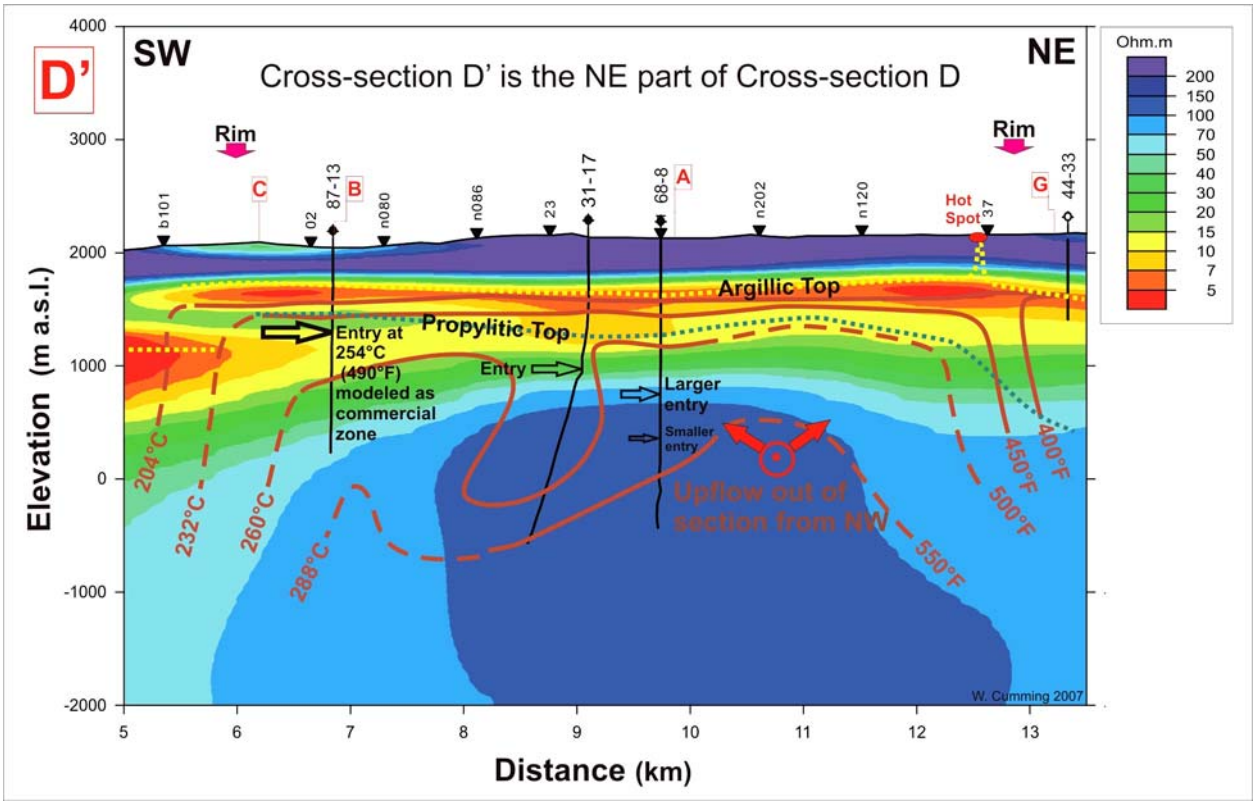

3.2.1.2 MT Cross-Section through Wells 87-13, 31-17 and 68-8

Cross-section D' (Figure 21) includes several bends (Figure 18) so that it ties the borehole temperature and alteration patterns in exploration wells 87-13, 31-17 and 68-8 and TGH 44-33 to the 3D MT resistivity. The boundary of the Medicine Lake Volcano ring fracture system is sub-parallel to this cross-section, 500 to 1000 m (1641 to 3281 ft) to the southeast. The label "D" in Figure 20 shows where cross-sections A' and D' intersect near an abrupt discontinuity in the low resistivity zone. Although cross-sections that parallel geologic strike close to such

discontinuities often exhibit off-trend irregularities that make it a poor choice for illustrating a resource conceptual model, cross-section D' summarizes the relationship between alteration, temperature and resistivity on the east side of the Glass Mountain resource.

The correlation of borehole temperatures and alteration with the resistivity pattern in cross-section A' is consistent with the smectite-illite model for geothermal resistivity interpretation. The top of the <10 ohm-m (yellow to red) argillic alteration zone characterized by high smectite content is at about 1650 masl (5414 fasl). Below the base of the (red) low resistivity argillic zone, the top of the propylitic alteration correlates with >10 to >15 ohm-m (blue to yellow) resistivity. The propylitic alteration is shallow at about 1500 masl (4922 fasl) at well 87-13 and dips down to 1300 m (4265 fasl) near well 31-17 where relatively low 7 to 10 ohm-m (orange) resistivity also extends to greater depth. The most permeable entry at Glass Mountain is 200 m (656 ft) below the base of the argillic clay cap in well 87-13, near the base of the 15 to 20 ohm-m (green) zone from 1250 to 1500 masl (4265 to 4922 fasl). The tabular 15 to 20 ohm-m zone appears to extend to the southwest of 87-13, although this is not well resolved because of a gap in coverage between MT stations 02 and b101. Resistivity decreases slightly to 10 to 15 ohm-m (yellow) below the entry in well 87-13. Hydrated smectite alteration is unlikely to account for such a decrease in resistivity at a temperature over 250°C (482°F) but some types of higher temperature mixed clays might (Flóvenz et al. 2005) and chlorite alteration derived from smectite is reported in the reservoir (Carrier, 1989b). Such smectite-derived alteration might correlate with lower permeability. Southwest of well 87-13, the reservoir is closed off by a 700 m thick <7 ohm-m (red) zone that extends from 500 to 1200 masl (1641 to 3937 fasl). This is interpreted as thick argillic alteration of low permeability volcanics. Although the correlation of low resistivity with the low permeability smectite clay cap works in a straightforward manner for this cross-section, the interpretation of isotherms requires a more subtle integration of data.

The conceptual interpretation of upflow presented in Figure 21 is not based on MT alone but on the integration of the temperature, permeability, petrography and MT resistivity data. One upflow is postulated to exist about 1000 m (3281 ft) northeast of well 68-8 and another to the north of well 87-13. A distributed uneven upflow along a fault trend just to the northwest of the line of section of A' is also compatible with the data. The temperature pattern in well 44-33 is consistent with it being beyond the upflow, close to an impermeable edge to the system, but with a more gradual resistivity closure than at most margins related to the rim structure.

Well 31-17 is slightly cooler than wells 68-8 and 87-13. Because profile A' parallels the outer rim to the southeast and the structural trend interpreted to the northwest, such conceptual inconsistencies are expected. Although the temperatures in 31-17 are near-boiling at the top of the propylitic zone (Lutz et al. 2000), they decline from >250°C (482°F) at 1138 masl (3732 fasl) to 236°C (457°F) near the entry at about 985 masl (3230 fasl). Therefore, the shallow part of the well is apparently heated by an upflow north or northwest of the southwesterly deviated course of well 31-17. The resistivity is also slightly lower and the transition to propylitic alteration slightly deeper at 31-17, consistent with this well being located farther from an upflow than wells 68-8 or 87-13. Due to difficult terrain, there is a gap in MT coverage east and west of 87-13 that

should be made a higher priority in any follow-up MT survey in order to constrain the conceptual origin of the cool 236°C (457°F) zone at 985 masl (3230 fasl) in 31-17.

5.3.2 MT Resistivity Cross-Sections and Reservoir Geometry

A larger scale view of implications of the MT resistivity pattern for geothermal exploration at the Glass Mountain KGRA is illustrated by the seven resistivity cross-sections, A to G, in Figures 22 and 23. Figures A and D are extensions of the cross-sections already discussed. The northwest extension of A has important implications for the interpretation of well 88A-28 but the extended version of cross-section D is mainly included to allow for easier comparison to the other sections.

Figure 22: Cross-Sections A, B and C with 3D MT Resistivity and Isotherm Conceptual Model

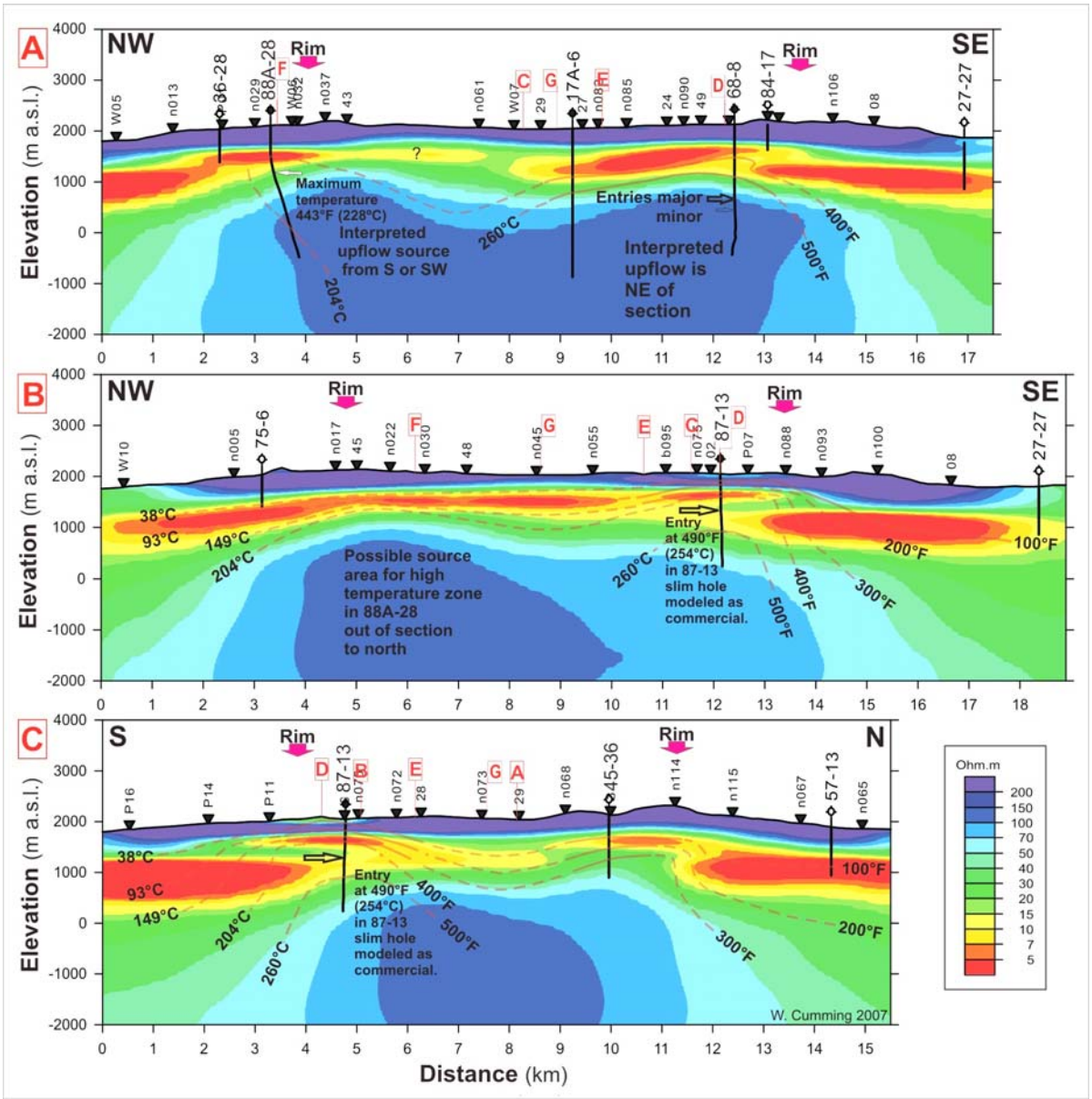

5.3.2.1 Cross-Section A with 3D Resistivity and Interpreted Isotherms

Cross-section A in Figure 22 includes only a few isotherms to illustrate how the Telephone Flat area to the southeast compares to the Fourmile Hill area in the northwest. The isotherms in the Telephone Flat part of this cross-section are discussed in Section 5.3.1. The pattern of the isotherms at Fourmile Hill includes elements of both the model for the resource proposed in Calpine-Siskiyou Geothermal Partners L.P. (2004) and an earlier model described in that report. The 204°C (400°F) isotherm mimics the shape of the deeper >100 ohm-m (blue) contour and shows a slight increase in resistivity where temperatures are lower and smectite alteration reappears near the bottom of the well. This shape might imply an upflow from the southeast although the lower intensity of overlying argillic alteration at MT stations n037 and 43 favoured the interpretation that the high temperature zone detected by well 88A-28 is more likely to originate from an upflow to the south or southwest.

5.3.2.2 Cross-Section B with 3D Resistivity and Interpreted Isotherms

Cross-section B in Figure 22 illustrates a possible source area for the high temperature zone in well 87A-13. Unfortunately, this cross-section has some significant data gaps larger than the projected MT stations would indicate. The section also shows well 87-13 from another perspective and it looks much the same as it does in cross-section D', with slightly better MT coverage making the 15 to 20 ohm-m (green) zone at about 1300 masl (4265 fasl) seem more reliable, although still possibly just an artefact of the lateral smoothing in the inversion.

5.3.2.3 Cross-Section C with 3D Resistivity and Interpreted Isotherms

Cross-section C illustrates the resistivity and temperature pattern on the north and south rims of the Medicine Lake Volcano. This is another cross-section in which well 87-13 looks like its entry is located at the base of a tabular 15 to 20 ohm-m reservoir zone below the <10 ohm-m clay cap. The generally similar zone on the north rim consists of a flat argillic cap at the water table overlying an aquifer with temperatures greater than the >150°C (300°F) encountered in TGH 45-36. Based on its temperature gradient, the well seems unlikely to reach temperatures over about 200°C (400°F) at depths less than 1500 m (4922 ft). Temperature could be higher near the rim because this zone does not have low resistivity clay beneath it that would indicate a decrease in temperature with depth. The thick <7 ohm-m (red) zone that appears to encase the area within the ring fracture is more sharply defined in this cross-section than in profiles A and B.

5.3.2.4 Cross-Section D with 3D Resistivity and Interpreted Isotherms

Cross-section D in Figure 23 is provided for comparison to the other cross-sections at this scale but all of the elements in this figure are addressed in the discussion of cross-section D' above.

5.3.2.5 Cross-Section E with 3D Resistivity and Interpreted Isotherms

Cross-section E in Figure 23 illustrates the resistivity pattern along the line of stations west of the upflow interpreted beneath the Glass Mountain rhyolite flow northwest of well 68-8. Because no MT stations could be recorded on the rhyolite flow, this line also borders the upflow rather than actually imaging it. Nevertheless, the resistivity pattern shows very intense alteration and a local high in the base of the <7 ohm-m (red) clay cap between wells 17A-6 and 28-32, consistent with an upflow existing southeast of this cross-section.

Figure 23: Cross-Sections D, E, F and G with 3D MT Resistivity and Isotherm Conceptual Model

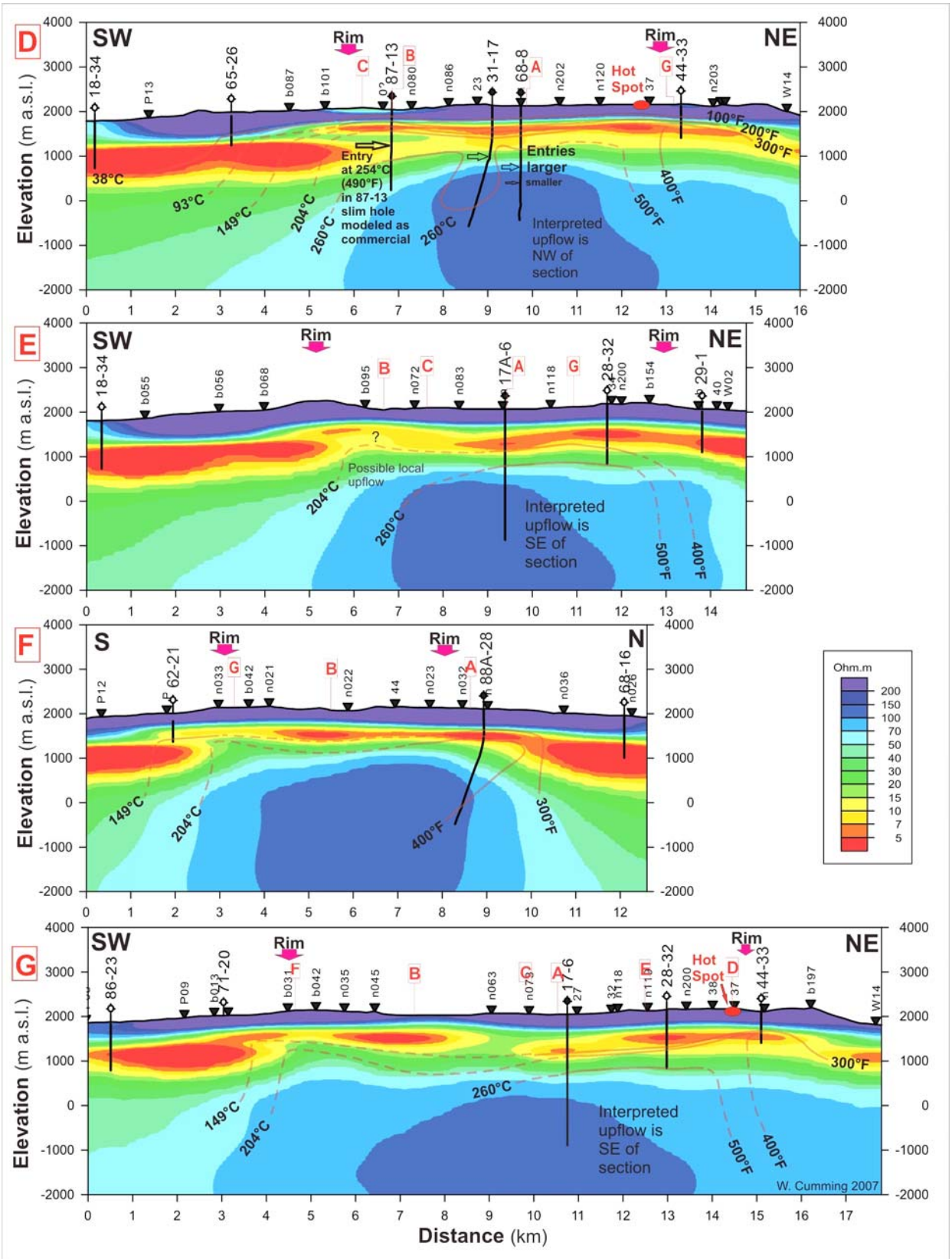

5.3.2.6 Cross-Section F with 3D Resistivity and Interpreted Isotherms

Cross-section F in Figure 23 trends through well 88A-28 and then south along the high in the base of the clay cap mapped in Figure 18. Well 62-21 at the south end of the line outside the volcanic rim has a maximum temperature of 149°C (300°F), consistent with it just penetrating the 700 m (2297 ft) thick <7 ohm-m (red) clay-rich zone close to the intersection of the SW Fault Zone and the rim to the north.

5.3.2.7 Cross-Section G with 3D Resistivity and Interpreted Isotherms

Cross-section G illustrates the pattern of resistivity and temperature at wells 86-23, 17-6, 28-32 and 44-33, with the interpreted high temperature upflow located just southeast of the line of section between wells 17-6 and 44-33, compatible with the measured temperature in 28-32.

5.4 MT Resistivity Maps

5.4.1 Interpreting Resistivity Maps at Different Elevations

Maps of resistivity extracted from the 3D MT inversion at a particular elevation (horizontal slices) can be tied to the cross-sections to understand the map patterns of conceptual elements identified in the cross-sections. Resistivity slices at four elevations, sea level, 1000 m, 1600 m and 1700 m, demonstrate most of the elements of the conceptual model.

Figure 24: Map of 3D MT Resistivity at Sea Level

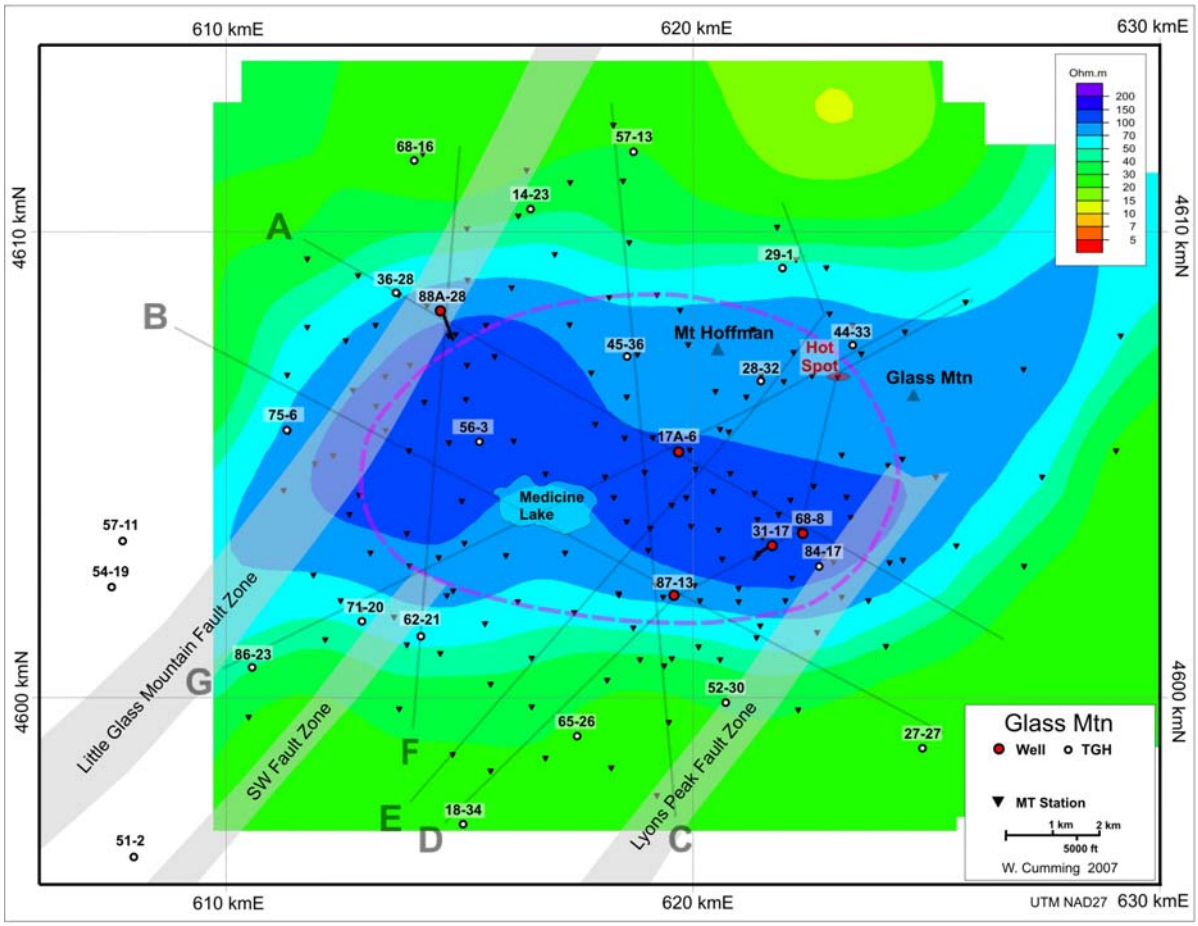

5.4.1.1 MT Resistivity at Sea Level

The map of resistivity at sea level in Figure 24 illustrates the smooth variations in deep resistivity resolved by the 3D MT inversion. Compaction, induration and alteration tend to homogenize rock properties in the propylitic alteration zone at intermediate values of 20 to 200 ohm-m (green to blue). The most likely explanation of the pattern of resistivity over 70 ohm-m in Figure 24 is that it includes indurated rocks in the propylitic alteration zone and granite intrusive. The east and west edges and the diversion of the contours near Medicine Lake correlate more strongly with the northeasterly trending regional structures than with the Medicine Lake Volcano rim structure. Although much lower resistivity would not be expected in a >290°C (550°F) upflow, the area of the proposed upflow zone northwest of well 68-8 has slightly lower resistivity than the average within the rim structure.

Figure 25: Map of 3D MT Resistivity at 1000 masl (3281 fasl) with Gravity Contours

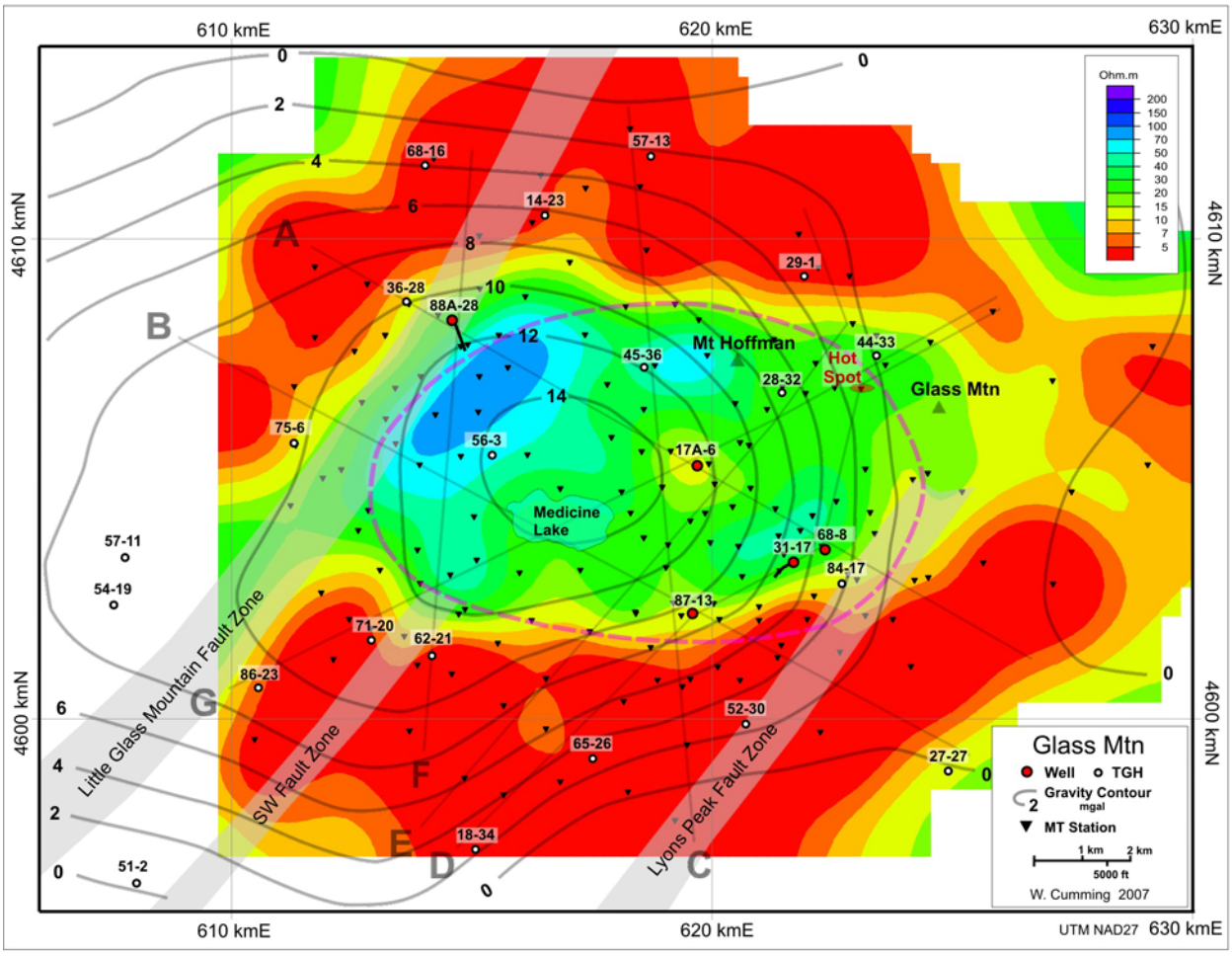

5.4.1.2 MT Resistivity at 1000 m (3281 ft) Elevation

The map of resistivity at 1000 masl (3281 fasl) in Figure 25 illustrates the distribution of a thick tabular <7ohm-m (orange-red) layer almost surrounding the rim of the Medicine Lake Volcano. The top of this 500 to 1000 m (1641 to 3281 ft) thick layer is generally above elevation 1500 masl

(4922 fasl) (Figures 15 and 22). It consists of porous but largely impermeable volcanics that form a barrier to flow around most of the volcanic rim. Its low resistivity is due to zeolite-smectite and argillic alteration. The apparent discontinuity in this barrier at the Glass Mountain Fault Zone may be just due to a gap in the MT data coverage, not to a gap in the clay alteration. On the west and northwest side of the topographic rim at the summit, the margin of the clay slab (red area in Figure 25) does not coincide with the rim as it does along the rest of the rim perimeter where there is enough MT data to constrain it. Near well 88A-28, the margin of the clay slab roughly parallels the topographic rim but over 1000 m (3281 ft) further west.

The TGH and exploration well temperature patterns are consistent with the interpretation of the <7 ohm-m (red) area in Figure 25 as a low permeability zone encasing the reservoir. None of the wells indicate significant fluid movement within this zone. TGH 44-33 lies at or just within this clay margin. Figure 21 shows that, in 44-33, about 450 m of cool, high permeability, high resistivity, unaltered surface volcanics overly a zone of impermeable clay less than 100 m (330 ft) thick that overlies, in turn, a 202°C (395°F) temperature peak indicative of minimal permeability in a zone thinner than 50 m (170 ft). Temperature decreases in the underlying low resistivity, impermeable altered zone. TGHs 62-21 and 84-17 are outside the rim and their cool permeable zone overlies a less abrupt increase in temperature to less than 150°C (302°F) in the impermeable clays, compatible with an impermeable area being heated by conduction without significant fluid movement. TGHs 27-27, 18-34 and 86-23 are located even farther from the rim and so the cool, permeable, unaltered surface volcanics are much thicker. The greater depth to the low resistivity, low permeability zone makes these appear to be on the edge of the <7 ohm-m (red) zone in Figure 23. The impermeable zone shows a more modest temperature increase to less than 100°C (212°F). Such a temperature profile on a volcano could be accounted for by heat conduction through low permeability rocks. In any case, the <7 ohm-m (red) area in Figure 25 is unlikely to host a >200°C (392°F) conventional geothermal resource.

The gravity contours shown in Figure 25 are filtered to remove the regional trend and minimize the effect of density variation in the topography in the gravity map from Wheeler (1985). The correlation of the 12 milligal gravity high centered north of Medicine Lake with the resistivity pattern in Figure 25 is consistent with Fink and Williams (1982) who modeled the high values of gravity as a dense intrusion within the rim surrounded by lower density volcanic materials. However, the wells and resistivity data indicate that the high density material is likely to include both granite intrusions like that encountered in well 17A-6 and the indurated volcanics in the propylitic alteration zone. The lower density volcanics would include both the thick, porous, clay-rich <7 ohm-m (red) zone in Figure 25 and, perhaps, some shallow rim volcanics.

The >70 ohm-m (blue) zone southeast of well 88A-28 in Figure 25 appears in cross-section A of Figure 22 to be a potential upflow source for the high temperature zone detected in well 88A-28. Smaller highs are located near TGH 45-36 and well 31-17. These high resistivity zones cannot be reliably attributed to low porosity granite. The granite in well 17A-6 (Figure 20) is over 700 m (2297 ft) deeper that the 70 ohm-m contour and 350 m (1148 ft) deeper than the 100 ohm-m contour. In cross-sections A' and D' (Figures 20 and 21), the transition to propylitic alteration occurs at resistivity lower than 70 ohm-m except in deeper, lower permeability parts of the

reservoir, for example, near well 17A-6 in Figure 20. Although the TDEM conductance to 600 m in Figure 11 seems to indicate more intense shallow alteration both southeast and southwest of 88A-28, the resistivity pattern in cross-section A does not detect an intensely altered clay cap to the southeast, as would be expected over a permeable upflow. Therefore, the high temperature zone in 88A-28 is more likely to originate from an upflow located to the south or southwest and less likely from an upflow associated with the >70 ohm-m zone in Figure 25 to the southeast.

5.4.1.3 MT Resistivity at 1600 m (5250 ft) Elevation

The map of MT resistivity at 1600 m (5250 ft) elevation in Figure 26 illustrates the resistivity pattern just below the water table in most parts of the map. Although many of the lowest values of resistivity are imaged in gaps between stations, the overall pattern seems valid. According to the isotherm interpretations of the cross-sections in Figures 22 and 23, the <7 ohm-m (red) contour probably corresponds to the clay cap over geothermal reservoir zones, albeit not necessarily the highest permeability part of such zones. The area southwest of well 88A-28, extending south to the rim north of 62-21 roughly defines the prospective Fourmile Hill and Southwest areas. The resistivity pattern near well 45-36 fits the Clausen et al. (2006) interpretation that the intense alteration and moderate temperature in 45-36 is due to an earlier hydrothermal system that has cooled. The <7 ohm-m contour bounding TGHs 44-33 and 28-32 and wells 87-13 and 68-8 outlines the conceptual resource that includes the Telephone Flat area.

Figure 26: Map of 3D MT Resistivity at 1600 masl (5250 fasl)

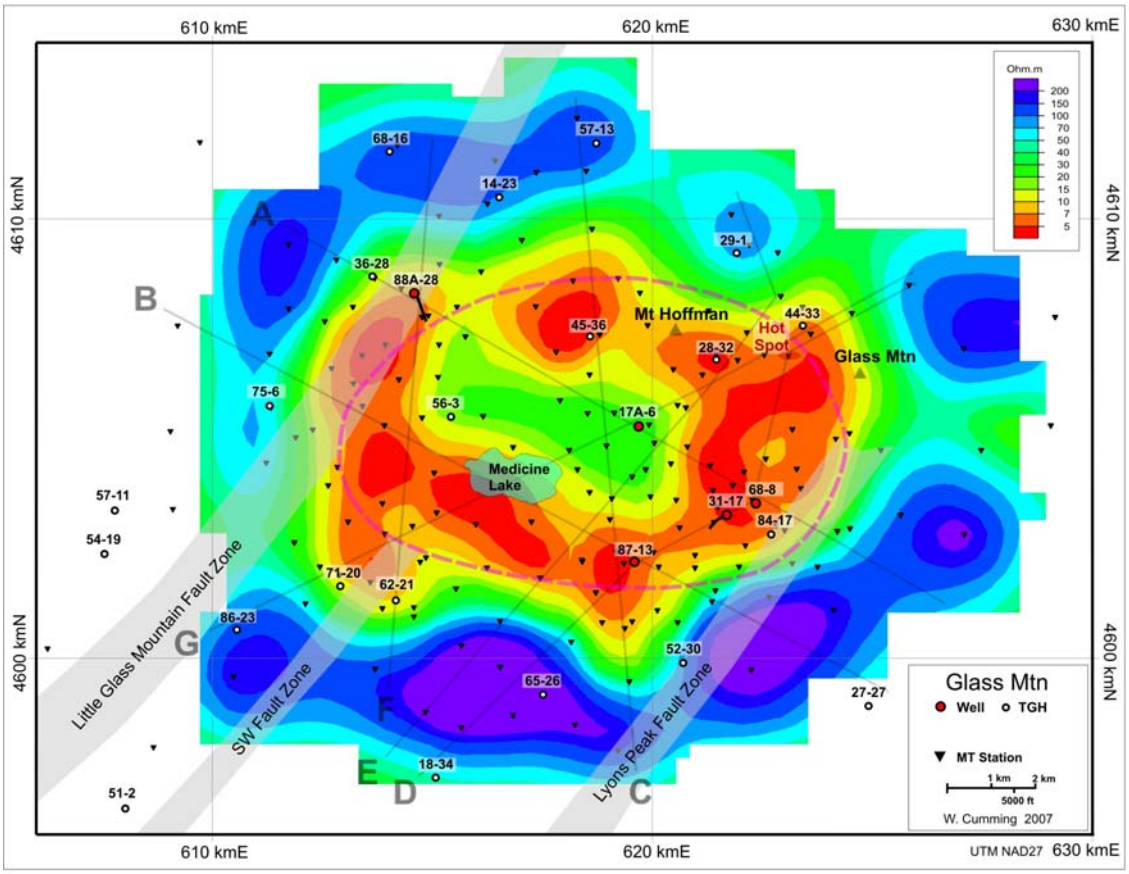

5.4.1.4MT Resistivity at 1700 m (5578 ft) Elevation

The map of MT resistivity at 1700 masl (5578 fasl) in Figure 27 illustrates the resistivity pattern just above the water table at Glass Mountain. Three areas are highlighted; 1) the trend from TGH 44-33 through the Telephone Flat area to well 87-13, 2) the area near 45-36, and 3) the area where the SW Fault intersects the rim. The first trend has two sub-sections, one around 87-13 in the south and the other centered north of 68-8. Alteration above a water table is consistent with boiling in the reservoir as Lutz et al (2003) indicated might be occurring at the top of the propylitic altered zone in well 31-17. The boiling indicated by the resistivity imaging must have occurred in geologically recent times but it is not necessarily occurring now. Although a lack of thermal manifestations over a currently boiling system is unusual, it is consistent with the very coherent clay cap isolating the reservoir from the surface described by Hulen and Lutz (1999).

Figure 27: Map of 3D MT Resistivity at 1700 masl (5578 fasl)

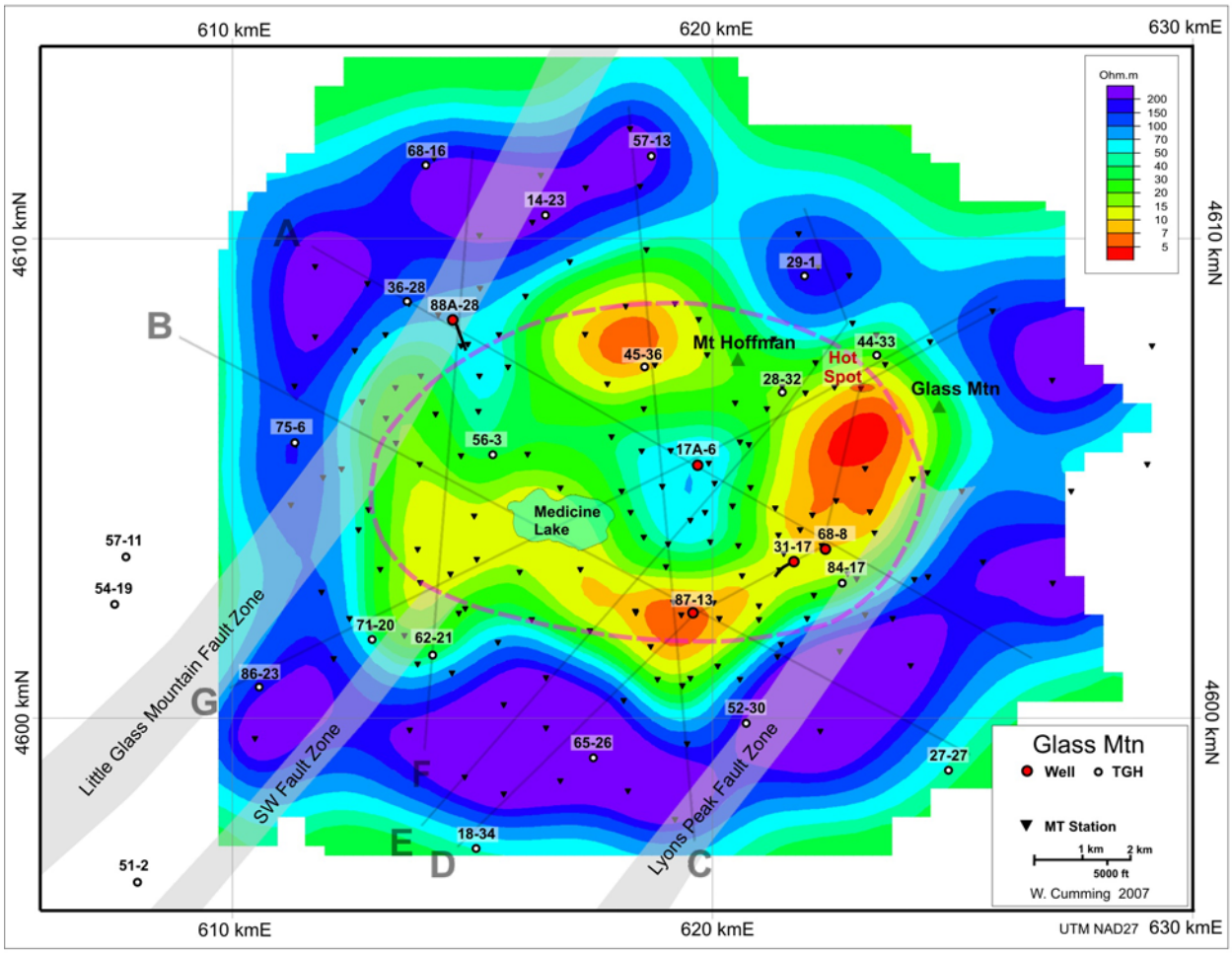

5.5 Integrated Geothermal Resource Interpretation

A wide variety of geoscience information has been considered in the process of interpreting the Glass Mountain MT resistivity images and so no separate integration step is needed. However,

because the elements of the conceptual model discussed in this report are unusually numerous, Figure 28 summarizes them.

5.5.1 Geothermal Resource Conceptual Model Elements

The elements of the Medicine Lake geothermal conceptual model detailed in Figure 28 are color coded. The red shades are the elements that are higher priority for well targeting. The green elements are features that are similar to the red ones but, for a variety of reasons are expected to be higher risk as drilling targets. The blue shading highlights areas that evidence more intense alteration near the top of the clay slab that encases the reservoir. The cross-sections are shown as profiles and their relevance can be inferred by the elements that they intersect. Charts are also considered Figures, and should be numbered sequentially.

Figure 28: Summary map of Conceptual Model Elements

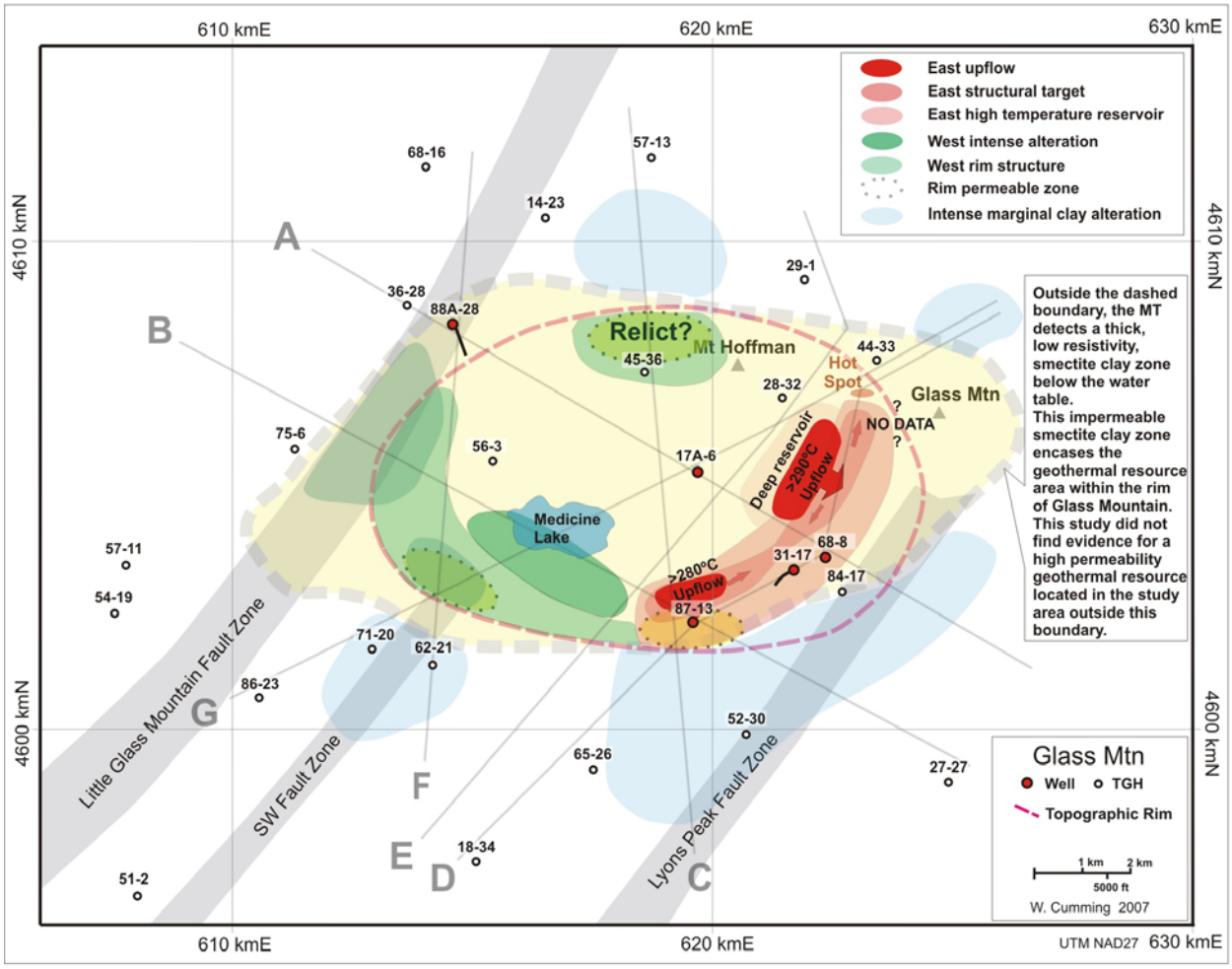

5.5.1.1 Background Geology

The background geology includes the fault zones, the volcanic rim, and the Hot Spot thermal manifestation, items that have appeared on every map in the report and influence all of the

other elements. For example, both the northeast trending fault zones and the Medicine Lake Volcano rim structure have an important influence on both permeable zones and boundaries. The mapped structures and resistivity geometry are consistent with a model of Medicine Lake Volcano as behaving more like a subsiding pull-apart zone than a Cascades volcano. The major fault zones in Figure 28 influence permeability associated with structures inside the rim of the volcano. The Lyons Peak Fault Zone may step left to account for the proposed permeability trend shown in red from well 87-13 northeast past well 68-8. The SW Fault Zone and Little Glass Mountain Fault Zone appear to be associated with permeability where they intersect the rim. The mapped faults do not host >200°C (392°F) geothermal reservoir permeability, except possibly in the case of Little Glass Mountain Fault Zone. However, they do define boundaries like the east and west sides of the thick clay layer that appears to form the outer boundary of the prospect area, shown as a dashed line in Figure 28.

5.5.1.2 Surrounding Clay Alteration Layer Boundary

A low resistivity, low permeability clay-rich slab is found outside of the dashed line in Figure 28, surrounding the rim of the Medicine Lake Volcano. The top of the clay slab is close to the water table above 1500 masl (4922 fasl) and, with a thickness of up to 1000 m (3281 ft); it isolates the reservoir within the volcanic rim. High resistivity rocks overlying the clay alteration are probably generally permeable but cold, consistent with a cold "rain curtain" above clay alteration as described by Hulen and Lutz (1999). Beneath the clay-rich slab of volcanics, some TGHs encountered cold water and then conductive regional thermal gradients. In others, the clay slab appears to be heated conductively by the nearby reservoir. Because of low permeability inferred from temperature patterns, alteration and resistivity imaging, the area outside the dashed line in Figure 28 would be very high risk for targeting a conventional geothermal production well.

5.5.1.3 More Intense Alteration in the Impermeable Clay Margins

Four areas shaded blue in Figure 28 outline areas with exceptionally low resistivity or shallower low resistivity in the upper part of the impermeable slab outside the dashed boundary. This very likely indicates more intense smectite alteration. In a manner analogous to the more intense alteration in the impermeable clay cap over a particularly permeable part of a reservoir, more intense smectite alteration can develop adjacent to permeable zones.

5.5.1.4 Geothermal Reservoirs Outside the Rim Fracture

A zone shaded in green in Figure 28 is located on the west margin where the rim intersects the Little Glass Mountain Fault Zone. Because the deep clay slab is imaged by the MT only on the west side of the fault zone more than 1000 m (3281 ft) outside the rim, the possibility of an upflow in the fault zone is considered in the shading. This is a candidate source area for the high temperature zone intersected by well 88A-28 to the northeast. However, the maximum temperature measured in the area is 238°C (460°F) in TGH 88-28 and the maximum geothermometry from 88A-28 production is 249°C (480°F), both much lower than temperatures at Telephone Flat. Moreover, the limited number of wells and sparse MT coverage makes the interpretation less reliable. Therefore, although the Fourmile Hill and western areas are

attractive exploration prospects, they are higher risk targets than those in the Telephone Flat area.

5.5.1.5Upflow in the Telephone Flat Area near the East Rm

The areas highlighted in red include the lowest risk geothermal exploration well targets based on the technical information presented in this report. Access, regulatory and long term development issues are not addressed here. There are six sub-areas shaded red; two upflows, a deep reservoir, a linear permeable zone, a lower permeability margin where wells 68-8 and 31-17 are located, and a possible zone of higher shallow permeability.

This area is lower risk both because of its superior indications of a geothermal reservoir and because the greater number of wells and closer spacing of MT and TDEM stations reduces uncertainty. The Telephone Flat prospect has the largest area of shallow argillic alteration detected by MT and TDEM in the Glass Mountain KGRA. The intensity and pattern of alteration are consistent with the existence of two nearby upflow zones. This is similar to the rationale that initially led to drilling at Telephone Flat and it is still valid even though the existing wells have modest productivity. Besides the likelihood that their productivity is adversely affected by the injection of drill cuttings, the existing wells are marginal to the lowest risk target areas identified by the 3D MT resistivity imaging.

A deep >288°C (550°F) upflow must exist to support the high temperature zones encountered in well 68-8 at 288°C (550°F) and in well 31-17. The Glass Mountain rhyolite flow prevents the acquisition of MT data that could more narrowly define an upflow target northwest of 68-8, but the location plotted in Figure 28 is conceptually reasonable. It would likely be associated with structures above a cooling dike intrusion. Targeting risk can be mitigated by drilling directionally across the apex in the base of the low resistivity cap, toward the upflow location.

The upflow area has an arrow that implies up-dip flow (as in cross-section A') connecting to a narrow NE-trending zone of fracture permeability shown in Figure 28. This interpretation is based on the elevation of the base of the clay cap from the 3D MT inversion in Figure 18 and from conductance and resistivity maps illustrating intense shallow smectite alteration. Around this zone is a lighter red area that outlines the reservoir that wells 68-8, 31-17 and 87-13 penetrated. Wells 68-8 and 31-17 had sub-economic permeability but this may be because they were adversely affected by cuttings disposal or they were drilled on a high temperature zone adjacent to the main structural upflow.

Well 87-13 is of great interest because reservoir engineering analyses indicated that it probably penetrated the most permeable >220°C (428°F) zone drilled at Glass Mountain. As cross-section D in Figure 21 illustrates, the most permeable zone in well 87-13 may be correlated with the base of a relatively high resistivity zone. The measured temperatures and resistivity trends indicate that 87-13 is likely located just south of an upflow zone.

5.5.1.6 West and North Drilling Target Areas

Several areas are highlighted in green in Figure 28 that are conceptually similar to the features highlighted in red but have higher drilling risk. To some extent, the higher risk can be

attributed to higher uncertainty where a fewer number of wells are already drilled and where a lower density of MT and TDEM stations provide less confidence in the interpretation. However, there is also an important conceptual component to the risk. The resistivity features that define the areas shaded in green are generally less prominent. Well 88A-28 and the surrounding TGHs encountered lower temperature than the comparable examples near Telephone Flat. Therefore, although the features shaded in green have conceptual similarities to Telephone Flat, they are likely to have higher drilling risk. The absolute risk can be reduced by collecting more MT data or by drilling sufficient resource capacity at Telephone Flat to sustain a power plant, although that would not change relative risk. Source: Oil Price Information Service (OPIS).

Figure 29: Resolution of Conceptual Model Elements and MT Station Coverage

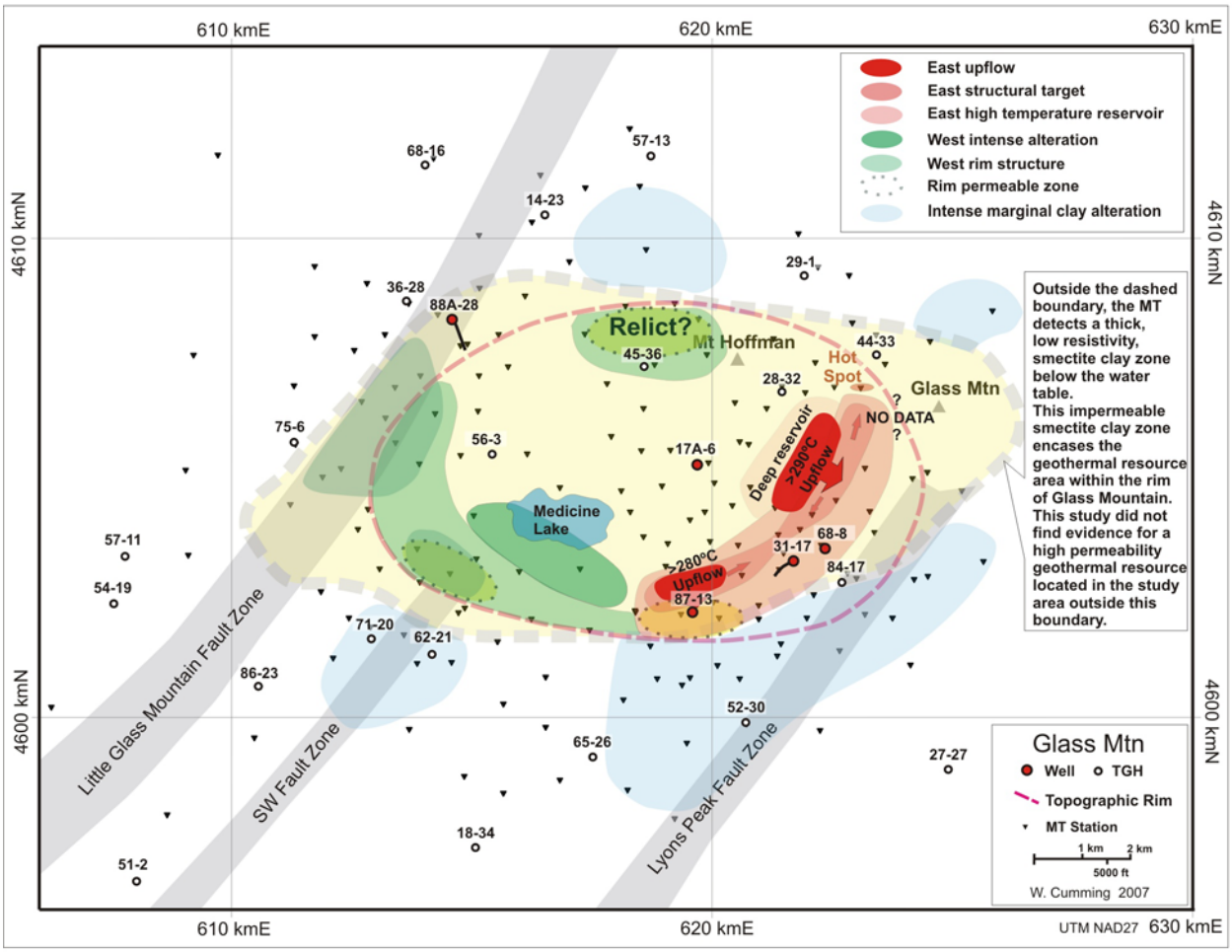

5.5.2 Conceptual Model Uncertainty

Although various MT inversion sensitivity parameters can indicate what parts of an image are best constrained by the MT data, a more intuitive understanding of the uncertainty in the conceptual model can be assessed by reviewing issues that most affect the MT resolution. This includes the MT station distribution and the MT data reliability summarized in Appendix A.

The uncertainty in the conceptual model derived from the MT is primarily illustrated by its consistency with well data. Because data besides the MT and TDEM are integrated into this interpretation, a review of the MT resolution alone would exaggerate uncertainty. For example, the lack of MT stations on the Glass Mountain rhyolite flow makes the location of the upflow uncertain but, because the isotherms require that an upflow be located in the vicinity, inferences drawn from neighboring MT stations are relevant. In any case, even if the upflow is located, say, beneath the Glass Mountain summit, the best place to target a high temperature zone adjacent to it is probably still at the nearest apex of the clay cap, which would still be northwest of well 68-8. The uncertainty in the upflow location does affect the risk of reaching higher temperature. However, in targeting such wells, there is a trade-off between the benefit of higher temperature at greater depth and the probability that permeability will decline with depth. A reservoir engineering analysis could help resolve this trade-off.

CHAPTER 6:
Conclusions and Recommendations

6.1 Conclusions

All of the conceptual goals of the project were met despite the long initial delay related to permitting difficulties and the challenges overcome during the course of the work, including recovering the legacy data, acquiring new MT data, imaging the 3D resistivity pattern, and interpreting a conceptual resource model consistent the well data.

6.1.1 Resource Imaged Using MT and TDEM Resistivity

6.1.1.1 Compiled and Imaged Resistivity and Integrated It with Well Data

All of the available resistivity data were reviewed and an optimized subset was extracted and optimized for comparison to supporting data sets. The preparation of the conceptual model emphasized the resistivity data and the well information including alteration, temperature and productivity. Analyses of wells 88A-28 and 17A-6 provided a detailed correlation between MT resistivity and alteration, temperature and permeability.

6.1.1.2 Confirmed Application of Smectite-Illite Approach to Geothermal Resistivity Interpretation

The detailed correlation of resistivity imaging with well data confirms the applicability of the smectite-illite clay approach to interpreting resistivity at Glass Mountain KGRA. The clay cap and upper reservoir in the Glass Mountain resource areas conform to the typical alteration pattern observed at other geothermal systems. The temperature-sensitive transition from low resistivity smectite and mixed layer smectite-illite in the impermeable cap to higher resistivity illite conforms to the isotherms near the top of the geothermal reservoir.

6.1.1.3 Confirmation 3D MT Imaging and Correlated It with Well Temperature and Productivity

The 3D MT inversions produced resistivity images that matched the intensity and geometry of the temperature-sensitive smectite clay alteration in the wells. A borehole log from well 17A-6 provided a direct confirmation of the MT resistivity imaging. Seven conceptual cross-sections including resistivity and interpreted temperature extend the conceptual interpretation through the survey area. Reservoir engineers emphasize the overall temperature pattern in the reservoir as the most reliable constraint on overall patterns of reservoir permeability. The resistivity pattern images the low permeability cap with little ambiguity. The generally high permeability reservoir can be inferred indirectly through the conformance of the upper reservoir isotherms with the resistivity change associated with the smectite-illite transition. Because clay alteration is more intense over permeable zones, the lower values of resistivity associated with the more intense alteration is also used to confirm the temperature and permeability patterns inferred from the geometry of the resistivity.

It was not expected that the 3D MT inversion would resolve features at the scale of individual entries in wells at the depth of a geothermal reservoir. Nor was this seen.

6.1.1.4 TDEM Surveys at Glass Mountain

Central loop TDEM using 300 m (984 ft) transmitter loops and portable generators produces resistivity maps that are valid to a depth of at least 300 m (984 ft) but may be misleading when extended to 600 m (1969 ft) depth at Glass Mountain. Therefore, it can image shallow alteration but not the base of the clay cap. A large non-portable generator and transmitter loops 1000 m (3281 ft) in diameter could probably image the base of the clay cap but would also cost as much as MT and its lack of portability would limit the effectiveness of surveys.

The relatively thick resistive zone at the surface over most of the Medicine Lake Volcano made the TDEM data acquired using systems powered by batteries and portable generators unreliable for MT static corrections. Fortunately, the consistency of the same resistive layer appeared to minimize the amplitude of the MT statics.

6.1.2 Well Targets

The integrated interpretation of the MT and well data suggested two well targeting strategies for the Telephone Flat resource area and a step-out direction from the Fourmile Hill area. The 3D MT imaging indicates that the original drilling mainly targeted peripheral zones rather than the most likely high temperature upflow. The drilling targets derived from the MT are either areas of higher permeability or higher temperature, ideally both.

6.1.2.1 Telephone Flat

In the Telephone Flat area, the temperature in the wells and the pattern of alteration inferred from MT resistivity suggest that a >290°C (550°F) upflow exists northwest of well 68-8, perhaps beneath the Glass Mountain rhyolite flow, and a smaller upflow exists just north of well 87-13. In many relatively low permeability reservoirs, more prolific production has been achieved by targeting deep exploration wells across the structural trend where upflow creates higher temperatures. Permeability is sometimes lower in such deep wells but this can be offset by the improvement in productivity related to higher temperature. A reservoir engineering evaluation would be needed to quantify the economics of this trade-off.

The lack of MT data over the Glass Mountain rhyolite lava flow is a significant source of uncertainty in this interpretation. Mitigating the dangerous access on the lava flow would be difficult and probably very costly. Mitigating the quality issues related to acquiring MT on the lava is also problematic. Technically, the most effective approach might be to use a high power TDEM system with 1000 m (3281 ft) loops to get adequate penetration, but this may be impractical given the difficult access. Acquiring more MT data near the margins of the lava flow might improve the imaging.

The highest reservoir permeability encountered in an exploration well at Glass Mountain is at well 87-13 and this alone gives it priority for consideration. The MT resistivity pattern and well temperature indicate that 87-13 is very likely near a local upflow at the southwest end of the structural trend that passes near wells 68-8 and 31-17. The interpretation of the resistivity and isotherms near well 87-13 indicate that the shallow permeability at this location may extend to greater depth to the north. An apex in the base of the clay cap is imaged by the 3D MT inversion north of 87-13 and northwest of 68-8 and 31-17. A local apex in the base of the clay cap,

especially if aligned along a trend, is likely to be associated with permeable structures. Targeting a structure north of well 87-13 would also be advantageous if it were hotter than other step-out options for this well, and further MT surveying would improve the assessment of this possibility.

6.1.2.2 Fourmile Hill

At Fourmile Hill, well 88A-28 is on the periphery of a reservoir upflow. More intense alteration caps the reservoir to the south and southwest, suggesting that a >250°C (480°F) upflow is located in those directions. The maximum 250°C (480°F) cation geothermometry of 88A-28 produced fluids implies that the reservoir may be cooler than the Telephone Flat resource.

6.1.2.3 Southwest

Although the Southwest area remains prospective, as a high temperature target it has higher risk than Telephone Flat. Its risk seems comparable to a step-out from Fourmile Hill. The 3D MT images imply that this area may be a zone conceptually similar to the reservoir near 87-13, although the Southwest has a lower likelihood of being connected to an upflow with a temperature over 260°C (500°F).

6.1.2.4 Low Eenthalpy

Areas where the temperature is interpreted to lie between 100 and 180°C (212 to 380°F) and so could be pumped for binary generation appear to have a very limited permeable volume based on TGH and MT data.

6.1.2.5 Higher Drilling Risk

Drilling risk is higher where the resistivity pattern shows that the base of the smectite zone is very deep or the smectite alteration is poorly developed.

Several significant discontinuities in the resistivity pattern are likely to be faults. However, the interpreted temperature pattern suggests that the fault discontinuities that lack a characteristic structural high in the base of the clay cap are likely to act as reservoir boundaries in the Glass Mountain KGRA.

6.2Recommendations

6.2.1 Well Targeting

Although this study concludes that the lowest risk drilling targets are near the Telephone Flat area, further work can be done at relatively low cost to refine the targeting and better constrain the relative risks between this area and the other drilling target areas. The lower risk well targets are more than 1000 m (3300′) from the existing wells.

6.2.1.1 Telephone Flat area

Two strategies for targeting wells at Telephone Flat are considered. The first involves targeting the highest temperature upflow zone northwest of 68-8. The second would target the interpreted upflow near the highest measured permeability in well 87-13. The relative risks of these targets can be constrained by geological analyses of alteration and other parameters that would promote conceptual comparisons to other geothermal. A reservoir engineering analysis

that considers the MT results with respect to the well test data could further characterize the relative economics of the targeting strategies in the Telephone Flat Area.

6.2.1.2 Fourmile Hill Area

A new well in the Fourmile Hill area should target the upflow zone that supported the high temperature zone in 88A-28. The upflow zone is most likely located 1000 to 2000 m (3300 to 6600 ft) south or southwest of 88A-28. Additional MT data would constrain this target better.

6.2.1.3 Rim Rargets

The MT resistivity imaging identified several areas of relatively high shallow reservoir permeability and likely elevated temperature along the rim structure of the Medicine Lake Volcano. Information from the drilling recommended in the Telephone Flat area would reduce the risk associated with these targets.

6.2.2 Further MT and Geoscience Interpretation

Because the Glass Mountain well targeting plan will necessarily consider issues other than the MT imaging such as well performance economics, environmental impacts and regulatory constraints, the MT plots and analyses used to support well targeting recommendations may prove to be more important than the recommendations themselves.

6.2.2.1 Revised 3D MT inversion

As rapidly improving computer capability continues to reduce the cost and improve the reliability of 3D MT inversion, companies can consider revising 3D MT inversions at geothermal fields, particularly when new data is acquired or well results allow a recalibration of the interpretation. At Glass Mountain, the main hurdle to revising the MT resistivity imaging is already overcome, recovering and editing the legacy MT data and making it available in a readily accessible format. As the cost of the computation is reduced, one option for improving the 3D imaging would be to further reduce the block size used to represent the topography so that related static distortion can be better compensated.

6.2.2.2 Geological Constraints on Resistivity Patterns and Permeability

As ongoing geological studies, reservoir analyses and new drilling are completed, they should be integrated with the MT imaging to further refine the recommendations. The assessment of relative value and risk of drilling options could be improved by further characterizing the geological controls on the deep resistivity variations. For example, the existing wells appear to be on the margins of the reservoir imaged by the 3D MT resistivity and this will probably result in a distinctive alteration pattern in the wells. Using analogies to other geothermal fields where alteration information is available in the upflow and on the margins, the relative risk of targeting deeper permeability closer to the reservoir upflow could be characterized.

6.2.2.3 New MT Acquisition at Glass Mountain

Although the geophysical assessment of the primary resource target is as thorough as is completed for most geothermal targets prior to drilling, uncertainty in the imaging remains. Because of problematic access, some gaps in MT station coverage are inevitable but the uncertainty related to the gaps might be mitigated by reducing the station spacing along the

perimeter of the lava flows and near Medicine Lake. The station spacing at the edges of the prospective trends shaded red in Figure 29 is large enough to leave significant uncertainty in the dimensions of targets, for example, at the proposed permeable target zone north of well 87-13. Uncertainty related to the large station spacing near the secondary targets shaded green in Figure 29 would commonly be considered too great to justify drilling. In general, the edges of the prospective trends shown in green and red could be better resolved by more data, perhaps affecting follow-up well targeting more than recommendation for the next few wells. However, in areas with exceptional access and environmental issues, resolving this as closely as possible before starting drilling might be justified.

6.2.3 Resistivity Methods

There are circumstances where alternative resistivity methods might be preferred but MT is likely to remain the dominant application for imaging resistivity at geothermal prospects like Glass Mountain.

6.2.3.1 MT Survey Design

Standard specifications for geothermal MT surveys are effective at Glass Mountain. This project indicates that, although a variety of approaches to reduce costs seem feasible from a technical point of view, practical constraints on access and permitting are likely to make these moot at Glass Mountain, although perhaps not elsewhere. For example, mixing telluric-only stations with the MT stations might reduce costs with little loss in data quality. However, this will only be effective if access to sites is quick enough to allow the crews to increase the number of stations occupied per crew-day.

When planning an MT survey, data should be acquired in standard EDI format. A 3D inversion should be considered for new geothermal MT surveys that have a distributed array of stations.

6.2.3.2 TDEM Survey Design

The reliability of the TDEM could be improved by using larger generators, more powerful transmitters and 300 to 1000 m (1000 to 3300 ft) diameter loops. This would probably resolve resistivity to the base of the clay cap in many areas at Glass Mountain and would provide better statics for MT in most areas. However, the lateral resolution of such TDEM stations would be poorer, the cost would be much higher than earlier surveys and moving such equipment off-road would be impractical. Permitting a much larger and noisier transmitter would be difficult.

A promising option to reduce costs of resistivity surveying is to no longer collect TDEM data in areas where thick, resistive rocks cover most of the surface, like at Glass Mountain. Unless very expensive large loops and generators are used, TDEM is likely to give misleading results in such conditions. Moreover, the MT in such areas is likely to have small, symmetrical static offsets that can be accommodated by 3D MT inversion, providing that an adequate MT station spacing is available and that the topography is represented in the 3D inversion by a sufficiently fine model mesh. In such cases, the budget for TDEM can be applied to decreasing the distance between MT stations.

6.2.3.3 Lower Cost MT and TDEM Surveys

MT and TDEM survey costs are much lower than they were 20 years ago and can be further reduced, although approaches to do this are site specific. In areas like Glass Mountain that have a consistently resistive surface layer, collecting only MT without TDEM can reduce costs by about 20 to 30 percent. When surveying resources shallower than 1000 m (3300 ft) in smaller areas with easy access and few permitting constraints, high frequency MT profiling can reduce station costs by 30 to 70 percent. For geothermal resources shallower than 300 m (984 ft) with easy access, TDEM or other shallow resistivity survey methods can be substituted for MT, reducing costs by 50 to 70 percent. A geoscientist familiar with current geothermal geophysics standards can evaluate these options at low cost.

6.2.3.4 Legacy Data Sets

If legacy MT data are not available in an industry standard digital format, fully reformatting the data for inclusion in a 3D inversion may not be cost-effective. A low cost test-of-concept can be completed by conducting a 1D analysis using averaged resistivity data digitized from paper plots. If this initial test is promising, then the investment in the conversion of the legacy digital data to modern EDI format might be justified. In some areas where power plants have been constructed since the legacy data were collected, even the simple 1D approach to analyzing the legacy data might provide better results than recording a new MT survey amongst geothermal field facilities and power lines.

6.2.4 Further Research Suggested by this Project

6.2.4.1 Geology

Research projects relevant to Cascades/Basin and Range geology might consider the tectonics, hydrology and alteration that could produce the some of the large scale patterns resolved by the MT at Glass Mountain.

A genetic model for the clay layer that encases the volcanic rim could be supported by the well and TGH data. This appears to keep the area within the rim of the Medicine Lake Volcano hydrologically closed. Of greater academic interest would be an explanation for the large scale geometry of the thick clay slab. The clay layer does not fit the rim of the volcano as well as it fits a trapezoid-shaped area between the Little Glass Mountain Fault Zone and the Lyons Peak Fault Zone. Others have proposed that Medicine Lake Volcano is less a part of the Cascades than it is a pull-apart basin on the west margin of the Basin and Range. These questions are more suitable for an academic thesis than an industry project.

6.2.4.2 MT Research

There are several areas of ongoing MT research that are likely to impact further work on geothermal MT interpretations like this Glass Mountain MT study. Of particular value would be improved analyses and displays to more efficiently and intuitively illustrate the reliable resolution and uniqueness of resistivity features in a 3D inversion. Inversions should explicitly allow for the station distribution so that conductance artifacts between stations are minimized. Approaches to smoothing the inversion could more explicitly consider geological likelihood in an intuitively appealing way, that is, a horizontally smooth model may be reasonable in a

sedimentary basin but perhaps not at the margin of a geothermal clay cap. Improved approaches to analyze the model uncertainty introduced by static distortion and to estimate corrections based on geologically plausible constraints or on reliable TDEM soundings would add value. On the other hand, topographic statics may be automatically addressed when 3D MT models can be computed with enough elements to accurately represent the effect of topography at a cost that is a very small fraction of the cost of the survey.

More extensive studies of the effect of clays other than smectite and illite on resistivity within the geothermal reservoir in the context of other rock properties including permeability would likely add value to geothermal resistivity interpretations.

6.3 Benefits to California

The validation of the MT interpretation model improves confidence in the conceptual model elements used to define well targeting priorities at Glass Mountain. By more fully characterizing the resource geometry and reducing the area considered prospective for geothermal production, this survey has reduced the area likely to be impacted by exploration well drilling and has reduced both the number and cost of wells required to explore the geothermal resource at Glass Mountain. Improved well targeting is especially beneficial in California geothermal resource areas where changes in drilling locations may cause regulatory delays.

This MT interpretation and further refinements to it based on the drilling required for an initial power plant will improve the success of follow-up drilling for makeup or expansion, making more efficient use of surface locations. For an initial power plant, the MT-TDEM survey might reduce the pads required by one or two and wells by two to four.

The applicability of the smectite-illite transition approach to interpreting geothermal MT resistivity data has been confirmed at Glass Mountain and, based on this analysis and international studies; this type of interpretation is likely to also apply to other volcanic, sediment and granite-hosted geothermal fields in California. For example, since this project began, MT surveys have been conducted at two large geothermal fields in California, the Salton Sea and Coso, but the publications on these fields have not yet fully examined the integrated smectite-illite approach to the interpretation of the MT data, focusing instead on temperature, porosity and, in the case of the Salton Sea, salinity variations (Hoversten et al. 2006, Kaspereit et al. 2006). In the case of the Salton Sea sediments, the smectite-illite transition corresponds to the rapid loss of wet shale porosity and so could be viewed as a shale porosity analysis of the type extensively researched in the petroleum industry. The application of this method to exploration and step-out development should increase the utilization of California's geothermal potential, help meet utilities mandate for their renewable energy portfolio and ultimately reduce the cost of California's energy.

Although published case histories from geothermal fields worldwide have shown that MT is the most effective geophysical approach to targeting geothermal wells and assessing resource capacity data, there are no public domain data sets that include sufficient MT and geological

information to validate applications of new MT imaging technologies like the 3D inversion method that was applied as part of this project. For most published case histories, only final results and not the underlying data sets are available, preventing their use in benchmarking new technology. The MT, TDEM and well data that support the conclusions of this report will be available to the public in a format that would allow other MT practitioners and geothermal experts to independently review the results.

The Fourmile Hill and Telephone Flat projects are expected to benefit Siskiyou County in jobs and generate several million dollars in annual property tax revenue, and will provide new renewable energy that can help utilities meet California's Renewable Portfolio Standard.

REFERENCES

Adams, M., Moore, J, Bjornstad, S., Norman, D. "Geologic history of the Coso Geothermal System." *Proceedings World Geothermal Congress 2000*. 2463–2469.

Anderson, C.A. 1941. "Volcanoes of the Medicine Lake Highland, California: University of California Publications." *Bulletin of the Department of Geological Sciences* 25 (7): 347–422.

Anderson, E., Crosby, D. and Ussher, G. 2000. "Bull's Eye! — Simple resistivity imaging to reliably locate the geothermal reservoir." *Proceedings World Geothermal Congress 2000*. 909–914.

Anderson, S., Stofan, E., Plaut, J., Crown, D. 1998. "Block size distributions on silicic lava flow surfaces: Implications for emplacement conditions." *GSA Bulletin* 110 (10): 1258–1267.

Anderson, W., Frischknecht, F., Raab, P., Bradley, J., Turnross, J., Buckley, T. 1983a. "Inversion results of time-domain electromagnetic soundings near Medicine Lake, California, geothermal areas." *USGS Open-File Report 83-233*. 31 p.

Anderson, W., Frischknecht, F., Bradley, J., Grette, R., and Grose, C. 1983b. "Inversion results of time-domain electromagnetic soundings near Medicine Lake, California, Part 2." *USGS Open-File Report 83-910*. 29 p.

Anderson, W., Frischknecht, F., Raab, P., Bradley, J., Turnross, J. 1983c. "Results and preliminary analysis of loop-loop frequency domain electromagnetic soundings near Medicine Lake, California." *USGS Open-File Report 83-830*. 126 p.

Anderson, W. 1988. "Interpretation of transient electromagnetic soundings at the Medicine Lake volcano, Siskiyou County, California." *USGS Open-File Report 88-582*. 29 p.

Bargar, K. and Keith, T. 1997. "Estimated temperatures for geothermal drill holes at Medicine Lake Volcano, north-eastern California, based on fluid inclusion and hydrothermal mineralogy studies." *USGS Open File Report 97-716*. 116 p.

Beamish, D. and Travassos, J. 1992. "The use of the D^+ solution in magnetotelluric interpretation." *Journal of Applied Geophysics, 29:* 1-19.

Broker, M., Christopherson, K., and Haller, R. 1982. "E-field ratio telluric survey near Medicine Lake in the Medicine Lake Highlands Caldera, Siskiyou County, California." *USGS Open File Report 82-900*. 11 p.

BRW Geotechnical, Inc. 1984. "Medicine Lake California gravity survey summer 1984." Proprietary report to Occidental Geothermal, Inc. Released to the California Energy Commission by Calpine Corporation. 43 p.

Calpine-Siskiyou Geothermal Partners L.P. 2004. "Draft final report: Fourmile Hill exploration well 88A-28." California Energy Commission, GRDA Geothermal Resources Development Account.

Carrier, D.L. 1987. "Analysis of mineralogy and fluid inclusion data from Glass Mountain area temperature boreholes." Proprietary Unocal memorandum to Alex Schriener, November 30, 1987. Released to the California Energy Commission by Calpine Corporation. 39 p.

Carrier, D.L. 1989a. "Summary report on the geology and geochemistry of Glass Mountain Geothermal Reservoir, Glass Mountain KGRA, California." Proprietary Unocal memorandum to David Sussman, June 23, 1989. Released to the California Energy Commission by Calpine Corporation. 12p.

Carrier, D.L. 1989b. "Hydrothermal alteration and well lithologies for Glass Mountain wells GMF68-8, GMF31-17 and GMF17A-6, Glass Mountain, CA." Proprietary Unocal memorandum to David Sussman, August 8, 1989. Released to the California Energy Commission by Calpine Corporation. 78 p.

CGG. 1982. "MT Survey, Glass Mountain Prospect: Prepared for UNOCAL Geothermal." Proprietary report to Unocal Corp. 470 p.

Clausen, S., Nemčok M., Moore , J., Hulen, J. and Bartley, J. 2006. "Mapping Fractures in the Medicine Lake Geothermal System." *Geothermal Resources Council Transactions* 30: 383–386.

Constable, S., Parker, R., and Constable, C. 1987. "Occam's inversion: A practical algorithm for generating smooth models from electromagnetic sounding data." *Geophysics* 52: 289–300.

Cumming, W., Nordquist, G., and Astra, D. 2000. "Geophysical exploration for geothermal resources, an application for combined MT-TDEM." *70th Ann. Internat. Mtg., Soc. Expl. Geophys. Expanded Abstracts*.

Donnelly-Nolan, J. 1985. "Geothermal Potential of Medicine Lake Volcano, In Proceedings of the Workshop of Geothermal Resources of the Cascade Range." *USGS Open-File Report 85-521*.

Donnelly-Nolan, J.M., and Nolan, K.M. 1986. "Catastrophic flooding and the eruption of ash-flow tuff at Medicine Lake volcano, California." *Geology* 14: 875–878.

Donnelly-Nolan, J.M. 1988. "A magmatic model of Medicine Lake volcano, California." *Journal of Geophysical Research* 93 (B5): 4412–4420.

Donnelly-Nolan, J.M. 1990. "Geology of the Medicine Lake Volcano, Northern California Cascade Range." *GRC Trans*. 14: 1395–1396.

Donnelly-Nolan, J.M. 1992. "Medicine Lake volcano and Lava Beds National Monument." *California Geology* 45 (5): 145–153.

Dzurisin, D., Donnelly-Nolan, J.M., Evans, J.R., and Walter, S.R. 1991. "Crustal subsidence, seismicity, and structure near Medicine Lake Volcano, California." *Journal of Geophysical Research* 96 (B10): 16319–16333.

Dzurisin, D., Poland, M., and Bürgmann, R. 2002. "Steady subsidence of Medicine Lake volcano, northern California, revealed by repeated leveling surveys." *J. Geophys. Res.* 107(B12): 2372.

Eichelberger, J. C. 1975. "Origin of Andesite and Dacite, Evidence of Mixing at Glass Mountain and at Other Circum-Pacific Volcanoes." *Geol. Soc. Am. Bull.* 86: 1381–1391.

Eichelberger, J.C. 1981. "Mechanism of magma mixing at Glass Mountain, Medicine Lake Highland volcano, California." in Johnson, D., and Donnelly-Nolan, J., eds., "Guides to some volcanic terranes in Washington, Idaho, Oregon, and northern California." *U.S. Geological Survey Circular 838*. 183–189.

Earth Technology Corporation 1985. "TEM Survey Medicine Lake California. Prepared for Unocal Geothermal Division. Job # G85143." Proprietary report to Unocal Corp. Released to the California Energy Commission by Calpine Corporation. 362 p.

Earth Technology Corporation 1986. "TEM Survey Medicine Lake Highland, California. Prepared for Unocal Geothermal Division, Santa Rosa CA. Job # G86179." Proprietary report to Unocal Corp. Released to the California Energy Commission by Calpine Corporation. 214 p.

ElectroMagnetic Surveys, Inc. 1982. "Transient electromagnetic depth sounding test survey at Glass Mountain - Medicine Lake, Northern California; Report #8246 Prepared for: Occidental Geothermal, Inc. Bakersfield, CA." Proprietary report to Occidental Geothermal, Inc. Released to the California Energy Commission by Calpine Corporation. 118 p.

ElectroMagnetic Surveys, Inc. 1983a. "Schlumberger electrical sounding survey, Medicine Lake Area, California; Report #8377C Prepared for Occidental Geothermal, Inc. Bakersfield, CA." Proprietary report to Occidental Geothermal, Inc. Released to the California Energy Commission by Calpine Corporation. 32 p.

ElectroMagnetic Surveys, Inc. 1983b. "TEM central induction soundings, Siskiyou County, California; Report #838101 Prepared for: Union Oil Company of California, Geothermal Division." Proprietary report to Union Oil Company of California. Released to the California Energy Commission by Calpine Corporation. 244 p.

ElectroMagnetic Surveys, Inc. 1985a. "TEM central induction sounding, Glass Mountain Prospect, California; Report #841201 Prepared for: Union Oil Company of California, Geothermal Division." Proprietary report to Union Oil Company of California. Released to the California Energy Commission by Calpine Corporation. 100 p.

ElectroMagnetic Surveys, Inc. 1985b. "TEM central induction sounding, Medicine Lake, California; Report #841301 Prepared for Occidental Geothermal, Inc. Bakersfield, CA." Proprietary report to Occidental Geothermal, Inc. Released to the California Energy Commission by Calpine Corporation. 173 p.

ElectroMagnetic Surveys, Inc. 1985c. "TEM central induction sounding, Medicine Lake Area, California; Report #850503 Prepared for Santa Fe Geothermal, Inc." Proprietary report to Santa Fe Geothermal, Inc. Released to the California Energy Commission by Calpine Corporation. 132 p.

GSY-USA, Inc. 2005. "Magnetotelluric survey Glass Mountain KGRA, California." Report prepared for the California Energy Commission, October 2005.

Essene, E. and Peacor, D. 1995. "Clay mineral thermometry – a critical perspective." *Clays and Clay Minerals*. 43. 540-553.

Evans, J. and Zucca, J. 1988. "Active high-resolution seismic tomography of compressional wave velocity and attenuation structure at Medicine Lake volcano, Northern California Cascade Range." *J. Geophys. Res.* 93: 15,016–15,036.

Fink, J. and Pollard, D. 1983. "Structural evidence for dikes beneath silicic domes, Medicine Lake volcano, California." *Geology* 11: 458–461.

Finn, C. and Spydell, D., 1982. "Principal facts for seventy-four gravity stations in the northern California Cascade Mountains." *U.S.G.S. Open File Report 82-1080*.

Finn, C., and Williams, D. 1982. "Gravity evidence for shallow intrusion under Medicine Lake Volcano, California." *Geology* 10: 503–507.

Fitterman, D., Stanley, W., and Bisdorf, R. 1988. "Electrical structure of Newberry Volcano, Oregon." *JGR* 93: 10, 119–10,134.

Flóvenz, O., Spangenberg, E., Kulenkampff, J., Árnason, K., Karlsdóttir, R., and Huenges, E. 2005. "The Role of Electrical Interface Conduction in Geothermal Exploration." *Proceedings World Geothermal Congress*.

Fournier, R. 1999. "Hydrothermal Processes Related to Movement of Fluid From Plastic into Brittle Rock in the Magmatic-Epithermal Environment." *Economic Geology* 94: 8, 1193-1211.

Heiken, G. 1978. "Plinian-Type Eruptions in the Medicine Lake Highland, California and the Nature of the Underlying Magma." *Journ. Volc. Geoth. Res.* 4: 375–402.

Hulen, J. and Lutz, S. 1999. "Altered volcanic rocks as hydrologic seals on the geothermal system of Medicine Lake Volcano, California." *Geothermal Resources Council Bulletin* 7: 217–222.

Geonomics, Inc. 1975. "Report No. 1 Magnetotelluric Survey Glass Mountain, California. Report for the Union Oil Company by Alan Lattanner and Tsvi Meidev." Proprietary report for Union Oil Company of California. Released to the California Energy Commission by Calpine Corporation. 55 p.

Geoterrex 1983. "Glass Mountain Unit Area 1983 HEM survey." Proprietary maps for Union Oil Company of California. Released to the California Energy Commission by Calpine Corporation. 2 p.

Goranson, C., and Combs, J. 2000. "Using slim holes for long-term monitoring of geothermal reservoir performance at Steamboat Springs, Nevada, USA." *Proceedings World Geothermal Congress*.

GSY-USA, Inc. 2005. "Magnetotelluric survey Glass Mountain KGRA, California." Report for the California Energy Commission. 35 p.

Gunderson, R. 1991. "Collected petrographic, fluid inclusion and rock property analyses of cores and drill cuttings from Glass Mountain wells." Unocal data summary. Released to the California Energy Commission by Calpine Corporation. 108 p.

Gunderson, R., Cumming, W., Astra, D., and Harvey, C. 2000. "Analysis of smectite clays in geothermal drill cuttings by the methylene-blue method: for well site geothermometry and resistivity sounding correlation." *Proceedings World Geothermal Congress*: 1175–1181.

Hoversten, M., Newman, G.A., and Gasperikova, E. 2006 "Further Analysis of 3D Magnetotelluric Measurements Over the Coso Geothermal Field." *GeothermalR esouces Council Transactions* 30: 133–137.

Hulen, J. and Lutz, S. 1999. "Altered volcanic rocks as hydrologic seals on the geothermal system of Medicine Lake Volcano, California." *Geothermal Resource Council Bulletin* 7: 217–222.

Kaspereit, D., Berard, B., Gutierrez, P., Nichols, E. and Chen, J. 2006. "Land and Marine Magnetotelluric Exploration at the Salton Sea Geothermal Field." *Geothermal Resources Council Transactions* 30: 985–990.

Larsen, J., Mackie, R., Manzella, A., Fiordelisi, A., and Rieven, S. 1996. "Robust Smooth MT transfer functions." *Geophys. J. Int*. 124: 801–819.

Lisowski, M., Poland, M., Dzurisan, Owen, S. 2004. "Volcano-tectonic deformation at Mount Shasta and Medicine Lake volcanoes, northern California, from GPS: 1996–2004." *Trans. AGU*. 85(47): Fall Meet. Suppl., Abstract G51A-0069.

Lowenstern, J., Donnelly-Nolan, J., Wooden, J., and Charlier, B. 2003. "Volcanism, plutonism and hydrothermal alteration at Medicine Lake Volcano, California." *Proceedings, Twenty-Eighth Workshop on Geothermal Reservoir Engineering, Stanford University*. 8 p.

Lutz, S., Hulen, J., Schriener, A. 2000. "Alteration, geothermometry, and granitoid intrusions in well GMF 31-17, Medicine Lake Volcano geothermal system, California." *Proceedings 25th Workshop on Geothermal Reservoir Engineering, Stanford University.* SGP-TR-165.

Mackie, R., Smith, J., and Madden, T. 1994. "Three-dimensional electromagnetic modeling using finite difference equations: The magnetotelluric example" *Radio Science* 29: 923–935.

Mariner R., Evans, W., and Huebner, M. 1998. "Preliminary chemical and isotopic data for waters from springs and wells on and near Medicine Lake Volcano, Cascade Range, Northern California." *USGS Open File Report 98-2*. 27 p.

Mariner R. and Jenik C. 1995. "Geochemical data and conceptual model for the Steamboat Hills geothermal system, Washoe County, Nevada." *Geothermal Resources Council Transactions* 19. 191–200.

Mase, C.W., Sass, J.H., Lachenbruch, A.H., and Munroe, R.J., 1982, Preliminary Heat Flow Investigations of the California Cascades, *U.S.G.S. Open-File Report 82-150*, 240 p.

McNutt, S. 1989. "Medicine Lake Highland September 1988 earthquake swarm." *California Geology*: 51–52.

Mertzman, S.A. 1981. "Pre-Holocene silicic volcanism on the northern and western margins of the Medicine Lake Highland, California." in Johnson, D., and Donnelly-Nolan, J., eds., "Guides to some volcanic terranes in Washington, Idaho, Oregon, and northern California." *U.S. Geological Survey Circular 838*: 163–169.

Moore, J. 2006. "Predicting fracture characteristics in volcanic environments as a guide to locating enhanced geothermal system reservoirs." Year 2 Technical Report for period ending September 30, 2006 for DOE Project DE-FG36-04GO14298.

Newendorp, P., and Schuyler, J. 2000. "Decision analysis for petroleum exploration, 2nd edition" Planning Press. 606 p.

Nordquist, G. 1985. "Glass Mountain Well 17A-6 Schlumberger Dual Induction Resistivity log, averaged at 100' intervals." Unocal Corporation Figure. Released to the California Energy Commission by Calpine Corporation. 1 p.

Pellerin, L., and Hohmann, G. 1990. "Transient electromagnetic inversion: A remedy for magnetotelluric static shifts." *Geophysics* 55: 1242–1250.

Phoenix Geoscience 1986. "MT Stations P01 to P17." Data report to Unocal. Released to the California Energy Commission by Calpine Corporation. 345 p.

Phoenix Geoscience 1989. "MT Stations 01 to 49." Data report to Unocal. Released to the California Energy Commission by Calpine Corporation. 981 p.

Poland, M., Dzurisan, D., Burgmann, R., Koenig, E., and Fink, J. 2000. "Modeling deformation at Medicine Lake Volcano in Northern California using regional tectonic and local volcanic sources." *Eos Trans. AGU.* 81 (48). Fall Meet. Suppl., Abstract G21A-11.

Poland, M., Dzurisan, D., Hammond, W., Endo, E., Iwatsubo, E., and Lisowski, M. 2003. "New results from a proposed PBO Cascade Volcano Cluster I: Deformation in the Medicine Lake region of Northeast California from leveling, GPS and InSAR." *GSA Annual Meeting Abstracts* 35(6): 563.

Quantech Consulting Inc. 2002. "Geophysical report on the transient electromagnetic (TEM) surveys conducted at the Fourmile Hill Project, Siskiyou County, California on behalf of Calpine Corporation." GCA Project C-364 report by Jon Powell. Released to the California Energy Commission by Calpine Corporation.

Ramsey, D., and Donnelly-Nolan, J. 2002. "Digital geologic map database of Medicine Lake Volcano, California." *GSA Annual Meeting Abstracts* 34(6).

Rodi, W. and Mackie, R. 2001. "Nonlinear conjugate gradients algorithm for 2-D magnetotelluric inversion" *Geophysics* 66: 174–187.

Sanyal, S., Morrow, J., Butler, S. and Robertson-Tait, A. 2007. "Cost of electricity from enhanced geothermal systems" *Proceedings 32nd Workshop on Geothermal Reservoir Engineering, Stanford University.* SGP-TR-183.

Simpson, F. and Bahr, K. 2005. "Practical Magnetotellurics" Cambridge University Press. 254 p.

Smith, J. and Booker, J. 1991. "Rapid inversion of two- and three-dimensional magnetotelluric data" J. *Geophys. Res.* 96: 3905–3922.

Smith, T. 1996. "Conservative modeling of 3-D electromagnetic fields, Part I: Properties and error analysis." *Geophysics* 61: 1308–1318.

Smith, T. 1995. "Understanding telluric distortion matrices." *Geophysics Jour. International* 122: 219–226.

Sorey, M. 2000. "Geothermal development and changes in surficial features: examples from the western United States." *Proceedings, World Geothermal Congress :*705–711.

Summit Engineering Inc. 1983. "Medicine Lake California gravity survey" Proprietary report to Occidental Geothermal, Inc. Released to the California Energy Commission by Calpine Corporation. 15 p.

Tikhonov, A. and Arsenin, V. 1977. "Solutions of ill-posed problems" V.H. Winston and Sons.

Uchida, T. 2005. "Three-dimensional magnetotelluric investigation in geothermal fields in Japan and Indonesia" *Proceedings World Geothermal Congress*.

Ussher, G., Harvey, C., Johnstone, R., and Anderson, E. 2000. "Understanding the Resistivities Observed in Geothermal Systems" *Proceedings World Geothermal Congress*.

Vozoff, K. 1991. "The magnetotelluric method" in *Electromagnetic Methods in Applied Geophysics Vol 2B*, pub Society of Exploration Geophysics: 641-711.

Wannamaker, P.E., Rose, P.E., Doerner, W.M., McCulloch, J., and Nurse, K. 2005. "Magnetotelluric Surveying and Monitoring at the Coso Geothermal Area, California, in Support of the Enhanced Geothermal Systems Concept: Survey Parameters, Initial Results." *Proceedings, World Geothermal Congress*.

Wannamaker, P.E. Wright, P.M., Zi-xing, Z., Xing-bin, L., and Jing-xiang, Z. 1991. "Magnetotelluric transect of Long Valley caldera: resistivity cross-section, structural implications, and the limits of a 2-D analysis." *Geophysics*, 56: 926–940.

Waff, H. 1983. "Glass Mountain MT." Data tables for CalEnergy, Inc. Released to the California Energy Commission by Calpine Corporation. 177 p.

Waff, H. 1984. "Shasta Region MT. Vol 1 to 4." Data tables and plots for CalEnergy, Inc. Released to the California Energy Commission by Calpine Corporation. 1028 p.

Wheeler, D. 1985. "Glass Mountain gravity map." Unocal Corporation Data Summary. Released to the California Energy Commission by Calpine Corporation. 43 p.

Wight, D. 1991. "MT/EMAP data interchange standard." Society of Exploration Geophysicists, Technical Standards Committee Report. 108 p.

Woodward-Clyde Consultants 1981. "Glass Mountain, California Magnetotelluric Data Prepared for Union Oil Company." Released to the California Energy Commission by Calpine Corporation.

Wright, P., Ward, S., Ross, H., and West, R. 1985. "State of the art geophysical exploration for geothermal resources." *Geophysics* 50: 2666–2696.

Yee, K.S., 1966, "Numerical solution of initial boundary value problems involving Maxwell's equations in isotropic media." *IEEE Trans. Ant. Prop.,* AP-14: 302-307.

Zohdy, A., and Bisdorf, R. 1982. "Schlumberger soundings in the Medicine Lake Area, California." *USGS Open File Report 82-887*.

GLOSSARY

Term	Definition
1D	One dimensional, in geophysics methods, usually describes a computation used to derive a series of rock property values versus depth. It also describes the underlying approximation that assumes property variations occur only with respect to depth. Areas with “layer cake” geology are 1D.
2D	Two dimensional, in geophysics methods, usually describes a computation used to derive a cross-section grid of rock property values. The cross-section extends below a profile line on a map. The 2D *strike* is the direction at right angles to the profile line. The term 2D also describes the underlying approximation used in the computation that assumes property variations occur only with respect to the depth and the horizontal axes of the cross-section, while no variations occur in the strike direction. A long, straight fault might be 2D with a strike direction parallel to the fault line.
3D	Three dimensional, in geophysics methods, usually describes a computation used to derive a three dimensional mesh of property values covering a volume. Properties variations can occur in any direction, for example, northing, easting, and elevation. This is the most general case for spatial imaging.
Argillic	In geothermal geology, the argillic zone is a section of rock alteration that forms over and adjacent to geothermal reservoirs, often forming a low permeability cap to the system. It is characterized by abundant mixed-layer smectite clay and is usually very low in resistivity because of its smectite content.
Brittle-Ductile Transition	The depth in the earth’s crust at which rock becomes less likely to fracture and more likely to deform by ductile creep.
Chlorite	In geothermal exploration, chlorite is a family of clay types that, as part of the hydrothermal alteration process, replaces primary minerals and lower temperature smectite clay alteration at temperatures over 150°C (~300°F). Along with illite clay, some types of chlorite clay are associated with the more permeable propylitic zone of a geothermal reservoir. Some types of chlorite clay have an electrical resistivity that is intermediate between smectite and illite clay.
Conductance	In geophysics, a measure of the ease with which a particular area of rock conducts electricity. Its units are siemens. High values imply easier movement of electrical current. In geothermal geophysics, maps of conductance of rocks from the surface to a particular depth typically correlate with the total amount of smectite clay alteration to that depth. Conductance is the reciprocal of resistance.
Conductivity	In geothermal geophysics, a rock property that is a measure of a rocks ability of conduct electricity. Its units are siemens/m or mhos/m. It is the reciprocal of resistivity.
Deliverability	In geothermal reservoir engineering, a measure of well productivity performance over a range of conditions, usually based on the mass flow of steam and water at two or more wellhead pressures.
Dike	A tabular body of igneous rock that is thin in its smallest dimension compared to its other dimensions. A dike is intruded as molten rock into a solid host rock along a vertically oriented fissure.

Term	Definition
EDI	The electronic data interchange format, in MT surveying, is the standard digital format supported by the Society of Exploration Geophysicists to store and exchange MT data. It is widely used by academic and industry groups.
EGI	Energy & Geoscience Institute, a research consultancy affiliated with the University of Utah and the employer of Dr. Joseph Moore who provided the geology and alteration analysis support for the Glass Mountain MT interpretation.
EGS	Enhanced Geothermal System, a geothermal research program of the US Department of Energy that seeks to enhance the permeability in parts of geothermal reservoirs that cannot currently be economically produced because of their low permeability. Dr. Joseph Moore of EGI has a research project funded under the EGS program that involves research in fracture permeability and alteration at Glass Mountain.
Entry	In geothermal reservoir engineering, a point at a particular depth in a well where water or steam enters a well bore from the reservoir, implying the existence of a permeable zone. The interaction of well and reservoir pressure sometimes results in permeable zones that are not observed as entries, although all entries are permeable zones.
Fracture Permeability	In geothermal reservoir engineering, structurally induced secondary porosity with high hydraulic conductivity.
Geothermometer	A chemical indication of temperature in water or rock. Water geothermometers are based on proportions of cations that have temperature sensitive solubility. Minerals that tend to form in rocks at particular temperature ranges also act as geothermometers .
Graben	A block of the earth's crust that has been faulted downward, often forming a valley between two almost parallel faults.
Illite	In geothermal exploration, illite is a type of clay that begins to replace other clay (see smectite) at temperatures over 90°C (~200°F). It is associated with the more permeable propylitic zone of a geothermal reservoir and has high electrical resistivity compared to other clays.
Impedance	The complex resistance to alternating electrical current flow, usually with real and imaginary components, analogous to resistance in direct current flow. Because MT uses electromagnetic waves, the basic result of an MT survey is a matrix of directional impedances from which apparent resistivity can be calculated in those directions at a particular frequency.
Inversion	In geophysics, a computation that converts data from the measurement units of a particular technique to a rock property variation with respect to spatial location. For example, a central loop TDEM detector typically records data as detector voltage versus time and a 1D inversion converts that data to rock resistivity versus depth below the station center.
Isotherm	A contour of equal temperature. The pattern of isotherms in the natural state of a geothermal reservoir, before exploitation, is usually considered to be the most revealing component of a geothermal conceptual model.
ka	Thousand years, in geological time scales.

Term	Definition
kph	Thousand pounds per hour, the mass rate of production of fluid from a geothermal well in the USA, usually total rate unless specified as steam or water rate.
MeB	Methylene-blue, a standard chemical dye and, in geothermal well cuttings and core analysis, a method of semi-quantitatively assessing how much smectite clay exists in a rock by grinding up the rock and measuring how much MeB it can absorb.
milligal	A unit of the acceleration due to gravity used in geophysical surveys. It is about one millionth of the acceleration at the Earth's surface, that is, 0.00001 m/s^2
Mode	In magnetotelluric analysis, a mode is one of the two apparent resistivity (and phase) curves that can be defined using a variety of criteria. For example, one mode could be the apparent resistivity and phase measured along the north axis of the electrodes in the field while the other mode would be along the east electrodes. The MT axes can be mathematically rotated to any direction, providing a variety of other modes. The choice of MT modes defined parallel and perpendicular to the interpreted resistivity strike, called the TE and TM modes respectively, is an important part of 2D inversion. The validity of the TE and TM mode choices is usually the most serious limitation to the 2D inversion. The TM mode is inherently easier to fit in 2D inversion because it is defined along the axis in the plane of the 2D cross-section in which the elements of the resistivity model are adjusted. The 2D inversion assumes that no variations occur in the perpendicular (TE mode) direction. Modes are not a significant consideration in 3D inversion.
MT	Magnetotellurics, a surface method of imaging resistivity from a few m deep to many km (over 100,000 ft) deep by measuring variations in magnetic and electric fields at the surface of the earth caused by natural sources like sun spots and lightning.
Ohm-m	Unit of resistivity and in geophysics, a rock property.
PA	Principal axes, in MT, is a mathematical rotation done so that the two orthogonal measurements made in the field are aligned in directions that more closely represent a 2D case, resulting in maximum and minimum values for the apparent resistivity modes if the data is 2D and has no static distortion.
Perched Aquifer	An aquifer that is separated from a deeper aquifer by a zone that is not saturated with water. The base of the upper aquifer, coinciding with the top of the unsaturated zone, is a low permeability layer on which the perched aquifer sits.
Permeability	In geothermal reservoir engineering, the capacity of a rock volume to transmit fluid. Geothermal wells require high permeability in order to produce enough hot fluid to be economically viable. In the deep parts of geothermal fields, such high permeability is associated with faults.

Term	Definition
Propylitic	In geothermal geology, the propylitic zone is a section of rock alteration that forms within geothermal reservoirs at temperatures over 200 to 260°C (400 to 500°F) and may extend to over 320°C (600°F). It is characterized at Glass Mountain by the consistent appearance of the temperature-sensitive mineral epidote and by the replacement of smectite clay by chlorite and illite clay. The propylitic zone typically has moderate resistivity but it is significantly higher in resistivity than the overlying argillic zone that contains very low resistivity smectite. The word propylitic comes from mineral deposit terminology but its meaning can differ in a geothermal context.
Resistance	In geothermal geophysics, a property of a particular path through a volume of rock that is a measure of the opposition to the flow of electrical current. Its units are ohms.
Resistivity	In geothermal geophysics, a rock property with units of ohm-m that is a measure of the opposition of the rock to the flow of electrical current. In geothermal areas, this depends mostly on how much wet clay alteration the rock contains. Resistivity is the reciprocal of conductivity.
Siemens	Unit of conductance.
Smectite	In geothermal geology, smectite is a type of clay alteration in rock that absorbs water and is particularly abundant near hydrothermal aquifers at 60°C (~100°F) to 180C (~380°F). Rocks that contain wet smectite tend to be impermeable and so smectite alteration usually forms a “cap” over geothermal aquifers. As temperature rises from 60 to 180°C, smectite either loses water or converts to illite clay. Wet smectite found at lower temperature has very low electrical resistivity whereas illite clay found at higher temperature has high resistivity. This is the basis for the smectite-illite interpretation model for geothermal resistivity surveys.
Static	In resistivity methods like MT that use electrodes to measure electric fields, a static is a type of distortion related to local accumulation of electrical charge at a discontinuity in earth resistivity near the electrodes. In MT, a static often results in a ratio between xy and yx apparent resistivity that is different from 1 but constant over a wide range of frequencies, starting from the highest recorded. Inductive methods like TDEM do not suffer from static effects and so can be used to provide corrections.
TE mode	Transverse electric field, in MT, the MT apparent resistivity and phase measured along the resistivity strike, that is, parallel to geological elements like faults that define resistivity discontinuities.
Telluric	A natural electrical current in the ground. As a survey, a surface method of imaging resistivity from a few m deep to many km by measuring only the electrical fields related to natural currents. It is MT without the magnetic measurements.
TDEM	Time domain electromagnetics, a surface method of imaging resistivity from depths of a few m to a few hundred m (up to ~3000 ft). The most common approach is to suddenly switch off a steady current in a large wire loop laid out on the ground and use a vertical coil as a detector to measure the time decay of the resulting magnetic field. The decay rate depends on the resistivity pattern of the underlying rocks. When the detector is located in the middle of the loop, the measurement is focused and so 1D computations are more reliable. Because no electrodes are used, the *static* distortions that electrodes sometimes cause are eliminated.

Term	Definition
TEM	Same as TDEM.
T-MT	A method in which one or more telluric stations are recorded at the same time as a nearby MT station to image resistivity in a manner similar to MT. In areas that lack abrupt lateral variations in resistivity, a telluric station can be processed as if it was MT using the magnetic field signals recorded at the nearby MT station. This avoids digging holes for magnetometers at the telluric station.
TGH	Temperature gradient hole. This is usually a small diameter well designed so that temperature logs can be run but no production is feasible. TGH cores and cuttings can be used for lithology and alteration descriptions. Also called a TGW or temperature gradient well.
TM mode	Transverse magnetic field, in MT, the MT apparent resistivity and phase measured across the resistivity strike, that is, across the geological elements like faults that define resistivity discontinuities.
VES	Vertical electrical sounding, sometimes called Schlumberger sounding, is a surface method of imaging resistivity, the resistance to the flow of electricity in rocks, from depths of a few m to a few hundred m (up to several thousand feet). At the surface, a current is put into the ground between two transmitter electrodes. The voltage they induce in the ground is measured between two detector electrodes, spaced close together between the more widely spaced transmitter electrodes. A sounding showing the variation of resistivity with respect to depth can be made by increasing the distance between the transmitter electrodes and repeating the measurement.
Xenoliths	Rock fragments that are unlike the type of volcanic or intrusive igneous rock in which they are found. Solid pieces of the foreign rock type became mixed with the molten igneous rock before the igneous rock cooled and solidified.
XRD	X-ray diffraction crystallography, in geology, is a method of characterizing the crystal structure of the minerals in a rock by transmitting X-rays through them.